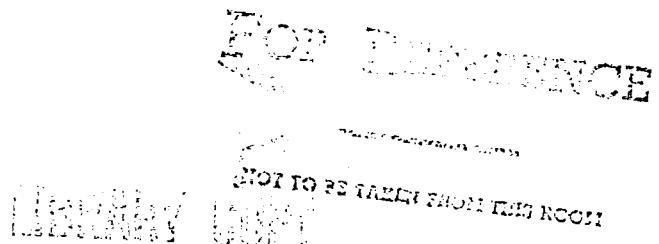NASA-TM-100057

NASA-TM-100057 19880016036

Diurnal Variations in Optical Depth at Mars: Observations and Interpretations

D. S. Colburn, J. B. Pollack and R. M. Haberle

May 1988

NASA

National Aeronautics and
Space Administration

$N88 - 25420\#$

Diurnal Variations in Optical Depth at Mars: Observations and Interpretations

D. S. Colburn
J. B. Pollack
R. M. Haberle, Ames Research Center, Moffett Field, California

May 1988

$N88 - 25420\#$

SUMMARY

Viking lander camera images of the Sun were used to compute atmospheric optical depth at two sites over a period of 1-1/3 martian years. The complete set of 1044 optical depth determinations is presented in graphical and tabular form. Error estimates are presented in detail. Optical depths in the morning (AM) are generally larger than in the afternoon (PM). The AM-PM differences are ascribed to condensation of water vapor into atmospheric ice aerosols at night and their evaporation in midday. A smoothed time series of these differences shows several seasonal peaks. These are simulated using a one-dimensional radiative-convective model which predicts martian atmospheric temperature profiles. A calculation combining these profiles with water vapor measurements from the Mars Atmospheric Water Detector (MAWD, on the Viking orbiters) is used to predict when diurnal variations of water condensation should occur. The model reproduces a majority of the observed peaks and shows the factors influencing the process. Diurnal variation of condensation is shown to peak when the latitude and season combine to warm the atmosphere to the optimum temperature, cool enough to condense vapor at night and warm enough to cause evaporation at midday. The diurnal variation is enhanced by increased water vapor, and is sometimes enhanced, sometimes diminished, by enhanced dust loading, depending on the other conditions. Often the model predicts condensation only at altitudes of 25 km or more, while at other times the condensation reaches ground level. Agreement between model and observations is also evident on a time scale of hours, when the data are available at more than two times in a single day.

INTRODUCTION

The atmosphere of Mars is known to contain water vapor as a minor constituent. The surface column abundance was measured by the Viking Mars Atmospheric Water Detector (MAWD) with typical values on the order of 10-100 precipitable micrometers (for water, 1 pr μm = 1 g m^{-2}) (Jakosky,1985, Farmer et al., 1977). The temperature of the martian atmosphere is often lowered to a point at which condensation would be expected, and the low temperature and pressure of the atmosphere indicates that the condensate would be solid rather than liquid. Thin frost deposits have been observed at the Viking Lander 2 (VL2) site (Jones et al., 1979, Hart and Jakosky, 1986, Gooding, 1986). Haze layers which are presumed to be condensed water have been observed at high altitudes by the orbiter camera (Jaquin et al., 1986).

The most prominent aerosol component of the martian atmosphere is dust. Obscuration of martian features by global dust storms was first observed from Earth and later confirmed by Mariner 9 (Hanel et al., 1972, Toon et al., 1977). During the first martian year (1 martian year = 687 Earth days) after the arrival of the Viking orbiters and landers numerous local dust storms and two global dust storms were observed.

The Viking lander cameras have provided measurements of atmospheric aerosols at the two lander sites (Pollack et al., 1977, Pollack et al., 1979, hereafter referred to as Papers I and II, respectively). The areocentric location of Lander 1 (VL1) is 22.27 N, 47.94 W, and of VL2, 47.67 N, 225.71 W (Mayo et al., 1977). Three types of measurements were performed: (a) Sky brightness measurements, consisting of images of the solar-illuminated sky viewed at three visible and three infrared (IR) wavelengths. (b) Twilight rescan images, a sequence of views of an area of the sky where the sun had set or was about to rise. Each of these two methods provided estimates of the particle size and composition of atmospheric aerosol particles. (c) Sun diode images, which were views of the Sun at a wavelength of 670 nm, yielding a measurement of the atmospheric optical depth. As previously reported (Papers I and II), images were obtained at various times during the daylight hours over a period of 1-1/3 martian years.

1

The best estimate of martian aerosol properties from these measurements was of nonspherical particles with a cross section weighted mean radius of 2.5 μm, a real index of refraction of 1.5 and an imaginary index on the order of 0.004 at a wavelength of 670 nm (Papers I and II).

The purpose of this paper is twofold: to present more completely the sun diode measurements, including their method of analysis and their limitations, and to examine a fairly consistent pattern of an increase of optical depth in the morning hours (AM) over that in the afternoon hours (PM), interpreted as a diurnal variation in atmospheric condensed H_2O.

For a more general understanding of the martian environment in which these observations were made, a listing of relative parameters on Mars and their corresponding values at Earth has been made in the following table.

	MARS	EARTH	
Distance to Sun	1.52	1.00	AU
Eccentricity	0.093	0.017	
Year	687	365	Earth days
	669		sols (Mars days)
Radius	3380	6378	km
Inclination	24.8	23.5	degrees
Day	24.66	24	hr
Atmosphere	CO_2	N_2, O_2	
Surface pressure (typical)	6.1	1013	mb
Scale height	11	6	km
Water vapor (typical)	10	30000	pr μm
Atmospheric temperature (typical, at surface)	200-250	293	K

PROCEDURE

Several hundred solar images were obtained by the sun diodes on cameras on both landers. Resolution of the image is determined by the size and spacing of the pixels. A pixel covers an area of about 0.12° in diameter and the step between pixels (for the sun diode images) is 0.04°. Since the diameter of the Sun at the orbit of Mars is about 0.35°, the number of pixels within the solar disk image is about 80. By inspection, a square is chosen at the center of the image, containing 16 pixels (in some cases 9), and a computer fit to the data is made, optimizing the position of the solar center in the square to 0.008°, and allowing for the field of view of each pixel and the solar limb darkening function (Paper I). This yields a brightness and also a variance obtained by comparing the 16 (or 9) pixel measurements to the value predicted by the model. The variance is expressed as a fractional deviation (FDV).

The optical depth τ for each observation is derived from Beer's Law

$$I = I_0 e^{-\tau M(e)} r^{-2} \qquad (1)$$

2

where I is the observed intensity, $M(e)$ is the airmass, which is a function of solar elevation angle (e), and $I_0 r^{-2}$ is the intensity that would have been obtained if optical depth were zero. The units for I and I_0 are arbitrary, since it was not feasible to calibrate the sun diode in absolute units. Radius r is the Mars-Sun distance normalized to its nominal value of 1.52 AU; the factor r^{-2} is introduced to make I_0 independent of the time of year. While for most values of e, $M(e)$ is nearly equal to $1/\sin(e)$, it is necessary at low elevation angles to allow for the curvature of the atmosphere. The algorithm for calculating $M(e)$ is detailed in the Appendix. In this calculation, the maximum value of $M(e)$, occurring at $e = 0$, is $\sqrt{\pi R/(2H)}$, where R is the radius of Mars (3380 km), and H is the atmospheric scale height. The use of a fixed scale height for the aerosols is an approximation which was chosen from observations (Paper I), and it suffices here because of the relative insensitivity of $M(e)$ to H. In these calculations, H = 11 km, which for CO_2 corresponds to an atmospheric temperature of 220 K. Rayleigh optical depths can be ignored in comparison with the minimum optical depths measured in this experiment (Paper I).

I_0 DETERMINATION

The accuracy of a determination of τ from I depends on the determination of I_0. For each of the four cameras a value can be obtained from a set of two or more measurements of I at significantly different values of e, assuming that τ is invariant. Since for a given set, τ might vary unpredictably, the value of I_0 should be assigned to the average of several determinations. We refer here to the two cameras on VL1 as 11 and 12 and the two on VL2 as 21 and 22. We looked for pairs from which I_0 could be calculated and the error estimated. We excluded values of high dust storm activity and all AM (i.e., from dawn until noon) readings as less likely to represent invariant τ. On camera 12 there were 10 pairs spread over 8 sols (3 observations on one sol produced 3 pairs). On camera 21 there were 24 pairs spread over 16 sols.

Values of I_0 were determined for cameras 12 and 21 that minimized the variance of the individual pairs. The deviation of the mean was computed from these data. For cameras 11 and 22 there were insufficient eligible observations to use the above method, so we used instead pairs of observations where two cameras on the same lander observed the Sun within a period of 30 min. In this way the values of I_0 for cameras 11 and 22 were derived from the values of I_0 for cameras 12 and 21. Periods of dust storm activity were excluded for these determinations. For VL1 there were six pairs and for VL2 four pairs. The resulting values of I_0 and deviations of the means for the four cameras are given in the table.

Lander	Camera	I_0	DIZ_a	DIZ_b	DIZ
1	11	178.351	–	0.046	0.271
1	12	187.100	0.267	–	0.267
2	21	146.454	0.150	–	0.150
2	22	185.281	–	0.051	0.159

In this table, DIZ is the deviation of the mean of I_0 divided by I_0. DIZ_a is the DIZ determined by pairs of observations from the same camera. DIZ_b is the DIZ determined by pairs of nearly simultaneous observations of both cameras of the same lander. For cameras 11 and 22, DIZ is the root mean square (rms) of the relevant DIZ_a and DIZ_b.

3

ERROR DETERMINATION

There are four errors associated here with the observations. The error in I is converted to an error in $M\tau$ by obtaining the average effect of plus and minus excursions in I. This error is divided by M to obtain the error in τ.

Digitization Error, EDG

Since the measurement of brightness is digitized into a 64-bit number before being transmitted from the lander, a digitization error is associated here with the uncertainty of the exact measurement due to digitization. Here we define E1 as the expected error in DN, i.e., the rms value of a random selection of digital errors ranging from +0.5 to -0.5. Then $E1 = \sqrt{1/12} = 0.28868$, and we define

$$EDG = \frac{0.5}{M} \log \frac{DN + E1}{DN - E1} \qquad (2)$$

as the uncertainty in τ due to digitization, where M is the airmass and DN is the average 64-bit number for the measurement.

Deviation Error, EDV

Since I is the average of nine (or 16) observations, the error of the mean, FDVM, is FDV divided by the square root of the number of observations. Then

$$EDV = \frac{0.5}{M} \log \frac{1. + FDVM}{1. - FDVM} \qquad (3)$$

Vignetting Error, EV

Camera calibration showed that at elevation angles in the upper range of each camera, the brightness diminished with increasing angle. It was necessary to compensate for vignetting at the higher elevations. A typical vignetting function for a camera is shown in the following table.

Solar elevation, degrees	Relative brightness
0 to 21	1.
22	0.993
23	0.987
29	0.930
30	0.883
34	0.616
35	0.532
40	0.108
41	0.060
42	0.001

For two of the four cameras the contamination cover causing the vignetting was removed by ground command after a period of time. Thus, there was no vignetting error for Camera 11 after 0900, Sol 470, and for Camera 22 after 0848, Sol 593.

The elevation angle of the sun is known to greater accuracy than the vignetting calibration of the camera, so that interpolation is used to determine the vignetting correction. Quantities VP and VM are the vignetting corrections at an elevation angle of the correct value plus and minus 0.5°, respectively. The error EV is then taken as

$$EV = \frac{0.5}{M} \log \frac{VM}{VP} \tag{4}$$

I_0 Error, ES

The error in τ due to uncertainty in determination of I_0 uses DIZ, described above. Then the error for each measurement ES is calculated as

$$ES = \frac{0.5}{M} \log \frac{1. + DIZ}{1. - DIZ} \tag{5}$$

Total Error, ET

The total error ET is taken as the rms of the relevant errors. In this case we exclude EDG because the digitization effect is implicit in EDV. Therefore,

$$ET = \sqrt{EDV^2 + EV^2 + ES^2} \tag{6}$$

The relative significance of the errors is shown in histogram form in figures 1(a) and 1(b). There were 460 measurements using VL1 in which values of deviation and the DN were available for this study. The histogram is cumulative; i.e., the ordinate indicates the fraction of the cases in which the error is less than that indicated by the abscissa, and consequently the median occurs where the curve crosses the 0.5 level. For EDG and EDV, this is 0.006 and 0.003, respectively. For EV, 217 of the cases had no vignetting because the elevation angle of the camera was sufficiently low; the median error of the remaining cases was 0.007. For ES the median is much larger, 0.109, making the median of ET 0.1095. The average errors are similar to the medians, although the average tabulated for EV is for the total number of cases. An analogous description can be made for VL2, and the results for both landers are summarized in the Table.

		EDG	EDV	EV	ES	ET	Total number	Number for vig.
Median	VL1	0.006	0.003	0.007	0.109	0.1095	460	243
	VL2	0.005	0.003	0.010	0.058	0.060	319	142
Average	VL1	0.013	0.006	0.013	0.107	0.108	460	243
	VL2	0.009	0.006	0.010	0.058	0.060	319	142

The table suggests that an error in τ of 0.11 can be associated with VL1, and 0.06 for VL2. However, since the error is largely due to determination of DIZ, as discussed above, any condition which will reduce

ES will reduce ET nearly proportionally. Such a condition results from the determination of the difference of optical depths at two times on the same lander. For the difference $\tau_1 - \tau_2$, using the same camera, ES is given by

$$ES = 0.5 \log \frac{1. + DIZ}{1. - DIZ} F \qquad (7)$$

where $F = abs(1./M_1 - 1./M_2)$ and abs indicates the absolute value of the argument. If τ_2 is an average of several tau values, the relation still holds provided that $1./M_2$ is taken as the average reciprocal of M.

Histograms of F were made for the optical depth differences discussed later in this article, and are shown in figure 2. The error ES for the median value of F is calculated using DIZ values of 0.271 and 0.159 for VL1 and VL2, respectively (ignoring the relatively small error sometimes occurring when the same camera is not used for both measurements). The results are shown in the following table.

Lander	DIZ	Median F	Average F	Total number	ES for median
1	0.271	0.082	0.095	209	0.022
2	0.159	0.102	0.105	146	0.016

Thus to optical depth differences discussed here, we can ascribe errors on the order of 0.02 or 0.03.

THE OPTICAL DEPTHS

To review briefly here the terminology used in Viking data interpretation, lander pictures were identified by sol number and time. The sol is a mean martian day of 24 hr 39 min 35.25 sec, and the sol number of a lander picture is the number of sols elapsed since the touchdown for that lander. The time is the elapsed time from nominal midnight. The length of the solar day varies because of the eccentricity of the orbit; so that while the Sun crossed the nadir meridian at midnight on the first sol, over the course of a martian year the time of crossing varied between 17 min before midnight and 72 min after midnight. The difference between tabulated time and local solar time (EQT) is of necessity taken into account when comparing observations with model predictions. The areocentric solar longitude (Ls) denotes the time of year, with Ls = 0 indicating northern vernal equinox. Year 1 includes times from touchdown to Ls = 360. The remaining times are labelled Year 2.

In Paper I we presented optical depths measured by the lander cameras during the first 220 sols of VL1 and the first 180 sols of VL2 over the Ls range 95 to 220. In Paper 2 the data set was extended to VL1 sol 530 and VL2 sol 490, or Ls = 35, Year 2. Here we present the total set of optical depth measurements taken by the cameras. The end of the set was determined by the end of the Viking continuation mission, after which no further sun diode pictures were taken. The final sun diode pictures for VL1 were on sol 920, Ls = 235, Year 2, and for VL2 on sol 872, Ls = 232, Year 2. The total number of useful optical depth measurements and their categories are shown in the table.

Lander	Number of Observations	Number in AM	Number in PM	Number Upper Bound	Number Lower Bound
1	592	380	212	13	75
2	452	252	200	35	17

The pictures are categorized as AM or PM depending on whether the local time is before or after 1200. Generally, the upper elevation limit of the camera prevented observations at times near noon, but during some sols at VL2 in the winter season the sun was viewable by the camera during the whole day.

The complete data set of optical depths from VL1 and VL2 is plotted in figures 3(a) and 3(b). Observations where only the upper or lower bounds of the optical depth were available are so labeled, and the others are marked as AM or PM. Data from the second martian year are plotted under that of the first. Consequently from Ls of 100 to 225, covering most of the northern summer and early autumn seasons, comparisons can be made between two successive martian years. At VL1 in the period from Ls = 360 to Ls = 180, Year 2, the optical depths are fairly constant at about 0.5, with a few peaks approaching 1.0 and only a few measurements above 1.0. The first 20° of Ls can be considered to be the final decrease from the second major global dust storm shown in the first year. The modest increase at Ls = 150 to 180, Year 2, may be similar to the increase shown at Ls=150 to 180, Year 1, which was believed to be connected with the triggering of the first global dust storm (Paper II). Whether a corresponding global dust storm occurred in the second year cannot be determined from the VL1 data because of a data gap following Ls = 184. All of the later observations occurred during one sol, VL1 sol 920 at Ls = 235. There were large variations in optical depth during this sol when the optical depth was seen to vary at least between 1.40 and 2.86. The lowest value was in the late afternoon, so that condensation as well as dust may have been observed.

The data from VL2 are similar to those of VL1 in that for the first 180° of the second year the optical depths are fairly low, in this case usually around 0.4 with excursions to perhaps 0.8. As with VL1, the year begins with the final decrease from the second storm, and there is a gradual increase between Ls values 150 to 180. With VL2 the data from 180 to 230 are consistently higher than earlier, which would seem to indicate the onset of a major dust storm at the same season as the first global dust storm of the previous year. However, the lander pressure measurements of semidiurnal tide, which is indicative of global dust storms, showed the absence of a global dust storm in the second year (Leovy et al., 1985).

In figure 4, we compare optical depths at both landers in the second year. Various small peaks are seen at both locations and these can be ascribed to local dust storms of short duration. Correlation between the two sites is not evident except that the optical depth peak at Ls = 56 observed at VL1 appears to coincide with a peak at VL 2. Since the two landers are nearly 180° apart in longitude, a regional storm affecting both landers would appear to be a substantial one.

The complete set of optical depths presented here are listed in the Appendix, which also contains information on the availability of a computer file of these data.

It is also apparent from the data in both years that AM optical depths tend to be higher on the average than the PM optical depths. These differences are analyzed in the following sections as possible indications of a diurnal cycle of H_2O condensation and evaporation.

AM-PM DIFFERENCES

A set of AM-PM differences was compiled consisting of the difference between an AM reading and the average of all PM readings on that sol and the one previous. The preponderance of these differences is positive, as shown in figure 5. However, because of the great variation in individual differences it is difficult to determine from this plot the seasonal variation. Consequently, a smoothed time series was created, first by averaging all differences in the same sol, and then by constructing a running average of all observations within plus or minus 15 sols of each sol. The running average is shown in figure 6, where points are suppressed for which all the data were either before or after the central sol.

7

The smoothed data in figure 6 show few points significantly negative, and the values range from -0.1 to +0.5 optical depth units. Several peaks are found—one can identify five in the VL1 data and three for VL2. In order to understand the causes of these peaks, one must assess the condensed water in the PM, how much water vapor is available, the amount of dust in the atmosphere, and the solar energy input as a function of time of day and time of year.

THE MODEL

A one-dimensional atmospheric model is combined with a partial pressure calculation to predict condensation at the appropriate latitude as a function of the time of year and the time of day for an assumed distribution of atmospheric dust. The dust used here is the value determined by the PM optical depth measurements, with a mixing ratio independent of altitude (Paper I).

Temperature profiles

A one-dimensional radiative-convective model has been constructed to obtain temperature profiles. It is based on heating routines used in a version of the Mars General Circulation Model currently under development at Ames Research Center. In this section we briefly describe the 1-D model.

For any given latitude and season, the program marches in time through the diurnal cycle computing ground temperatures every 6.16495 minutes (1/240 of a sol) and atmospheric temperatures every half-hour. Ground temperatures are computed as in Pollack et al. (1981). The method is similar to the "force-restore" technique discussed by Deardorff (1978). Values of the surface albedo and emissivity are 0.284 and 1.0, respectively. The thermal inertia value is 264. $Jm^{-2}K^{-1}sec^{-1/2}$, corresponding to the value determined by Kieffer et al. (1976) from Viking IRTM data.

Atmospheric temperatures are calculated at the midpoint of each of the model's 49 tropospheric layers which are spaced approximately uniformly in pressure (the lower 40 layers are spaced uniformly, while the upper nine are closer together to resolve adequately the higher altitudes). The surface pressure for this model is 6.1 mb, and the pressure at the tropopause is 0.002 mb. The remainder of the atmosphere above the tropopause is lumped into a single layer, the stratosphere, that is included in the radiative parts of the calculation. The altitudes associated with the pressure levels vary considerably according to the temperature profiles. Thus, the altitude of the tropopause varies from 56 km (AM, wintertime, at VL2) to 82 km (PM, summertime, at VL1). Likewise, the thicknesses of the pressure layers vary, being on the order of 10% of the altitude at the higher altitudes, and about 0.2 km at altitudes of 0 to 2 km. The calculations proceed sequentially. First, temperatures are advanced by radiative processes alone. These processes are described below. Next, the radiatively predicted temperature profile is convectively adjusted, if necessary. The convective adjustment eliminates regions where the temperature profile becomes superadiabatic. It occurs instantaneously, and it is meant to represent the stabilizing effect of small-scale turbulence. Finally, temperatures within the continuous convective layer adjacent to the surface are changed due to the exchange of sensible heat with the surface (see Pollack et al., 1981).

The radiative processes considered by the model are the absorption of solar and infrared (IR) radiation by dust and CO_2 gas. The abundance of the dust is specified by lander data for the seasonal date of interest, and the mixing ratio is assumed constant with altitude. Solar heating in the near-infrared CO_2 bands is calculated from equivalent width formulae (Pollack et al., 1981) while that due to suspended dust is calculated from a look-up table. The table itself was created from a multiple-scattering doubling code

using optical properties deduced by Pollack et al.(1979). Because of the dominance of dust heating at solar wavelengths, we have neglected the increase in gaseous absorption by CO_2 that would result from multiple scattering by dust particles.

In the IR, we distinguish between two regions: the 15-μm band (667-1047 cm^{-1}), and everything else. Within the 15-μm band, both dust and CO_2 gas contribute to the opacity. Outside the 15-μm band dust is the only contributor. Radiative fluxes are calculated by integrating the transfer equation cast in terms of emissivities. The emissivities are calculated off-line for each constituent in each region. For CO_2, the emissivity is calculated from the band model of Pollack et al. (1981) with the temperature along all paths fixed at 200 K. For dust, the emissivity is calculated from a delta-Eddington code with a 200 K thermal emission source function. Values of the optical constants were obtained from a Mie scattering code with refractive indices appropriate for montmorillonite 219B, a material which Toon et al. (1977) found to give a reasonable fit to Mariner 9 IRIS observations. The assumed 200 K path length temperature was found by Haberle at al.(1982) to give a good fit to the Viking lander entry data. The dust emissivity varies very little over the gamut of martian atmospheric temperatures.

Within the 15-μm band, we use a combined emissivity to calculate fluxes. This combined emissivity ε_{com} is obtained from the relation

$$\varepsilon_{com} = 1 - (1 - \varepsilon_{dust})(1 - \varepsilon_{CO_2}) \tag{8}$$

where ε_{dust} is the emissivity of the dust and ε_{CO_2} is the emissivity of CO_2. Thus, we have neglected any correlation between dust continuum opacity and CO_2 lines within the 15-μm band, as well as multiple scattering effects (except in the calculation of the dust emissivity).

Estimate of Water Condensation

Using calculated temperature profiles, a simplified model is used to determine the corresponding water condensation profiles expected to occur. The required input is an estimate of the local column water vapor density, given here in units of precipitable micrometers. The assumption is also made that the mixing ratio is invariant with altitude. Then at any level denoted by the atmospheric pressure, p_{CO_2}, the water vapor pressure is given by

$$p_{H_2O} = R_M p_{CO_2} \tag{9}$$

where R_M is the volume mixing ratio.

The dewpoint temperature is related to the vapor pressure, to good approximation, by the Clausius-Clapeyron equation

$$p = A e^{-B/T} \tag{10}$$

where A and B are constants over a given temperature range. Values used here are A = 3.93519 $\times$ 10^{12} Nm^{-2} and B = 6162.56 K; they reproduce within 1% the published values of vapor pressure of ice in the temperature range 175 K to 273 K (American Institute of Physics Handbook, 1963). At each altitude, the saturation water vapor density is calculated for the temperature predicted by the model, and if this is exceeded by the amount of water vapor predicted by the assumption of a uniform mixing ratio, the excess is assumed to condense out. The condensed water overburden at a given altitude is then the integral of this excess from the top of the atmosphere down to that point.

To obtain profiles of condensed water, the derivative of the overburden profile is plotted. A smooth curve is obtained by tabulating corresponding altitude and overburden values, fitting a cubic spline to the

tabulation, and plotting the derivative of the spline. Except for small end effects the area under the curve accurately represents the tabulated overburden.

A consistent calculation would take into account the sedimentation of condensed ice and its modification of the mixing ratio as a function of altitude. This would require refinements in the model not attempted here; however, the profiles shown here are a first approximation for typical situations in which most of the water condensed at night reevaporates during the day. Hence little sedimentation is expected over such a cycle. At a later date the model may include microphysical processes for a more accurate assessment.

APPLICATION OF THE MODEL

Temperature Profiles

Using the model, we plot temperature profiles at the latitudes of each of the landers for various times of the year and various dust loadings. Since the martian pole is tilted 24° to the ecliptic, the VL1 location (latitude = 22.3N) is approximately on the northern tropic, while the VL2 location (latitude = 47.7N) is in the temperate zone. The maximum temperatures should be reached approximately at the time of the northern summer solstice (Ls = 90), but the eccentricity of the orbit with the aphelion at Ls = 71 causes the maximum to occur somewhat later than the solstice. Similarly, the minimum occurs somewhat later than the northern winter solstice Ls = 270. In figure 7, we show temperature profiles for VL1 at two times of day and two times of year, Ls = 90 and 270. The assumed dust loading is $\tau = 0.3$, where τ is the optical depth due to dust; since the level seldom dropped below $\tau = 0.3$, this is considered to be a background level.

The AM time is approximately an hour before sunrise, when temperatures are minimum, and the PM time is late afternoon, when they are at a maximum. Figure 7 shows this temperature difference and also shows the decrease of temperature with increasing altitude. It is also shown that temperatures are lower in the winter (Ls = 270, dotted lines) than in the summer (Ls = 90, solid lines). In figure 8 we show profiles for the same conditions, with the exception that the optical depth of the dust is set at $\tau = 2.0$ (a high level observed during the two major dust storms). The major difference seen in this figure in comparison with the previous one is the increased temperature difference between AM and PM profiles. Figures 9 and 10 compare profiles of two different dust loadings at the same season, Ls = 90 for figure 9 and Ls = 270 for figure 10.

The most apparent effect of the increased dust loading is that the PM upper atmospheric temperature is raised with the increased absorption of solar energy by the dust, making the profiles more isothermal. In addition, the AM-PM difference is enhanced because of the ability of the dust to radiate energy during the nighttime. The combination of these two effects generally causes the AM temperature to be higher with increased dust loading , but at some low altitudes the radiating property of the dust causes a temperature decrease. An additional contribution to this temperature decrease is seen in figure 10, where the slope of the PM $\tau = 2.0$ curve becomes decidedly more isothermal as the altitude decreases. This is believed to be due to the obscuration of solar energy by the overlying dust, decreasing the PM temperature. At the same altitude the radiating ability of the dust is still high, decreasing the AM temperature as at higher altitudes. Thus, although the addition of dust generally raises the AM temperatures, for certain altitudes and seasons it can lower them.

To the right of the curves are indicated altitude levels in kilometers corresponding to the pressure levels on the ordinate scale. For a given pressure the altitude varies both diurnally and seasonally, since it depends upon the temperature profiles. The altitudes in the figures are averages of AM and PM values; seasonal variations are shown in figures 7 and 8, and dust loading variations in figures 9 and 10.

Figures 11, 12, 13, and 14 show the corresponding profiles for VL2, at a latitude 25° higher than that of VL1. Figure 11 shows that for low dust loading, while the summer profiles for the two landers are similar, the winter temperatures at VL2 are much lower than at VL1, with the winter surface temperature determined by the sublimation of CO_2 frost. Thus at low altitudes a positive temperature gradient is observed along with an unusually small diurnal temperature swing at the surface. At the latitude of VL2, for Ls = 270 the solar elevation angle never exceeds 17.5°, so that M(e) always exceeds 3.3. The low slant path of the Sun's rays increases the effect of the dust in obscuring the Sun, and surface heating is minimized. Figure 12 shows the same differences as figure 11, but the positive temperature gradient is more pronounced in the winter profiles for these τ = 2.0 calculations. A comparison of figures 9 and 13 shows that the latitude difference of the landers seems to have little effect in the summer. However, a comparison of figures 10 and 14 indicates that while winter temperatures at both lander sites are similar at higher altitudes, the VL2 winter temperatures become much lower at lower altitudes, because of the low slant path of the Sun described above. Figure 14 shows that surface temperatures for both values of dust loading are similar, but that in the VL2 winter atmosphere at low altitudes, as the dust load is increased, both AM and PM temperatures decrease.

Water Condensation Profiles

Temperature profiles from the foregoing model are compared with profiles of dewpoint temperature in order to obtain profiles of condensed water. Figure 15 shows a set of dewpoint temperature curves for the assumed martian atmosphere. Each curve is a profile of the dewpoint temperature for a given water vapor content of the atmosphere. The curves are independent of latitude, season or time of day. These profiles can be compared with temperature profiles from the model to indicate where condensation can occur. If, for example, assuming the total content to be 10 pr μm, at any altitude where the temperature drops below the dewpoint curve for that content, condensation is predicted until a local content consistent with the lower temperature can be achieved, the excess being condensed H_2O. The curves are nearly always steeper than the temperature profiles, so that condensation tends to occur at the higher altitudes, but the large diurnal variation in surface temperature can sometimes result in AM condensation near the surface. A further discussion of this effect is given in Jakosky (1985).

In the following parametric analysis the water content is 11 pr μm, a typical value for the MAWD measurements, held constant here to illustrate the effect of other variables in the condensation process. Figures 16(a),(b) and 17(a),(b) show the condensation profiles for VL1 at two seasons, corresponding to the temperature profiles of figure 7. In both figures τ = 0.3; for figure 16, Ls = 90, while for figure 17 Ls = 270. In figure 16(a) the AM and PM temperature profiles are shown along with the dewpoint temperature curve for 11 pr μm. Figure 16(b) shows the condensed water profile. The total amount of condensed water for the AM curve is 0.58 pr μm, all of which occurs above 24 km, where the temperature curve intersects the dewpoint curve. For the PM curve the total is 0.07 pr μm, cutting off at 43 km, also shown by the temperature curves. The limitation in condensed water above 50 km is seen to be the availability of water vapor, since the temperature profiles indicate that nearly all of the water has condensed out above this altitude. While the high level haze might settle out if persisting day and night, the difference between the

11

two curves should represent the AM-PM difference, i.e., the water condensing at night and evaporating in the afternoon. The bulk is seen to lie between 25 and 40 km altitude.

In figure 17(a), the PM temperature curve intersects the dewpoint curve at 25 km with the corresponding water profile shown in figure 17(b). For the AM case, however, the temperature curve shows an intersection at 11 km and a second one at a low altitude. Correspondingly in figure 17(b) a low-lying layer is found containing 14% of the total overburden. (The total overburden in the AM is 2.15 pr μm, of which the amount above 10 km is 1.85 pr μm, while the total overburden in the PM is 0.41 pr μm.) The low layer is confined to the bottom two model pressure layers, i.e., below 0.48 km. The maximum density is 1.3 pr μm /km, occurring at the surface and in the figure indicated by a tick mark on the horizontal axis. The low-altitude component is a frequent but not universal component of condensation plots, being caused by the generally wide temperature swing of the surface in comparison to the atmosphere.

In figure 18 the AM and PM temperature profiles are shown for Ls = 90, τ = 2.0, along with the dewpoint temperature curve. It is seen that for both times of day, for the assumed amount of water vapor, no condensation will occur. Figure 19(a) shows profiles for Ls = 270, for the same value of τ. A small amount of AM condensation is predicted at all altitudes, evaporating in the afternoon. The condensation profile is shown in figure 19(b), the total amount of condensed water being 4.1 pr μm, with 7% in the lowest 0.48 km.

Figures 20-23 show the corresponding water condensation at the latitude of VL2. Figures 20(a) and 20(b) show that for Ls = 90 and τ = 0.3, the condensation is similar to that shown for VL1, but because of the higher summer temperatures the total is less (0.28 pr μm in AM, 0.05 pr μm in PM). Figures 21(a) and 21(b) show that for Ls = 270 and τ = 0.3, temperatures are so low that essentially all of the water is expected to be condensed, with no measurable AM-PM difference. Figure 22 predicts no condensation for Ls = 90 and τ = 2.0, because the dust has heated the atmosphere above the dewpoint temperature. Figures 23(a) and 23(b), along with Figures 21(a) and 21(b), show that at Ls = 270 essentially total AM and PM condensation is predicted for both dust loading values. It is apparent that the assumed water vapor content of 11 pr μm is too large for the latitude of VL2 in the winter season.

In summary, figure 24 shows expected condensation over the course of a year at the latitude of VL1 for a water vapor content of 11 pr μm, at two different values of τ. For a dust load of τ = 0.3, AM condensation is always present, minimizing at approximately Ls = 135 and maximizing somewhat later than Ls = 270. The curve is not symmetrical around Ls = 270 because of the eccentricity of the Mars orbit. The PM condensation is negligible in comparison. For τ = 2.0, the AM condensation is nearly zero, except at Ls = 270 where it surpasses that for τ = 0.3. Figure 25 shows the expected condensation at the latitude of VL2. The AM condensation for τ = 0.3 surpasses that of τ = 2.0 in the summer but not in the winter. At Ls = 270, at both values of τ, the AM-PM difference is negligible because condensation is nearly complete throughout the day. Before and after Ls = 270, the AM-PM difference for τ = 2.0 is greater than for τ = 0.3, for reasons discussed earlier, while near the summer solstice the AM-PM difference is greater for τ = 0.3. This summary of model predictions over the course of a Mars year is useful in evaluating the measurements presented in the following section.

APPLICATION OF THE MODEL TO LANDER MEASUREMENTS

Peaks in the lander measurements of AM-PM differences shown in figure 6 can in most cases be predicted by the model, using the values of latitude, season, dust and water vapor associated with the peaks. In order to assign an appropriate value of water vapor, estimates are obtained from the MAWD on

the orbiters (Jakosky and Farmer, 1982). Data used here are averages of the measurements in a time period of 15° of Ls, in a region of dimensions 10° in latitude and longitude, encompassing the location of the appropriate lander. The water vapor averages used here are shown in figure 26. Since the measurements were made at various times of day they can only approximate the level of water vapor at the time of the AM and PM measurements. Linear interpolation was used for intermediate values of Ls. For VL1 it was assumed that the level did not drop below 11 pr μm, and the averages in the Ls range 280-360 were raised where necessary to reach this level. This period was in the midst of the global dust storm when the dust level may have prevented the instrument from detecting all of the vapor deep in the atmosphere. For VL2, measurements were not available near Ls = 270, and interpolated values have been plotted. Probably the water vapor content was much lower, since the model predicts low temperatures throughout the day, as discussed in the previous section.

Comparisons between measured AM-PM differences and model predictions are shown in the following two figures. It is simplest to begin the comparison with VL2. Figure 27 shows three peaks in the record of VL2 measured differences, at Ls values of 217 and 355, Year 1, and 145, Year 2. The peak at 217 coincides with the peak of the first dust storm (see fig. 3(b)). The dust level is high at this point and drops off gradually. The seasonal factor contributing to this peak was shown in figure 25 where Ls = 217 is seen to lie between the season where AM and PM condensation are both low and the season where temperatures are apparently too cold to support appreciable water vapor. At Ls = 180 and 225, figure 25 shows that the AM-PM difference increases with dust level. Thus both the season and the high dust level contribute to this peak.

The peak at Ls = 355 is also predicted by the model, for the same reasons ascribed to the previous peak: a high dust level and a time of year favoring a large diurnal variation in condensation.

The peak at Ls = 145, Year 2, also predicted by the model, is attributable to a large increase in water vapor content as measured by MAWD and shown in figure 26.

Profiles of the condensed water were calculated for these peaks. For peaks at Ls = 217 and 355 they show condensation occurring at all altitudes, with nearly all of the water condensed in the AM. The AM-PM difference also occurs at all altitudes. For the peak at Ls = 145, Year 2, approximately 8% of the condensation is predicted to be ground fog and the rest to be above 20 km altitude, with only 10% of the condensation remaining in the PM.

Figure 28 shows five peaks in the record of VL1 AM-PM differences, at Ls values of 212 and 312, Year 1, and 33, 95 and 131, Year 2. The peak at 312 corresponds to a model peak at Ls = 290, when a measurement of AM-PM difference was not available. As shown earlier in figure 24, AM condensation tends to peak at Ls = 270 at VL1, when temperatures are coldest, and PM condensation is negligible. The model also predicts enhanced condensation for larger values of optical depth, and figure 3(a) shows this period to be at the height of the second global dust storm. Thus the dust load and the season are both factors contributing to this peak.

The observed peak at Ls = 131, Year 2, occurs when the dust load is fairly low, in late summer, and the model shows a corresponding peak due to high water vapor content measured by the MAWD experiment.

The other three peaks in AM-PM difference for Lander 1 do not have an obvious explanation provided by the model. The peak at Ls = 212, Year 1, may not be significant because it is based on only a few measurements, as shown in figure 3(a). It is comprised of a difference at Ls = 206 in which two AM readings on sol 208 are compared to two PM readings the previous afternoon, and a second difference at Ls = 215, during the height of the first dust storm, comparing four AM readings with one PM reading, all on sol 222. Likewise, the peak at Ls = 33, Year 2, is due to one AM reading of 1.38 at

Ls = 33 on sol 528, compared to one PM reading on the previous afternoon and followed by a two sol data gap. The third peak in this category at Ls = 95, Year 2, appears to occur over several mornings, but is not predicted by the MAWD observations of water vapor, which peak at an earlier time, or by the PM optical depth observations, which are higher at this point. In this season a larger dust loading should decrease the condensation predicted by the model.

Thus, three of the VL2 peaks and two of the VL1 peaks are predicted by the model, while three more peaks at VL1 are not explained by the limited observations available.

Profiles for VL1 peaks show water condensation occurring only above altitudes of 12-28 km. Less than 15% of the available water vapor is condensed, and more than 85% of the condensed water evaporates in the PM.

The record of lander optical depths includes certain sols in which there were more than two optical depth measurements. In these cases, the observed time at which condensation or evaporation commences compares favorably with model predictions. One such case is shown in figure 29, which plots predicted condensation vs time over a 24 hr period, for Sol 420 of VL2. Also shown in the figure are the optical depths measured during this sol. It is seen that the predicted maximum of condensation is 1.2 pr μm at a time of about 0700, while the measured optical depth peaks broadly at about $\tau = 0.89$ at a local Sun time of 0810. The remaining three observations for this sol appear to support the model prediction of a steady drop toward a minimum at 1700.

Using simplified assumptions about the particles, one can compare a change in optical depth with a corresponding change in condensed water, W, thereby estimating a column number of particles n and a mean particle radius r. Here we assume scattering efficiency to be 2.0 and the particles to be spherical. Then in a column of unit area (1 m^2), the volume V of condensed water is

$$V = 4\pi r^3 n/3 \tag{11}$$

and

$$W = 4 \times 10^6 \pi r^3 n/3 \tag{12}$$

where the units of W are pr μm. The optical depth τ is given by

$$\tau = 2\pi r^2 n \tag{13}$$

so that the radius in micrometers r_μ is given by

$$r_\mu = 1.5 W/\tau \tag{14}$$

Thus, for Sol 420 of VL2, if the optical depth difference of 0.37 is ascribed to the condensation difference of 1.1 pr μm, the condensed water column can be described as a collection of particles of radius 4.5 μm with a density of 2.9 $\times$ 10^5 particles per cm^2. The example is not necessarily representative of the sols in which condensation is observed.

Jaquin et al.(1986) have analyzed images of the martian limb observed by the Viking orbiters and from them have derived profiles of aerosol extinction. Often a detached haze is observed at altitudes of tens of km with reflectance properties similar to water ice, as compared to reflectance properties of the lower layer more like that of dust. In one case they show a detached haze at 50-60 km in the AM which is not observed in the PM, and also an AM increase as the altitude drops to the lowest value. They report many observations of aerosols at 50-80 km altitude. These observations seem to correspond in a general sense to profiles predicted here.

14

SUMMARY OF RESULTS

Viking lander camera observations have produced 1044 measurements of optical depth spread over 1-1/3 martian years at various times of day. The comparison of afternoon and morning observations, when smoothed by a running average, shows that the optical depth in the morning is larger than that in the afternoon, and that this AM-PM difference in optical depth reaches peaks at various seasonal dates. These peaks were simulated using a model of the martian atmosphere that computes the radiation balance to produce a temperature profile, along with a calculation that determines the dewpoint temperature for a given water vapor profile. From this calculation, estimates of AM and PM water condensation, and their differences, were plotted over the time period of the lander observations, and correlations were found with a majority of the optical depth peaks. It is consequently apparent that diurnal variations in water vapor condensation have been observed at the two lander sites, and that changes over time of these variations can be explained by the amount of water vapor, the amount of atmospheric dust and the seasonal variations in solar energy input. This correspondence has been highlighted by certain martian days in which a series of optical depth measurements has been compared with the model predictions for the same times. In this comparison, the time of optical depth reduction appears to correlate with the predicted time of the evaporation of morning fog. Thus the Viking lander observations of optical depth and the model computations of condensed water are in substantial agreement.

APPENDIX A

Calculation of Airmass

This section shows the expression used for the calculation of the airmass factor, and its derivation. We postulate that the optical depth is caused by a substance of density ρ with scale height H, so that

$$\rho = \rho_0 e^{-\alpha z} \tag{A1}$$

where ρ_0 is the density at the surface, z is the altitude, and $\alpha = 1/H$.

The extinction E is given by

$$E = K \int_0^\infty \rho_0 e^{-\alpha z} \, ds \tag{A2}$$

where s is the slant path of the optical beam and K is the absorption per unit length per unit density.

The airmass M is the ratio of the extinction along the slant path to the extinction along the vertical, so that

$$M = K \int_0^\infty \rho_0 e^{-\alpha z} \, ds \bigg/ K \int_0^\infty \rho_0 e^{-\alpha z} \, dz \tag{A3}$$

or, simplifying,

$$M = \alpha \int_0^\infty e^{-\alpha z} \, ds \tag{A4}$$

Figure 30 shows the relation of slant height s to altitude z for a planet of radius r, when the solar zenith angle is θ. From the law of cosines,

$$r^2 + 2rz + z^2 = r^2 + s^2 + 2rs \cos \theta \tag{A5}$$

Solving for ds/dz,

$$s = -r \cos \theta + \sqrt{r^2 \cos^2 \theta + 2rz + z^2} \tag{A6}$$

$$\frac{ds}{dz} = (r + z)(r^2 \cos^2 \theta + 2rz + z^2)^{-1/2} \tag{A7}$$

$$\left(\frac{ds}{dz}\right)^{-2} = \frac{(r + z)^2 - r^2 \sin^2 \theta}{(r + z)^2} \approx 1 - \sin^2 \theta \left(1 - 2\frac{z}{r}\right) \tag{A8}$$

$$\left(\frac{ds}{dz}\right)^{-2} \approx (r^2 \cot^2 \theta + 2rz)\frac{\sin^2 \theta}{r^2} \tag{A9}$$

Combining equations 4 and 9,

$$M \approx \alpha \int_0^\infty e^{-\alpha z} \frac{r \, dz}{\sin \theta \sqrt{r^2 \cot^2 \theta + 2rz}} \tag{A10}$$

But from Abramowitz and Segun (1968)

$$\int_0^\infty \frac{e^{-at} \, dt}{\sqrt{t + w^2}} = \sqrt{\frac{\pi}{a}} e^{aw^2} \text{erfc}(w\sqrt{a}) \tag{A11}$$

where the complementary error function, erfc, is defined by

$$\text{erfc}(x) = 1 - \text{erf}(x) = \frac{2}{\sqrt{\pi}} \int_0^\infty e^{-t^2} \, dt \tag{A12}$$

Combining equations 10 and 11,

$$M \approx \frac{\sqrt{.5 r \alpha \pi}}{\sin \theta} \exp(.5 r \alpha \cot^2 \theta) \operatorname{erfc}(\sqrt{.5 r \alpha} \cot \theta) \tag{A13}$$

Numerical integration tests have shown equation 13 to be more accurate than a previous expression in which $\sin \theta$ is replaced by unity and $\cot \theta$ by $\cos \theta$; however, for the martian radius and scale height the maximum improvement is a mere 0.3%.

Values of erfc are generally available in computer libraries, but for large values of the argument the following expansion is used (Abramowitz and Segun, 1968):

$$\sqrt{\pi} u e^{u^2} \operatorname{erfc}(u) = 1 + \sum_{m=1}^{\infty} (-1)^m \frac{(1)(3) \cdots (2m-1)}{(2u^2)^m} \tag{A14}$$

or

$$M \approx \frac{1}{\cos \theta} \left[1 + \sum_{m=1}^{\infty} (-1)^m \frac{(1)(3) \cdots (2m-1)}{(2u^2)^m} \right] \tag{A15}$$

where

$$u^2 = .5 r \alpha \cot^2 \theta \tag{A16}$$

It is thus apparent that for $\theta = 0$, $M = 1$, and for $\theta = 90$, $M = \sqrt{.5 r \alpha \pi}$.

APPENDIX B

OPTICAL DEPTH MEASUREMENTS

This appendix contains the complete set of optical depths obtained from the two Viking landers from touchdown until the sun diodes were no longer monitored. The camera column indicates both the lander and the camera – 11 and 12 representing cameras 1 and 2 of VL1, and 21 and 22 representing cameras 1 and 2 of VL2. The sol is the martian day measured from touchdown, the time is local lander time in hours and minutes, and tau is the measured atmospheric optical depth. The sol, time, and tau entries are offset: observations made before noon (AM) are on the left and those after noon (PM) are on the right. The parameter K is normally 0; if K = 1, the measurement is a lower bound, and if K = 2, an upper bound. This information is repeated in the limitation tag column. The day column is the fractional 1976 day number; for example, 1.5 would represent noon, January 1, Universal Time. The solar longitude LS indicates the season, with LS = 0 representing northern vernal equinox. When values in this column are greater than 360, the viking year number is year 2 and the LS values should be treated modulo 360. The error columns EDG, EDV, EV, ES, and ETOT are described in the text.

This data set has been made available as a computer file on the Prototype Atmospheres Node Data Access System, at the University of Colorado. The file can be accessed by contacting

> Dr. Steven Lee
> University of Colorado
> Laboratory for Atmospheric and Space Physics
> Campus Box 392
> Boulder CO 80309

Dr Lee's telephone number is 303-492-5348, and the computer address on the SPAN network is ORION::LEE.

VL1

VIKING OPTICAL DEPTH MEASUREMENTS
DAY IS 1976 DAY NUMBER.
LS IS LONG OF SUN RELATIVE TO N, VERNAL EQUINOX.
LIMITATION TAG IDENTIFIES LOWER AND UPPER BOUND ESTIMATES, DEFINED BY COLUMN K.
ERROR EDG IS DIGITIZATION ERROR.
ERROR EDV IS ERROR COMPUTED FROM DEVIATION.
ERROR EV IS ERROR DUE TO VIGNETTING CORRECTION.
ERROR ES IS ERROR ESTIMATED FROM USE OF IZERO.
ERROR ETOT IS ROOT SUM OF SQUARES OF ABOVE ERRORS. EXCEPT DIGITIZATION.

CAM	SOL	TIME	TAU	K	DAY	LS	LIMITATION TAG	EDG	EDV	EV	ES	ETOT
11	6	1754	0.503	0	208.751	99.701		0.011	0.009	0.000	0.083	0.084
11	7	706	0.660	0	209.316	99.948		0.015	0.032	0.000	0.098	0.103
11	12	1736	0.518	0	214.903	102.395		0.003	0.000	0.001	0.098	0.098
11	12	1823	0.515	0	214.936	102.410		0.004	0.000	0.000	0.054	0.054
11	12	1847	0.485	0	214.953	102.418		0.012	0.000	0.000	0.032	0.032
11	12	1858	0.435	0	214.961	102.421		0.026	0.000	0.000	0.023	0.023
11	13	535	0.399	1	215.416	102.621	LOWER BOUND	0.040	0.001	0.000	0.019	0.019
11	13	547	0.605	1	215.424	102.625	LOWER BOUND	0.065	0.002	0.000	0.031	0.031
11	13	611	0.550	0	215.441	102.633		0.006	0.000	0.000	0.050	0.050
11	13	659	0.647	0	215.476	102.648		0.004	0.000	0.000	0.096	0.096
12	28	1806	0.525	0	231.364	109.749		0.002	0.000	0.000	0.066	0.066
11	29	554	0.457	0	231.869	109.978		0.002	0.000	0.000	0.035	0.035
11	29	621	0.513	0	231.888	109.987		0.002	0.000	0.000	0.060	0.060
11	29	721	0.582	0	231.931	110.006		0.003	0.000	0.001	0.117	0.117
12	41	1719	0.429	0	244.688	115.857		0.004	0.000	0.001	0.106	0.106
12	41	1751	0.413	0	244.711	115.867		0.002	0.001	0.000	0.076	0.076
12	101	1715	0.360	0	306.334	145.922		0.003	0.001	0.001	0.090	0.090
12	101	1741	0.350	0	306.353	145.932		-1.000	0.000	0.000	0.000	-1.000
12	115	1659	0.645	0	320.708	153.360		0.007	0.002	0.000	0.100	0.100
12	115	1752	0.581	0	320.746	153.380		0.007	0.003	0.000	0.048	0.048
12	155	1644	0.753	0	361.797	175.513		0.010	0.003	0.000	0.095	0.095
12	155	1731	0.742	0	361.830	175.531		0.039	0.002	0.000	0.048	0.048
12	168	1739	0.753	1	375.193	183.021	LOWER BOUND	0.077	0.001	0.000	0.035	0.035
11	169	621	0.906	1	375.737	183.329	LOWER BOUND	0.083	0.001	0.000	0.039	0.039
11	169	709	1.010	0	375.771	183.348		0.026	0.009	0.000	0.087	0.087
11	169	814	1.050	0	375.818	183.374		0.014	0.005	0.015	0.148	0.149
12	174	1639	0.803	0	381.316	186.576		0.012	0.004	0.001	0.091	0.091
12	174	1726	0.959	0	381.349	186.595		-1.000	0.000	0.000	0.000	-1.000
11	175	632	0.981	1	381.910	186.919	LOWER BOUND	0.101	0.001	0.000	0.047	0.047
11	175	722	0.961	0	381.946	186.940		0.018	0.006	0.000	0.097	0.097
12	183	1635	1.110	0	390.560	191.942		0.015	0.001	0.001	0.090	0.090
12	183	1720	1.210	1	390.592	191.961	LOWER BOUND	0.101	0.001	0.000	0.046	0.046
11	185	636	1.130	0	392.188	192.892		0.057	0.000	0.000	0.047	0.047
11	185	721	1.300	0	392.220	192.911		0.027	0.009	0.000	0.092	0.092
12	207	1624	0.873	0	415.212	206.493		0.007	0.003	0.001	0.091	0.091
12	207	1644	0.862	0	415.226	206.501		0.005	0.002	0.000	0.073	0.073
11	208	722	0.947	0	415.853	206.876		0.006	0.002	0.000	0.079	0.079
11	208	805	0.911	0	415.884	206.894		0.006	0.001	0.001	0.119	0.119
12	209	1536	1.260	0	417.233	207.701		0.013	0.001	0.021	0.133	0.135
12	209	1626	1.380	0	417.269	207.722		0.018	0.001	0.000	0.089	0.089
11	210	742	2.470	1	417.922	208.114	LOWER BOUND	0.210	0.002	0.000	0.096	0.096
11	210	822	3.060	1	417.951	208.131	LOWER BOUND	0.289	0.003	0.001	0.131	0.131
11	210	854	3.130	1	417.973	208.145	LOWER BOUND	0.346	0.003	0.025	0.157	0.160
12	211	1537	1.840	0	419.289	208.933		0.043	0.003	0.019	0.132	0.133
12	211	1554	1.890	0	419.301	208.940		0.059	0.001	0.004	0.117	0.117
12	211	1632	2.060	0	419.328	208.956		0.265	0.044	0.000	0.083	0.094
12	222	816	2.600	0	430.276	215.557		0.162	0.001	0.000	0.116	0.116

CAM	SOL	TIME	TAU	K	DAY	LS	LIMITATION TAG	EDG	EDV	EV	ES	ETOT
12	222	849	2.690	0	430.300	215.571		0.079	0.003	0.010	0.142	0.142
12	222	906	2.630	0	430.312	215.579		0.063	0.018	0.024	0.154	0.157
11	222	909	2.730	0	430.314	215.580		0.075	0.116	0.026	0.159	0.199
11	222	1526	2.490	0	430.583	215.743		0.082	0.034	0.022	0.139	0.144
12	222	1616	2.260	1	430.619	215.765	LOWER BOUND	0.211	0.002	0.001	0.095	0.095
12	239	1536	1.980	0	448.058	226.425		0.031	0.003	0.011	0.124	0.125
12	239	1608	1.970	0	448.080	226.439		0.037	0.024	0.000	0.098	0.101
12	240	834	2.000	0	448.784	226.873		0.019	0.012	0.000	0.116	0.117
12	240	851	2.020	0	448.796	226.880		0.026	0.007	0.002	0.130	0.130
11	240	855	2.010	0	448.799	226.882		0.025	0.017	0.001	0.134	0.135
12	240	921	1.970	0	448.817	226.893		0.019	0.005	0.021	0.151	0.152
11	246	831	2.000	0	454.947	230.684		0.050	0.001	0.000	0.110	0.110
11	248	837	2.000	0	457.006	231.963		0.046	0.034	0.000	0.113	0.118
11	251	833	1.830	0	460.086	233.880		0.036	0.023	0.000	0.107	0.110
11	252	834	1.820	0	461.114	234.521		0.037	0.031	0.000	0.107	0.111
11	254	829	1.790	0	463.165	235.802		0.040	0.028	0.000	0.101	0.105
11	256	829	1.840	0	465.220	237.087		0.050	0.029	0.000	0.099	0.104
11	257	831	1.680	0	466.249	237.732		0.031	0.009	0.000	0.100	0.100
12	258	841	1.670	0	467.284	238.381		0.012	0.005	0.000	0.106	0.106
11	258	906	1.700	0	467.302	238.392		0.016	0.001	0.000	0.127	0.127
11	258	947	1.700	0	467.331	238.410		0.012	0.011	0.022	0.154	0.156
12	258	1519	1.590	0	467.568	238.559		0.012	0.004	0.020	0.135	0.137
12	258	1549	1.620	0	467.589	238.572		0.016	0.003	0.001	0.114	0.114
12	258	1619	1.590	0	467.611	238.586		0.017	0.006	0.000	0.090	0.090
11	259	831	1.570	0	468.304	239.021		0.024	0.001	0.000	0.099	0.099
11	262	833	1.670	0	471.388	240.961		0.032	0.016	0.000	0.098	0.099
11	263	833	1.630	0	472.416	241.608		0.031	0.001	0.000	0.097	0.097
11	264	934	1.660	0	473.487	242.284		0.011	0.010	0.008	0.141	0.142
11	265	934	1.590	0	474.514	242.932		0.010	0.007	0.007	0.141	0.141
11	266	934	1.600	0	475.542	243.581		0.010	0.005	0.006	0.140	0.141
11	267	935	1.590	0	476.570	244.232		0.010	0.003	0.001	0.140	0.140
11	268	935	1.480	0	477.597	244.882		0.008	0.008	0.009	0.139	0.140
11	270	936	1.510	0	479.653	246.185		0.009	0.007	0.001	0.138	0.138
11	272	937	1.350	0	481.709	247.491		0.006	0.005	0.001	0.137	0.137
11	274	938	1.340	0	483.764	248.799		0.006	0.002	0.002	0.136	0.136
11	275	904	1.370	0	484.768	249.438		0.007	0.007	0.002	0.135	0.135
11	277	905	1.360	0	486.823	250.750		0.005	0.004	0.000	0.110	0.110
11	279	920	1.390	0	488.889	252.071		0.006	0.005	0.000	0.108	0.109
11	280	920	1.390	0	489.916	252.728		0.005	0.007	0.000	0.119	0.119
11	282	901	1.340	0	491.958	254.037		0.006	0.002	0.000	0.103	0.103
11	283	901	1.300	0	492.985	254.697		0.005	0.002	0.000	0.102	0.102
11	288	903	1.180	0	498.124	258.005		0.004	0.001	0.000	0.101	0.101
12	288	1623	1.140	0	498.438	258.207		0.004	0.001	0.000	0.093	0.093
11	289	904	1.160	0	499.152	258.668		0.004	0.006	0.000	0.101	0.101
12	289	1554	1.170	0	499.445	258.857		0.005	0.002	0.001	0.122	0.122
12	290	934	1.280	0	500.201	259.346		0.006	0.002	0.000	0.120	0.120
11	291	905	1.290	0	501.208	260.334		0.005	0.003	0.000	0.100	0.100
11	292	905	1.240	0	502.236	260.997		0.005	0.002	0.000	0.100	0.100
11	293	905	1.260	0	503.263	261.659		0.005	0.015	0.000	0.099	0.100
11	294	906	1.320	0	504.291	262.321		0.006	0.003	0.000	0.099	0.099
11	295	906	1.420	0	505.319	262.982		0.008	0.003	0.000	0.098	0.099
11	297	907	1.240	0	507.374	264.300		0.005	0.001	0.000	0.098	0.098
12	297	1617	1.130	0	507.681	264.497		0.003	0.002	0.000	0.101	0.101
11	298	908	1.300	0	508.403	264.958		0.006	0.002	0.000	0.098	0.098
11	299	908	1.410	0	509.430	265.615		0.008	0.000	0.000	0.097	0.097
11	300	908	1.190	0	510.458	266.271		0.005	0.001	0.000	0.096	0.096
12	301	804	1.120	1	511.439	266.897	LOWER BOUND	0.095	0.001	0.000	0.042	0.042
12	301	839	1.160	0	511.464	266.913		0.018	0.009	0.000	0.071	0.072
12	301	904	1.190	0	511.482	266.925		-1.000	0.000	0.000	0.000	-1.000
12	301	934	1.160	0	511.504	266.938		-1.000	0.000	0.000	0.000	-1.000

CAM	SOL	TIME	TAU	K	DAY	LS	LIMITATION TAG	EDG	EDV	EV	ES	ETOT
12 301		1004	1.150	0	511.525	266.952		-1.000	0.000	0.000	0.000	-1.000
12 301		1034	1.130	0	511.547	266.966		0.008	0.002	0.022	0.150	0.152
12 301		1109	1.150	0	511.571	266.981		0.013	0.007	0.056	0.167	0.176
12 301		1134	1.080	0	511.589	266.993		0.025	0.006	0.125	0.175	0.215
12	301	1209	1.450	0	511.614	267.009		0.187	0.000	-1.000	0.183	-1.000
12	301	1404	1.190	0	511.696	267.061		0.083	0.002	0.212	0.175	0.275
12	301	1439	1.120	0	511.721	267.077		0.020	0.004	0.089	0.162	0.185
12	301	1504	1.150	0	511.739	267.088		0.013	0.000	0.041	0.150	0.156
12	301	1534	1.160	0	511.761	267.102		0.005	0.003	0.017	0.133	0.134
12	301	1604	1.200	0	511.782	267.116		0.006	0.002	0.001	0.113	0.113
12	301	1634	1.220	0	511.803	267.129		0.010	0.003	0.000	0.091	0.091
12	301	1709	1.230	0	511.828	267.145		0.021	0.002	0.000	0.063	0.063
12	301	1734	1.100	1	511.846	267.156	LOWER BOUND	0.094	0.001	0.000	0.042	0.042
12 302		804	1.180	0	512.467	267.552		0.193	0.000	0.000	0.042	0.042
12 302		839	1.300	0	512.492	267.568		0.031	0.002	0.000	0.071	0.071
12 303		805	1.330	0	513.495	268.206		-1.000	0.000	0.000	0.000	-1.000
12 303		840	1.130	0	513.520	268.221		0.017	0.001	0.000	0.071	0.071
11 303		910	1.110	0	513.542	268.235		0.004	0.004	0.000	0.096	0.096
12 304		805	1.090	1	514.523	268.858	LOWER BOUND	0.092	0.001	0.000	0.041	0.041
12 304		845	1.190	0	514.551	268.876		0.017	0.002	0.000	0.074	0.074
12	304	1625	1.150	0	514.879	269.085		0.013	0.008	0.000	0.099	0.100
11 305		915	1.140	0	515.600	269.542		0.007	0.003	0.000	0.099	0.099
11 306		916	1.090	0	516.628	270.193		0.006	0.003	0.000	0.099	0.099
11 307		916	1.060	0	517.656	270.843		0.006	0.002	0.000	0.098	0.098
11 308		917	1.060	0	518.684	271.492		0.006	0.004	0.000	0.098	0.098
11 309		917	1.220	0	519.711	272.140		0.009	0.003	0.000	0.098	0.098
11 310		917	1.210	0	520.739	272.788		0.009	0.004	0.000	0.097	0.097
11 311		918	1.320	0	521.767	273.435		0.012	0.003	0.000	0.098	0.098
11 312		923	1.620	0	522.798	274.082		0.025	0.008	0.000	0.101	0.101
11 313		924	1.880	0	523.826	274.727		0.052	0.026	0.000	0.101	0.105
11 314		924	2.370	1	524.854	275.371	LOWER BOUND	0.222	0.002	0.000	0.101	0.101
11 315		925	2.370	1	525.882	276.015	LOWER BOUND	0.222	0.002	0.000	0.101	0.101
11 316		925	2.370	1	526.910	276.657	LOWER BOUND	0.222	0.002	0.000	0.101	0.101
12	316	1635	2.100	1	527.216	276.848	LOWER BOUND	0.220	0.002	0.001	0.099	0.099
11 317		925	2.360	1	527.937	277.298	LOWER BOUND	0.221	0.002	0.000	0.101	0.101
11 318		926	2.360	1	528.965	277.939	LOWER BOUND	0.221	0.002	0.000	0.101	0.101
11 319		931	2.450	1	529.996	278.580	LOWER BOUND	0.230	0.002	0.000	0.105	0.105
11 320		932	2.450	1	531.025	279.219	LOWER BOUND	0.230	0.002	0.000	0.105	0.105
11 321		932	2.450	1	532.052	279.857	LOWER BOUND	0.230	0.002	0.000	0.105	0.105
11 321		1126	3.440	1	532.133	279.907	LOWER BOUND	0.377	0.003	0.070	0.171	0.185
11 321		1132	3.370	1	532.138	279.910	LOWER BOUND	0.382	0.003	0.087	0.174	0.194
11 322		932	2.440	1	533.080	280.494	LOWER BOUND	0.229	0.002	0.000	0.104	0.104
11 323		933	2.450	1	534.108	281.130	LOWER BOUND	0.230	0.002	0.000	0.105	0.105
11	323	1638	2.690	1	534.411	281.318	LOWER BOUND	0.224	0.002	0.000	0.102	0.102
11 324		858	2.360	1	535.110	281.750	LOWER BOUND	0.168	0.002	0.001	0.077	0.077
12	324	1638	1.990	1	535.439	281.952	LOWER BOUND	0.225	0.002	0.000	0.101	0.101
11 325		934	2.700	1	536.163	282.400	LOWER BOUND	0.230	0.002	0.000	0.105	0.105
11 326		934	2.420	1	537.191	283.033	LOWER BOUND	0.229	0.002	0.001	0.104	0.104
11 327		934	3.060	1	538.218	283.666	LOWER BOUND	0.229	0.002	0.001	0.104	0.104
11 328		955	2.700	1	539.261	284.306	LOWER BOUND	0.262	0.003	0.000	0.119	0.119
11 328		1035	3.350	1	539.289	284.324	LOWER BOUND	0.320	0.003	0.014	0.145	0.146
11 328		1155	2.540	1	539.347	284.359	LOWER BOUND	0.399	0.004	0.168	0.181	0.247
11	328	1500	2.670	1	539.479	284.440	LOWER BOUND	0.365	0.003	0.101	0.166	0.194
12	328	1610	2.930	1	539.529	284.471	LOWER BOUND	0.277	0.003	0.010	0.124	0.124
12	328	1650	2.480	1	539.557	284.488	LOWER BOUND	0.212	0.002	0.001	0.095	0.095
11 329		935	2.690	1	540.274	284.928	LOWER BOUND	0.230	0.002	0.000	0.104	0.104
11 330		936	2.690	1	541.302	285.559	LOWER BOUND	0.230	0.002	0.000	0.104	0.104
11 331		936	2.690	1	542.330	286.188	LOWER BOUND	0.230	0.002	0.000	0.104	0.104
11 333		942	2.790	1	544.389	287.445	LOWER BOUND	0.238	0.002	0.000	0.108	0.108
11 337		944	2.800	1	548.500	289.946	LOWER BOUND	0.239	0.003	0.000	0.109	0.109

CAM	SOL	TIME	TAU	K	DAY	LS	LIMITATION TAG	EDG	EDV	EV	ES	ETOT
11 338		944	2.800	1	549.528	290.569	LOWER BOUND	0.239	0.003	0.000	0.109	0.109
11 339		944	2.820	1	550.555	291.191	LOWER BOUND	0.240	0.003	0.000	0.109	0.109
11 340		945	2.830	1	551.584	291.813	LOWER BOUND	0.241	0.003	0.000	0.110	0.110
12	340	1650	2.710	1	551.887	291.996	LOWER BOUND	0.232	0.002	0.000	0.104	0.104
11 341		945	2.830	1	552.611	292.433	LOWER BOUND	0.241	0.003	0.000	0.110	0.110
11 342		946	2.840	1	553.639	293.053	LOWER BOUND	0.242	0.003	0.000	0.110	0.110
12 343		1001	3.140	1	554.678	293.678	LOWER BOUND	0.266	0.003	0.001	0.119	0.119
12 343		1111	3.930	1	554.728	293.708	LOWER BOUND	0.362	0.003	0.044	0.162	0.168
12	343	1546	3.580	1	554.924	293.826	LOWER BOUND	0.333	0.003	0.042	0.149	0.155
12	343	1636	3.020	1	554.959	293.847	LOWER BOUND	0.259	0.003	0.001	0.116	0.116
12	343	1726	2.010	1	554.995	293.869	LOWER BOUND	0.171	0.002	0.000	0.077	0.077
12 344		912	2.100	1	555.670	294.274	LOWER BOUND	0.181	0.002	0.000	0.081	0.081
12 344		1001	3.150	1	555.705	294.295	LOWER BOUND	0.267	0.003	0.001	0.120	0.120
11 345		952	2.950	1	556.726	294.908	LOWER BOUND	0.251	0.003	0.001	0.114	0.114
11 346		952	2.960	1	557.754	295.524	LOWER BOUND	0.252	0.003	0.001	0.115	0.115
11 347		953	2.970	1	558.782	296.140	LOWER BOUND	0.253	0.003	0.001	0.115	0.115
11 348		954	2.980	1	559.810	296.754	LOWER BOUND	0.254	0.003	0.001	0.116	0.116
11 349		954	2.980	1	560.838	297.367	LOWER BOUND	0.254	0.003	0.001	0.116	0.116
12	350	1609	3.190	0	562.133	298.139		0.156	0.006	0.023	0.139	0.141
11 351		959	3.090	1	562.896	298.593	LOWER BOUND	0.264	0.003	0.002	0.120	0.120
11 352		1000	3.110	1	563.924	299.204	LOWER BOUND	0.265	0.003	0.002	0.121	0.121
11 353		1030	3.550	0	564.973	299.827		0.258	0.059	0.010	0.142	0.154
11 354		1031	3.400	0	566.001	300.436		0.179	0.007	0.010	0.143	0.143
11 355		1036	3.710	0	567.032	301.046		0.321	0.252	0.014	0.146	0.291
11 356		1036	3.430	0	568.060	301.653		0.169	0.000	0.015	0.147	0.147
11 357		1037	3.560	0	569.088	302.260		0.218	0.007	0.015	0.147	0.148
11 358		1037	3.230	0	570.116	302.865		0.112	0.037	0.016	0.147	0.153
11 359		1038	3.170	0	571.144	303.470		0.098	0.040	0.016	0.148	0.154
11 364		1045	2.950	0	576.286	306.483		0.061	0.055	0.022	0.153	0.165
11 365		1045	2.760	0	577.314	307.082		0.043	0.007	0.023	0.154	0.156
11 366		1045	2.750	0	578.341	307.680		0.042	0.008	0.023	0.154	0.156
12	366	1615	2.520	0	578.577	307.817		0.042	0.011	0.038	0.146	0.152
11 367		1036	2.690	0	579.362	308.274		0.039	0.004	0.017	0.148	0.149
11 368		1036	2.570	0	580.390	308.871		0.031	0.027	0.017	0.149	0.152
11 369		1037	2.600	0	581.418	309.467		0.033	0.008	0.018	0.150	0.151
11 370		1037	2.460	0	582.446	310.062		0.025	0.009	0.019	0.150	0.152
11 371		1038	2.340	0	583.474	310.656		0.020	0.008	0.019	0.151	0.152
11 372		1043	2.350	0	584.505	311.251		0.020	0.008	0.023	0.154	0.156
12	372	1643	2.150	0	584.762	311.399		0.021	0.006	0.017	0.131	0.132
11 373		1043	2.280	0	585.532	311.844		0.018	0.006	0.024	0.155	0.157
12	373	1638	2.100	0	585.786	311.989		0.019	0.007	0.021	0.135	0.136
11 374		1044	2.250	0	586.560	312.435		0.017	0.017	0.025	0.156	0.159
11 375		1044	2.190	0	587.588	313.026		0.015	0.018	0.025	0.157	0.160
11 376		1035	2.980	0	588.609	313.612		0.065	0.035	0.019	0.151	0.156
12	376	1640	1.990	0	588.869	313.761		0.015	0.005	0.021	0.135	0.137
11 377		1044	2.130	0	589.643	314.204		0.014	0.007	0.026	0.157	0.160
11 378		1046	2.070	0	590.672	314.793		0.013	0.005	0.028	0.159	0.161
12	378	1636	1.900	0	590.922	314.936		0.013	0.004	0.027	0.140	0.142
11 379		1046	2.050	0	591.699	315.380		0.012	0.005	0.029	0.159	0.162
11 380		1046	1.920	0	592.727	315.966		0.010	0.009	0.030	0.160	0.163
11 382		1052	1.810	0	594.786	317.138		0.009	0.004	0.041	0.165	0.170
11 384		1052	1.660	0	596.841	318.305		0.007	0.011	0.043	0.166	0.172
11 385		1053	1.710	0	597.869	318.887		0.008	0.014	0.045	0.166	0.173
12	386	1629	1.400	0	599.137	319.603		0.006	0.002	0.048	0.150	0.157
12	389	1630	1.380	0	602.220	321.341		0.006	0.002	0.052	0.151	0.160
12	390	1645	1.420	0	603.258	321.924		0.005	0.002	0.029	0.140	0.143
11 393		947	1.410	0	606.042	323.484		0.009	0.007	0.001	0.120	0.120
11 393		1022	1.430	0	606.067	323.498		0.007	0.004	0.015	0.148	0.149
11 394		947	1.430	0	607.070	324.058		0.010	0.004	0.001	0.120	0.121
11 395		1023	1.420	0	608.123	324.645		0.007	0.005	0.017	0.149	0.150

CAM	SOL	TIME	TAU		K	DAY	LS	LIMITATION TAG	EDG	EDV	EV	ES	ETOT
11	396	948	1.270		0	609.125	325.203		0.007	0.003	0.001	0.122	0.122
11	396	1023	1.270		0	609.150	325.217		0.005	0.003	0.018	0.150	0.151
11	397	938	1.360		0	610.146	325.771		0.009	0.005	0.000	0.114	0.114
11	397	1013	1.360		0	610.171	325.785		0.006	0.005	0.010	0.143	0.144
11	398	939	1.360		0	611.174	326.342		0.009	0.012	0.001	0.115	0.116
11	398	1014	1.370		0	611.199	326.355		0.013	0.004	0.011	0.144	0.145
11	399	939	1.260		0	612.201	326.911		0.007	0.004	0.001	0.116	0.116
11	399	1014	1.270		0	612.226	326.925		0.010	0.005	0.012	0.145	0.146
11	400	940	1.270		0	613.230	327.480		0.007	0.004	0.001	0.117	0.117
11	400	1015	1.320		0	613.255	327.494		0.011	0.004	0.013	0.146	0.146
11	401	920	1.340		0	614.243	328.040		0.012	0.003	0.000	0.100	0.100
11	401	1015	1.330		0	614.282	328.062		0.012	0.003	0.014	0.147	0.147
11	402	920	1.760		0	615.270	328.607		0.038	0.024	0.000	0.101	0.104
11	402	1015	1.710		0	615.310	328.629		0.024	0.007	0.015	0.148	0.148
12	402	1700		1.310	0	615.599	328.788		0.015	0.004	0.022	0.135	0.136
12	402	1730		1.250	0	615.620	328.800		0.007	0.002	0.001	0.109	0.109
11	403	926	1.190		0	616.302	329.176		0.007	0.002	0.000	0.106	0.106
11	403	1016	1.190		0	616.338	329.196		0.009	0.002	0.016	0.148	0.149
11	404	926	1.300		0	617.330	329.741		0.009	0.005	0.000	0.107	0.107
11	404	1016	1.290		0	617.365	329.761		0.011	0.006	0.017	0.149	0.150
11	405	927	1.260		0	618.358	330.306		0.008	0.002	0.000	0.108	0.108
11	405	1017	1.280		0	618.393	330.326		0.011	0.005	0.018	0.150	0.151
11	406	927	1.230		0	619.385	330.870		0.007	0.003	0.000	0.109	0.109
11	406	1002	1.230		0	619.410	330.883		0.010	0.003	0.002	0.139	0.139
11	407	927	1.300		0	620.413	331.432		0.009	0.003	0.000	0.110	0.110
11	407	1007	1.310		0	620.441	331.448		0.011	0.004	0.011	0.144	0.144
11	408	848	1.380		0	621.412	331.979		0.042	0.000	0.000	0.073	0.073
11	408	913	1.320		0	621.430	331.989		0.013	0.008	0.000	0.097	0.097
11	408	933	1.330		0	621.444	331.996		0.008	0.007	0.001	0.115	0.115
11	408	1008	1.350		0	621.469	332.010		0.012	0.005	0.012	0.145	0.145
12	408	1653		1.250	0	621.758	332.168		0.015	0.006	0.036	0.143	0.148
12	408	1723		1.260	0	621.780	332.179		0.013	0.003	0.008	0.119	0.119
12	408	1758		1.290	0	621.805	332.193		0.014	0.004	0.000	0.087	0.087
12	409	933	1.630		0	622.472	332.557		0.016	0.004	0.001	0.114	0.114
12	409	1008	1.510		0	622.497	332.571		0.016	0.006	0.013	0.143	0.144
11	410	934	1.130		0	623.500	333.118		0.005	0.003	0.001	0.117	0.117
12	410	1719		1.110	0	623.832	333.298		0.009	0.002	0.012	0.123	0.124
11	411	934	1.670		0	624.528	333.677		0.018	0.006	0.001	0.118	0.118
11	412	935	1.060		0	625.556	334.235		0.004	0.003	0.001	0.119	0.119
11	412	1010	1.070		0	625.581	334.249		0.007	0.002	0.015	0.148	0.149
11	413	940	1.410		0	626.587	334.795		0.009	0.004	0.001	0.124	0.124
11	414	940	1.330		0	627.614	335.351		0.007	0.002	0.001	0.125	0.125
12	414	1715		1.220	0	627.939	335.527		0.006	0.002	0.016	0.128	0.129
12	416	1711		0.950	0	629.991	336.635		0.003	0.001	0.021	0.133	0.134
11	418	942	1.010		0	631.726	337.570		0.003	0.002	0.001	0.128	0.128
12	418	1707		0.893	0	632.043	337.740		0.003	0.001	0.025	0.137	0.139
11	419	947	1.050		0	632.757	338.124		0.004	0.008	0.001	0.134	0.134
12	419	1707		1.030	0	633.071	338.292		0.004	0.003	0.025	0.137	0.139
11	420	908	1.250		0	633.757	338.660		0.010	0.003	0.000	0.098	0.098
12	420	1738		1.150	0	634.120	338.855		0.006	0.002	0.001	0.111	0.111
11	421	908	1.250		0	634.784	339.211		0.010	0.007	0.000	0.099	0.099
12	421	1738		1.190	0	635.148	339.405		0.006	0.005	0.001	0.111	0.111
11	422	914	1.200		0	635.816	339.762		0.008	0.007	0.000	0.105	0.105
12	422	1734		1.100	0	636.173	339.953		0.005	0.003	0.003	0.115	0.115
12	423	1734		1.240	0	637.200	340.501		0.006	0.003	0.003	0.115	0.115
11	424	914	1.610		0	637.871	340.859		0.021	0.006	0.000	0.107	0.107
11	425	915	1.500		0	638.899	341.406		0.015	0.005	0.000	0.108	0.108
11	426	920	1.580		0	639.930	341.954		0.016	0.003	0.000	0.113	0.114
12	426	1730		0.930	0	640.280	342.140		0.003	0.001	0.009	0.119	0.120
11	427	921	0.930		0	640.958	342.500		0.003	0.001	0.000	0.114	0.115

CAM	SOL	TIME	TAU	K	DAY	LS	LIMITATION TAG	EDG	EDV	EV	ES	ETOT
11	428	921	0.981	0	641.986	343.044		0.004	0.001	0.001	0.116	0.116
12	428	1741	1.060	0	642.343	343.233		0.005	0.002	0.001	0.110	0.110
11	429	922	1.080	0	643.014	343.588		0.005	0.003	0.001	0.117	0.117
12	429	1742	1.130	0	643.371	343.777		0.006	0.002	0.001	0.110	0.110
12	430	1737	0.986	0	644.395	344.317		0.004	0.002	0.002	0.114	0.114
11	431	922	1.120	0	645.069	344.672		0.005	0.004	0.001	0.119	0.119
11	432	928	1.190	0	646.101	345.215		0.005	0.002	0.001	0.124	0.124
11	433	928	0.926	0	647.128	345.755		0.003	0.003	0.000	0.125	0.125
12	433	1733	0.837	2	647.474	345.937	UPPER BOUND	0.002	0.002	0.008	0.118	0.119
11	434	929	0.935	0	648.156	346.295		0.003	0.002	0.000	0.126	0.126
11	435	929	0.949	2	649.184	346.833	UPPER BOUND	0.003	0.002	0.001	0.127	0.127
11	437	935	0.947	2	651.243	347.909	UPPER BOUND	0.003	0.002	0.001	0.134	0.134
12	439	1741	0.815	0	653.645	349.160		0.005	0.002	0.001	0.113	0.113
12	440	846	0.924	0	654.291	349.495		0.004	0.001	0.011	0.088	0.089
12	440	911	0.946	0	654.309	349.505		0.006	0.002	0.000	0.112	0.112
12	440	1746	0.841	0	654.676	349.695		0.005	0.002	0.001	0.108	0.108
12	442	852	0.990	0	656.350	350.563		0.005	0.002	0.000	0.095	0.095
12	442	912	1.010	0	656.364	350.570		0.007	0.003	0.001	0.114	0.114
12	442	1737	0.908	0	656.725	350.756		0.006	0.003	0.008	0.118	0.118
12	443	912	0.915	0	657.392	351.101		0.006	0.002	0.001	0.115	0.115
12	445	838	1.510	0	659.422	352.149		0.034	0.014	0.000	0.084	0.085
12	446	858	0.891	0	660.464	352.685		0.003	0.001	0.000	0.103	0.103
12	446	1809	1.010	0	660.857	352.887		0.006	0.003	0.000	0.088	0.088
12	447	859	0.974	0	661.492	353.213		0.004	0.002	0.000	0.105	0.105
12	448	904	0.805	2	662.523	353.742	UPPER BOUND	0.002	0.002	0.000	0.111	0.111
12	449	900	0.895	0	663.548	354.266		0.003	0.003	0.000	0.107	0.107
12	453	1716	0.745	0	668.012	356.541		0.005	0.003	0.029	0.138	0.141
12	453	1756	0.806	0	668.040	356.556		0.005	0.003	0.000	0.101	0.101
12	454	907	0.886	0	668.691	356.886		0.005	0.002	0.001	0.117	0.117
12	454	932	0.872	0	668.708	356.895		0.005	0.003	0.008	0.140	0.140
12	455	912	0.911	0	669.722	357.408		0.005	0.003	0.001	0.123	0.123
12	457	1743	0.775	0	672.141	358.631		-1.000	0.000	0.000	0.000	-1.000
12	458	919	0.835	0	672.809	358.968		-1.000	0.000	0.000	0.000	-1.000
12	466	907	0.740	0	681.020	3.078		0.004	0.002	0.001	0.125	0.125
12	466	1722	0.663	0	681.374	3.253		0.004	0.002	0.023	0.134	0.136
12	467	907	0.647	0	682.048	3.588		0.003	0.001	0.001	0.126	0.126
12	467	1722	0.588	0	682.401	3.763		0.004	0.001	0.023	0.134	0.136
12	468	908	0.877	0	683.076	4.098		0.005	0.003	0.001	0.127	0.128
12	469	913	0.934	0	684.107	4.608		0.005	0.002	0.001	0.133	0.133
12	469	1803	0.911	0	684.485	4.795		0.008	0.002	0.001	0.096	0.096
12	470	807	0.821	0	685.088	5.093		0.005	0.001	0.000	0.070	0.070
11	470	809	0.779	0	685.089	5.093		0.004	0.011	0.000	0.072	0.073
12	470	833	0.816	0	685.106	5.102		0.006	0.003	0.000	0.096	0.096
11	470	835	0.812	0	685.108	5.102		0.006	0.002	0.000	0.098	0.098
12	470	918	0.852	0	685.138	5.118		0.004	0.002	0.006	0.139	0.139
11	470	920	0.866	0	685.140	5.118		0.004	0.003	0.009	0.143	0.143
12	470	958	0.844	0	685.167	5.132		0.010	0.005	0.075	0.173	0.189
11	470	1803	0.886	0	685.513	5.302		0.007	0.002	0.001	0.097	0.097
11	471	859	0.938	0	686.152	5.618		0.006	0.004	0.001	0.123	0.123
11	472	904	0.862	0	687.183	6.125		0.005	0.002	0.001	0.129	0.129
11	472	1759	0.879	0	687.565	6.313		0.006	0.001	0.000	0.101	0.101
11	473	905	0.867	0	688.211	6.631		0.005	0.003	0.001	0.130	0.130
11	473	1800	0.800	0	688.593	6.818		0.005	0.003	0.000	0.101	0.101
11	474	800	0.720	0	689.193	7.112		0.004	0.002	0.000	0.066	0.066
11	474	905	0.751	0	689.239	7.135		0.004	0.003	0.001	0.131	0.131
11	474	1755	0.689	0	689.617	7.320		0.004	0.010	0.001	0.106	0.106
11	474	1845	0.694	0	689.653	7.338		0.005	0.002	0.000	0.055	0.055
11	475	906	0.717	0	690.267	7.639		0.003	0.001	0.001	0.132	0.132
11	476	911	0.712	0	691.298	8.143		0.003	0.001	0.001	0.138	0.138
11	476	1751	0.681	0	691.669	8.324		0.003	0.002	0.001	0.110	0.110

CAM	SOL	TIME	TAU	K	DAY	LS	LIMITATION TAG	EDG	EDV	EV	ES	ETOT
11	477	911	0.709	0	692.326	8.645		0.003	0.001	0.002	0.139	0.139
11	477	1751	0.624	0	692.697	8.826		0.003	0.002	0.001	0.109	0.109
11	478	912	0.626	0	693.354	9.146		0.003	0.001	0.004	0.140	0.140
11	481	828	0.635	0	696.405	10.627		0.003	0.002	0.000	0.100	0.100
11	481	1828	0.665	0	696.833	10.835		0.003	0.002	0.000	0.072	0.072
11	482	833	0.605	0	697.436	11.126		0.003	0.002	0.000	0.106	0.106
11	482	1828	0.646	0	697.861	11.332		0.002	0.001	0.000	0.072	0.072
11	483	834	0.655	0	698.464	11.623		0.003	0.001	0.000	0.107	0.107
11	483	1824	0.687	0	698.885	11.826		0.003	0.002	0.000	0.076	0.076
11	484	834	0.625	0	699.492	12.119		0.003	0.002	0.000	0.108	0.108
11	484	1824	0.607	0	699.913	12.321		0.002	0.001	0.000	0.076	0.076
11	485	835	0.633	0	700.520	12.614		0.003	0.002	0.000	0.109	0.109
11	485	1820	0.771	0	700.937	12.814		0.003	0.002	0.000	0.080	0.080
11	486	835	0.711	0	701.547	13.107		0.004	0.001	0.000	0.110	0.110
11	486	1815	0.661	0	701.961	13.306		0.002	0.002	0.000	0.085	0.085
11	487	835	0.626	0	702.575	13.600		0.003	0.002	0.000	0.112	0.112
11	487	1815	0.609	2	702.989	13.799	UPPER BOUND	0.002	0.001	0.000	0.084	0.084
11	488	841	0.583	0	703.607	14.094		0.003	0.002	0.001	0.117	0.117
11	489	1811	0.579	0	705.041	14.780		0.003	0.001	0.000	0.089	0.089
11	490	737	1.280	1	705.616	15.054	LOWER BOUND	0.114	0.003	0.000	0.054	0.054
11	490	802	0.622	0	705.634	15.063		0.002	0.002	0.000	0.080	0.080
11	490	827	0.632	0	705.652	15.071		0.003	0.001	0.000	0.105	0.105
11	490	1807	0.613	0	706.066	15.268		0.003	0.002	0.001	0.093	0.093
11	490	1842	0.608	0	706.090	15.280		0.003	0.001	0.000	0.058	0.058
11	491	827	0.563	0	706.679	15.560		0.003	0.001	0.000	0.106	0.106
11	491	1807	0.592	0	707.093	15.757		0.003	0.001	0.001	0.093	0.093
11	494	828	0.613	0	709.762	17.024		0.003	0.001	0.000	0.109	0.109
11	494	1758	0.595	0	710.169	17.216		0.003	0.002	0.000	0.102	0.102
11	500	841	0.589	0	715.937	19.930		0.003	0.002	0.000	0.125	0.125
11	501	841	0.524	0	716.964	20.411		0.002	0.002	0.000	0.126	0.127
11	502	847	0.567	0	717.996	20.893		0.002	0.001	0.001	0.132	0.132
11	502	1742	0.624	0	718.378	21.071		0.003	0.001	0.007	0.118	0.118
11	503	842	0.625	0	719.020	21.370		0.003	0.002	0.001	0.129	0.129
11	503	1742	0.583	0	719.405	21.550		0.003	0.002	0.007	0.117	0.117
11	505	848	0.628	0	721.079	22.327		0.003	0.002	0.001	0.135	0.135
11	505	1733	0.575	0	721.454	22.501		0.002	0.001	0.015	0.126	0.127
11	506	843	0.653	0	722.103	22.802		0.003	0.002	0.001	0.132	0.132
11	506	1728	0.596	0	722.478	22.976		0.003	0.002	0.019	0.130	0.132
11	508	849	0.665	0	724.162	23.754		0.003	0.002	0.002	0.139	0.139
11	508	1729	0.638	0	724.533	23.925		0.003	0.001	0.015	0.129	0.130
11	509	850	0.650	0	725.190	24.228		0.003	0.001	0.004	0.140	0.140
11	509	1730	0.582	0	725.561	24.399		0.003	0.001	0.017	0.129	0.130
11	510	855	0.623	2	726.221	24.703	UPPER BOUND	0.003	0.002	0.012	0.145	0.146
11	510	1725	0.577	0	726.585	24.870		0.002	0.002	0.021	0.133	0.135
12	511	730	0.582	0	727.188	25.147		0.002	0.001	0.000	0.062	0.062
11	511	800	0.608	0	727.210	25.157		0.003	0.001	0.000	0.093	0.093
11	511	855	0.635	0	727.249	25.175		0.003	0.001	0.013	0.146	0.147
11	511	920	0.715	2	727.267	25.183	UPPER BOUND	0.003	0.003	0.048	0.169	0.175
11	511	1720	0.610	0	727.609	25.340		0.003	0.002	0.026	0.137	0.140
11	511	1835	0.606	0	727.663	25.364		0.003	0.001	0.000	0.063	0.063
11	513	856	0.631	0	729.305	26.116		0.003	0.003	0.015	0.148	0.149
11	513	1716	0.592	0	729.661	26.279		0.003	0.002	0.033	0.141	0.145
11	515	902	0.739	0	731.364	27.056		0.003	0.001	0.023	0.155	0.156
11	515	1712	0.640	0	731.714	27.215		0.003	0.002	0.040	0.145	0.150
11	516	902	0.659	2	732.391	27.523	UPPER BOUND	0.003	0.003	0.024	0.156	0.157
11	518	903	0.823	0	734.447	28.456		0.004	0.003	0.025	0.158	0.160
11	518	1758	0.681	0	734.829	28.629		0.004	0.002	0.000	0.100	0.100
11	521	819	0.584	0	737.498	29.834		0.003	0.001	0.001	0.118	0.118
11	521	1744	0.561	0	737.901	30.016		0.003	0.001	0.001	0.113	0.113
11	523	830	0.742	0	739.561	30.762		0.004	0.002	0.001	0.130	0.130

CAM	SOL	TIME	TAU	K	DAY	LS	LIMITATION TAG	EDG	EDV	EV	ES	ETOT
11	523	1740	0.568	0	739.953	30.938		0.003	0.003	0.006	0.117	0.117
11	525	821	0.597	0	741.610	31.679		0.003	0.003	0.001	0.122	0.122
11	525	1736	0.581	0	742.006	31.856		0.003	0.001	0.010	0.121	0.121
11	526	702	0.531	0	742.581	32.113		0.004	0.002	0.000	0.044	0.044
11	526	827	0.622	0	742.641	32.140		0.003	0.002	0.001	0.128	0.128
11	526	1737	0.551	0	743.034	32.315		0.002	0.002	0.010	0.120	0.120
11	527	832	0.648	0	743.672	32.595		0.003	0.003	0.001	0.134	0.134
11	527	1737	0.534	0	744.061	32.766		0.002	0.001	0.009	0.120	0.120
11	528	802	1.380	0	744.678	33.037		0.022	0.014	0.000	0.106	0.107
11	530	803	0.733	0	746.734	33.939		0.004	0.002	0.000	0.108	0.108
11	530	1729	0.636	0	747.138	34.117		0.003	0.002	0.017	0.128	0.129
11	532	809	0.656	0	748.793	34.844		0.003	0.002	0.001	0.115	0.115
11	532	1729	0.611	0	749.193	35.019		0.003	0.001	0.016	0.127	0.128
11	535	811	0.626	0	751.877	36.198		0.003	0.002	0.001	0.118	0.118
11	535	1721	0.579	0	752.270	36.371		0.002	0.001	0.022	0.134	0.136
11	537	817	0.607	0	753.937	37.104		0.003	0.002	0.000	0.124	0.124
11	539	817	0.554	0	755.992	38.007		0.002	0.002	0.001	0.126	0.126
11	539	1802	0.516	0	756.409	38.191		0.002	0.002	0.001	0.093	0.093
11	540	823	0.654	0	757.023	38.461		0.003	0.004	0.001	0.132	0.132
11	542	719	0.524	0	759.033	39.345		0.002	0.002	0.000	0.070	0.070
12	542	748	0.542	0	759.053	39.354		0.003	0.002	0.000	0.098	0.098
11	542	823	0.573	0	759.078	39.365		0.002	0.001	0.001	0.134	0.134
11	542	1749	0.513	0	759.482	39.542		0.002	0.001	0.001	0.107	0.107
11	543	824	0.523	0	760.107	39.817		0.002	0.002	0.001	0.135	0.135
11	544	659	0.431	0	761.073	40.242		0.001	0.001	0.000	0.052	0.052
11	544	1744	0.477	0	761.534	40.445		0.002	0.000	0.001	0.110	0.110
11	546	700	0.444	0	763.129	41.147		0.001	0.001	0.000	0.054	0.054
11	546	1740	0.495	0	763.586	41.348		0.002	0.000	0.003	0.114	0.114
11	548	706	0.548	0	765.188	42.054		0.004	0.002	0.000	0.061	0.061
11	548	1736	0.510	0	765.638	42.252		0.002	0.001	0.008	0.118	0.118
11	553	708	0.565	0	770.327	44.318		0.004	0.002	0.000	0.066	0.066
11	553	1728	0.557	0	770.770	44.513		0.002	0.001	0.014	0.125	0.126
11	554	708	0.590	0	771.355	44.770		0.004	0.001	0.000	0.067	0.067
11	554	1729	0.520	0	771.798	44.966		-1.000	0.000	0.000	0.000	-1.000
11	555	714	0.627	0	772.386	45.225		0.004	0.001	0.000	0.073	0.073
11	557	1819	0.643	0	774.916	46.340		0.005	0.020	0.000	0.074	0.077
11	558	645	0.633	0	775.448	46.575		0.006	0.010	0.000	0.047	0.048
11	560	651	0.627	0	777.508	47.484		0.004	0.014	0.000	0.053	0.055
11	560	1821	0.590	0	778.000	47.701		0.004	0.020	0.000	0.072	0.075
11	562	652	0.718	0	779.563	48.391		0.006	0.021	0.000	0.055	0.059
11	562	1817	0.678	0	780.052	48.606		0.005	0.019	0.000	0.076	0.078
11	564	653	0.674	0	781.619	49.298		0.004	0.005	0.000	0.057	0.057
11	564	1813	0.614	0	782.104	49.512		0.004	0.002	0.000	0.080	0.080
11	567	654	0.582	0	784.702	50.659		0.003	0.001	0.000	0.060	0.060
11	567	1809	0.667	0	785.184	50.872		0.004	0.004	0.000	0.083	0.083
11	570	1805	0.707	0	788.263	52.232		0.005	0.002	0.000	0.087	0.087
11	571	656	0.667	0	788.813	52.476		0.003	0.003	0.000	0.063	0.063
11	572	701	0.702	0	789.845	52.931		0.006	0.004	0.000	0.069	0.069
11	572	1826	0.694	0	790.333	53.147		0.007	0.002	0.000	0.066	0.066
11	574	702	0.700	0	791.900	53.840		0.006	0.004	0.000	0.071	0.071
11	574	1827	0.683	0	792.389	54.056		0.007	0.002	0.000	0.065	0.065
11	577	703	0.875	0	794.983	55.203		0.011	0.002	0.000	0.073	0.073
11	577	1828	0.854	0	795.472	55.420		0.015	0.003	0.000	0.063	0.063
12	579	704	0.850	0	797.039	56.113		0.010	0.006	0.000	0.074	0.074
11	579	705	0.841	0	797.040	56.113		0.009	0.004	0.000	0.076	0.077
12	579	1809	0.897	0	797.514	56.323		0.010	0.002	0.000	0.080	0.080
11	579	1811	0.905	0	797.515	56.323		0.010	0.004	0.000	0.080	0.080
11	580	704	0.905	0	798.067	56.568		0.012	0.002	0.000	0.076	0.076
11	583	1811	0.865	0	801.625	58.143		0.009	0.003	0.000	0.080	0.080
11	584	711	0.811	0	802.182	58.389		0.007	0.003	0.000	0.084	0.084

CAM	SOL	TIME	TAU	K	DAY	LS	LIMITATION TAG	EDG	EDV	EV	ES	ETOT
11	585	1801	0.751	0	803.673	59.050		0.005	0.001	0.000	0.088	0.088
11	586	642	0.746	0	804.216	59.290		0.006	0.006	0.000	0.057	0.057
11	586	1802	0.708	0	804.701	59.505		0.005	0.002	0.000	0.088	0.088
11	587	617	0.585	0	805.226	59.737		0.011	0.008	0.000	0.034	0.035
11	587	642	0.629	0	805.243	59.745		0.003	0.004	0.000	0.058	0.058
11	587	722	0.675	0	805.272	59.758		0.004	0.001	0.000	0.096	0.096
11	587	827	0.705	0	805.318	59.778		0.006	0.002	0.025	0.157	0.159
11	587	1717	0.791	0	805.696	59.946		0.008	0.002	0.019	0.130	0.131
11	587	1807	0.765	0	805.732	59.962		0.006	0.002	0.000	0.082	0.082
11	587	1902	0.723	1	805.771	59.979	LOWER BOUND	0.064	0.001	0.000	0.031	0.031
11	589	643	0.709	0	807.299	60.656		0.005	0.005	0.000	0.059	0.059
11	589	1758	0.716	0	807.781	60.870		0.005	0.003	0.001	0.091	0.091
11	591	644	0.690	0	809.355	61.567		0.004	0.003	0.000	0.061	0.061
11	591	1753	0.658	0	809.832	61.779		0.004	0.001	0.001	0.095	0.095
11	593	1755	0.657	0	811.888	62.691		0.004	0.002	0.001	0.094	0.094
11	594	651	0.631	0	812.442	62.936		0.006	0.001	0.000	0.064	0.064
11	595	1755	0.647	0	813.943	63.602		0.004	0.002	0.001	0.093	0.093
11	596	651	0.596	0	814.497	63.848		0.004	0.001	0.000	0.069	0.069
11	597	651	0.641	0	815.525	64.304		0.005	0.002	0.000	0.070	0.070
11	597	1746	0.669	0	815.992	64.511		0.007	0.002	0.000	0.101	0.101
11	600	628	0.779	0	818.591	65.664		0.007	0.005	0.000	0.058	0.058
11	600	1817	0.648	0	819.097	65.889		0.005	0.002	0.000	0.071	0.071
11	602	628	0.638	0	820.646	66.577		0.005	0.005	0.000	0.050	0.051
11	602	1813	0.629	0	821.149	66.800		0.004	0.002	0.000	0.075	0.075
11	605	630	0.639	0	823.730	67.947		0.004	0.004	0.000	0.052	0.053
11	605	1810	0.589	0	824.229	68.168		0.004	0.001	0.000	0.078	0.078
11	611	1832	0.569	0	830.410	70.916		0.003	0.001	0.000	0.056	0.056
11	612	607	0.899	1	830.906	71.136	LOWER BOUND	0.073	0.001	0.000	0.035	0.035
11	612	1832	0.530	0	831.437	71.373		0.002	0.001	0.000	0.055	0.055
11	615	609	0.485	0	833.990	72.508		0.002	0.003	0.000	0.037	0.037
11	615	1834	0.553	0	834.521	72.745		0.003	0.001	0.000	0.054	0.054
11	619	605	0.902	1	838.097	74.336	LOWER BOUND	0.073	0.001	0.000	0.035	0.035
11	619	615	0.578	0	838.104	74.339		0.005	0.003	0.000	0.044	0.044
11	619	645	0.705	0	838.125	74.349		0.003	0.003	0.000	0.072	0.072
11	619	740	0.711	0	838.164	74.366		0.003	0.002	0.000	0.124	0.124
11	619	827	0.680	0	838.198	74.381		0.006	0.002	0.042	0.165	0.170
11	619	1830	0.524	0	838.628	74.573		0.002	0.001	0.000	0.057	0.057
11	621	606	0.489	0	840.152	75.251		0.002	0.004	0.000	0.036	0.036
11	621	1831	0.548	0	840.684	75.488		0.002	0.001	0.000	0.056	0.056
11	627	614	0.510	0	846.323	78.001		0.003	0.002	0.000	0.044	0.044
11	627	1819	0.563	0	846.840	78.232		0.002	0.001	0.000	0.067	0.067
11	639	619	0.564	0	858.656	83.504		0.003	0.002	0.000	0.051	0.051
11	639	1819	0.572	0	859.170	83.733		0.002	0.000	0.000	0.065	0.065
11	642	610	1.030	1	861.733	84.878	LOWER BOUND	0.092	0.001	0.000	0.044	0.044
11	645	611	1.180	1	864.816	86.256	LOWER BOUND	0.096	0.001	0.000	0.046	0.046
11	645	1841	0.544	0	865.351	86.495		0.004	0.001	0.000	0.044	0.044
11	647	1842	0.547	0	867.407	87.414		0.004	0.001	0.000	0.043	0.043
11	648	1837	0.604	0	868.430	87.872		0.005	0.002	0.000	0.047	0.047
11	649	613	0.578	0	868.927	88.094		0.004	0.002	0.000	0.048	0.048
11	649	1838	0.560	0	869.459	88.332		0.004	0.001	0.000	0.046	0.046
11	650	1838	0.526	0	870.486	88.792		0.003	0.001	0.000	0.046	0.046
11	651	614	0.692	0	870.983	89.014		0.007	0.005	0.000	0.049	0.049
11	651	1643	0.655	0	871.432	89.215		-1.000	0.000	0.000	0.000	-1.000
11	652	549	0.713	1	871.992	89.466	LOWER BOUND	0.058	0.001	0.000	0.028	0.028
11	652	614	0.662	0	872.010	89.474		0.006	0.005	0.000	0.049	0.050
11	652	644	0.729	0	872.032	89.483		0.006	0.002	0.000	0.077	0.077
11	652	719	0.749	0	872.057	89.494		0.008	0.003	0.000	0.110	0.110
11	652	754	0.763	0	872.082	89.506		0.007	0.002	0.011	0.142	0.143
12	652	1709	0.487	0	872.478	89.683		0.006	0.002	0.018	0.127	0.128
11	652	1839	0.488	0	872.542	89.712		-1.000	0.000	0.000	0.000	-1.000

CAM	SOL	TIME	TAU	K	DAY	LS	LIMITATION TAG	EDG	EDV	EV	ES	ETOT
11	660	619	0.841	0	880.234	93.156		-1.000	0.000	0.000	0.000	-1.000
12	660	1705	0.692	0	880.695	93.362		-1.000	0.000	0.000	0.000	-1.000
11	666	619	0.690	0	886.399	95.919		-1.000	0.000	0.000	0.000	-1.000
12	666	1706	0.685	0	886.860	96.126		-1.000	0.000	0.000	0.000	-1.000
11	672	625	0.859	0	892.568	98.687		-1.000	0.000	0.000	0.000	-1.000
12	672	1706	0.704	0	893.025	98.893		-1.000	0.000	0.000	0.000	-1.000
11	678	625	0.797	0	898.733	101.456		-1.000	0.000	0.000	0.000	-1.000
12	678	1720	0.588	0	899.200	101.666		-1.000	0.000	0.000	0.000	-1.000
11	684	623	0.659	0	904.896	104.226		-1.000	0.000	0.000	0.000	-1.000
12	684	1646	0.533	0	905.341	104.426		-1.000	0.000	0.000	0.000	-1.000
11	690	620	0.588	0	911.059	106.999		-1.000	0.000	0.000	0.000	-1.000
12	690	1657	0.464	0	911.514	107.204		-1.000	0.000	0.000	0.000	-1.000
11	697	619	0.532	0	918.251	110.238		0.002	0.016	0.000	0.058	0.060
12	697	1706	0.493	0	918.713	110.446		0.005	0.007	0.014	0.122	0.123
11	703	619	0.519	0	924.416	113.017		0.002	0.017	0.000	0.058	0.061
12	703	1706	0.519	0	924.878	113.225		0.005	0.006	0.012	0.121	0.122
11	709	629	0.682	0	930.588	115.802		0.003	0.025	0.000	0.068	0.072
12	709	1706	0.530	0	931.042	116.007		0.005	0.006	0.010	0.119	0.119
11	715	625	0.705	0	936.750	118.585		0.004	0.016	0.000	0.064	0.066
12	715	1719	0.478	0	937.217	118.796		0.004	0.005	0.001	0.105	0.105
11	721	623	0.578	0	942.914	121.371		0.002	0.018	0.000	0.062	0.064
12	721	1657	0.631	0	943.366	121.580		0.007	0.005	0.015	0.124	0.125
11	727	610	0.727	0	949.069	124.239		0.009	0.004	0.000	0.048	0.048
12	727	1657	0.449	0	949.531	124.455		0.004	0.037	0.014	0.122	0.128
11	734	629	0.725	0	956.275	127.639		0.004	0.018	0.000	0.067	0.069
12	734	1720	0.496	0	956.740	127.860		0.005	0.005	0.000	0.099	0.100
11	740	619	0.685	0	962.433	130.581		0.005	0.003	0.000	0.057	0.057
12	740	1705	0.476	0	962.894	130.803		0.002	0.006	0.001	0.111	0.111
11	746	630	0.710	0	968.606	133.563		0.004	0.006	0.000	0.066	0.067
12	746	1706	0.428	2	969.060	133.784	UPPER BOUND	0.002	0.003	0.001	0.108	0.108
11	752	625	0.567	0	974.767	136.573		0.002	0.004	0.000	0.062	0.062
12	752	1719	0.442	0	975.234	136.802		0.002	0.006	0.001	0.093	0.093
11	758	633	0.429	2	980.938	139.621	UPPER BOUND	0.001	0.016	0.000	0.068	0.070
12	758	1657	0.403	2	981.383	139.842	UPPER BOUND	0.002	0.008	0.003	0.112	0.112
11	764	619	0.428	0	987.093	142.693		0.001	0.010	0.000	0.055	0.056
12	764	1639	0.407	2	987.535	142.916	UPPER BOUND	0.002	0.007	0.018	0.127	0.128
12	771	629	0.484	0	994.292	146.330		0.001	0.005	0.000	0.063	0.063
12	771	1705	0.393	2	994.746	146.561	UPPER BOUND	0.002	0.004	0.000	0.099	0.099
12	777	619	0.488	0	1000.450	149.476		0.002	0.002	0.000	0.052	0.052
12	777	1705	0.443	0	1000.911	149.713		0.002	0.004	0.001	0.096	0.097
12	783	626	0.548	0	1006.620	152.661		0.002	0.021	0.000	0.057	0.061
12	783	1657	0.512	0	1007.070	152.895		0.002	0.021	0.001	0.102	0.104
12	789	625	0.507	0	1012.784	155.877		0.002	0.012	0.000	0.056	0.058
12	789	1705	0.485	0	1013.241	156.117		0.002	0.005	0.001	0.091	0.091
12	795	632	0.623	0	1018.954	159.129		0.003	0.004	0.000	0.062	0.062
12	795	1657	0.526	0	1019.400	159.366		0.003	0.019	0.001	0.096	0.098
12	801	1639	0.564	0	1025.552	162.644		0.003	0.016	0.001	0.111	0.112
12	808	1705	0.597	0	1032.763	166.528		0.003	0.004	0.000	0.082	0.082
11	814	620	0.563	0	1038.468	169.633		0.004	0.013	0.000	0.045	0.047
12	814	1705	0.583	0	1038.928	169.885		0.003	0.005	0.000	0.079	0.079
11	820	629	0.605	0	1044.639	173.024		0.004	0.006	0.000	0.054	0.054
12	820	1657	0.603	0	1045.088	173.272		0.003	0.004	0.000	0.083	0.084
11	826	625	0.685	0	1050.802	176.443		0.008	0.029	0.000	0.048	0.056
12	826	1706	0.746	0	1051.259	176.698		0.007	0.004	0.000	0.073	0.073
11	832	632	0.611	0	1056.971	179.900		0.004	0.003	0.000	0.053	0.053
12	838	1658	0.846	0	1063.583	183.641		0.010	0.010	0.000	0.075	0.075
12	920	719	1.060	1	1147.424	234.391	LOWER BOUND	0.069	0.022	0.000	0.042	0.048
12	920	744	1.470	1	1147.442	234.403	LOWER BOUND	0.105	0.033	0.000	0.064	0.072
12	920	824	2.250	1	1147.471	234.421	LOWER BOUND	0.162	0.049	0.000	0.098	0.110
12	920	859	2.860	1	1147.496	234.437	LOWER BOUND	0.207	0.060	0.001	0.125	0.139
12	920	939	2.820	0	1147.524	234.456		0.089	0.038	0.024	0.153	0.159
12	920	1019	2.460	0	1147.553	234.474		0.082	0.015	0.099	0.174	0.200
12	920	1444	2.680	0	1147.742	234.595		0.135	0.041	0.071	0.158	0.178
12	920	1609	1.400	1	1147.802	234.634		0.015	0.008	0.001	0.097	0.097
12	920	1709	1.040	1	1147.845	234.662	LOWER BOUND	0.075	0.023	0.000	0.045	0.051

28

VL2

VIKING OPTICAL DEPTH MEASUREMENTS
DAY IS 1976 DAY NUMBER.
LS IS LONG OF SUN RELATIVE TO N, VERNAL EQUINOX.
LIMITATION TAG IDENTIFIES LOWER AND UPPER BOUND ESTIMATES, DEFINED BY COLUMN K.
ERROR EDG IS DIGITIZATION ERROR.
ERROR EDV IS ERROR COMPUTED FROM DEVIATION.
ERROR EV IS ERROR DUE TO VIGNETTING CORRECTION.
ERROR ES IS ERROR ESTIMATED FROM USE OF IZERO.
ERROR ETOT IS ROOT SUM OF SQUARES OF ABOVE ERRORS. EXCEPT DIGITIZATION.

CAM	SOL	TIME	TAU	K	DAY	LS	LIMITATION TAG	EDG	EDV	EV	ES	ETOT
21	6	1757	0.275	0	254.467	120.428		0.002	0.000	0.010	0.055	0.056
21	7	612	0.283	0	254.992	120.675		0.001	0.000	0.000	0.044	0.044
21	15	1822	0.245	0	263.733	124.827		0.004	0.001	0.000	0.043	0.043
21	15	1907	0.249	0	263.765	124.843		0.002	0.001	0.000	0.024	0.024
21	22	1806	0.266	0	270.914	128.284		0.003	0.001	0.001	0.047	0.047
21	22	1840	0.284	0	270.938	128.295		0.003	0.001	0.000	0.034	0.034
22	25	521	0.451	0	273.450	129.514		0.005	0.000	0.000	0.023	0.023
22	25	606	0.514	0	273.482	129.530		0.006	0.000	0.000	0.041	0.041
22	25	646	0.502	0	273.511	129.544		0.005	0.000	0.000	0.058	0.058
21	28	1818	0.314	0	277.087	131.287		0.004	0.000	0.001	0.040	0.040
21	28	1903	0.309	0	277.119	131.303		0.002	0.000	0.000	0.023	0.023
21	31	1806	0.287	0	280.161	132.794		0.003	0.000	0.001	0.044	0.044
21	31	1904	0.296	0	280.202	132.814		0.002	0.000	0.000	0.022	0.022
22	40	520	0.423	0	288.862	137.099		0.003	0.000	0.000	0.019	0.019
22	40	602	0.446	0	288.892	137.114		0.005	0.000	0.000	0.036	0.036
22	40	644	0.457	0	288.922	137.129		0.008	0.000	0.000	0.053	0.053
22	44	529	0.353	0	292.978	139.156		0.001	0.000	0.000	0.022	0.022
22	44	559	0.364	0	293.000	139.167		0.002	0.000	0.000	0.034	0.034
21	48	1816	0.181	0	297.635	141.500		0.002	0.000	0.000	0.034	0.034
21	48	1856	0.172	0	297.664	141.514		0.001	0.000	0.000	0.019	0.019
21	52	1652	0.368	0	301.685	143.551		0.007	0.000	0.027	0.065	0.071
21	52	1757	0.341	0	301.732	143.575		0.004	0.000	0.001	0.040	0.040
21	52	1842	0.364	0	301.764	143.591		0.004	0.000	0.000	0.022	0.022
21	54	1652	0.272	0	303.740	144.597		0.005	0.000	0.025	0.064	0.069
21	54	1757	0.237	0	303.787	144.621		0.003	0.000	0.001	0.039	0.039
21	54	1838	0.246	0	303.816	144.636		0.002	0.000	0.000	0.023	0.023
22	55	513	0.329	0	304.269	144.867		0.002	0.000	0.000	0.013	0.013
22	55	533	0.464	0	304.283	144.874		0.004	0.000	0.000	0.021	0.021
22	55	608	0.485	0	304.308	144.887		0.003	0.000	0.000	0.035	0.035
21	73	1736	0.324	0	323.294	154.715		0.004	0.002	0.001	0.040	0.040
21	73	1816	0.356	0	323.323	154.730		0.003	0.001	0.000	0.024	0.024
21	88	1719	0.254	0	338.694	162.895		0.003	0.001	0.001	0.039	0.039
21	88	1758	0.282	0	338.722	162.910		0.002	0.001	0.000	0.024	0.024
22	111	647	0.792	0	361.876	175.557		0.018	0.001	0.000	0.031	0.031
22	111	742	0.805	0	361.915	175.578		0.012	0.007	0.000	0.054	0.054
21	111	1709	0.422	0	362.320	175.803		0.006	0.002	0.000	0.033	0.033
21	111	1747	0.452	0	362.347	175.818		0.010	0.003	0.000	0.018	0.018
22	120	652	1.070	1	371.127	180.727	LOWER BOUND	0.109	0.002	0.000	0.029	0.029
22	120	825	1.160	0	371.193	180.764		0.022	0.001	0.000	0.066	0.066
22	120	914	1.150	0	371.228	180.784		0.016	0.007	0.001	0.082	0.082
22	120	1019	1.140	0	371.274	180.810		0.018	0.007	0.028	0.098	0.102
21	131	1635	1.180	1	382.845	187.460	LOWER BOUND	0.144	0.002	0.000	0.036	0.037
21	131	1725	0.652	1	382.881	187.481	LOWER BOUND	0.069	0.001	0.000	0.018	0.018
22	132	815	1.440	0	383.516	187.848		0.066	0.003	0.000	0.056	0.057
21	145	1611	0.916	0	397.213	195.834		0.034	0.002	0.000	0.039	0.039
21	145	1711	0.778	1	397.256	195.859	LOWER BOUND	0.066	0.001	0.000	0.017	0.017
22	146	831	0.908	0	397.912	196.245		0.015	0.000	0.000	0.054	0.054

CAM	SOL	TIME	TAU	K	DAY	LS	LIMITATION TAG	EDG	EDV	EV	ES	ETOT
22	159	1501	0.850	0	411.548	204.308		0.012	0.003	0.001	0.058	0.058
22	159	1611	0.864	0	411.598	204.338		0.019	0.002	0.000	0.034	0.034
22	160	847	0.858	0	412.308	204.761		0.004	0.001	0.000	0.052	0.052
22	160	947	0.863	0	412.351	204.786		0.005	0.002	0.000	0.069	0.069
22	160	1052	0.849	0	412.398	204.814		0.004	0.001	0.002	0.081	0.081
22	160	1217	0.773	0	412.458	204.850		0.009	0.004	0.023	0.086	0.089
22	173	1100	1.910	0	425.761	212.826		0.022	0.009	0.000	0.075	0.075
22	173	1207	1.960	0	425.809	212.855		0.044	0.003	0.008	0.079	0.079
22	173	1312	1.740	0	425.855	212.883		0.033	0.013	0.011	0.075	0.077
22	173	1400	1.580	0	425.889	212.904		0.005	0.011	0.001	0.067	0.068
22	173	1500	1.660	0	425.932	212.930		0.090	0.002	0.000	0.052	0.052
22	173	1522	1.590	0	425.948	212.939		0.064	0.076	0.000	0.045	0.088
22	174	930	2.510	1	426.724	213.408	LOWER BOUND	0.214	0.002	0.000	0.056	0.056
22	174	1015	2.300	0	426.756	213.427		0.085	0.064	0.000	0.067	0.092
22	184	1014	1.900	0	437.030	219.664		0.046	0.020	0.000	0.061	0.064
22	184	1048	1.830	0	437.055	219.678		0.027	0.007	0.000	0.066	0.067
22	184	1129	1.770	0	437.084	219.696		0.020	0.007	0.001	0.071	0.071
22	184	1209	1.730	0	437.112	219.714		0.017	0.004	0.001	0.073	0.073
22	184	1249	1.700	0	437.141	219.731		0.017	0.004	0.001	0.071	0.072
22	184	1327	1.660	0	437.168	219.748		0.018	0.004	0.001	0.067	0.067
22	184	1417	1.740	0	437.204	219.769		0.035	0.012	0.000	0.058	0.059
22	184	1447	1.710	0	437.225	219.782		0.057	0.052	0.001	0.051	0.073
22	187	1035	1.030	0	440.128	221.556		0.004	0.002	0.000	0.063	0.063
22	188	1035	1.520	0	441.155	222.185		0.016	0.001	0.000	0.062	0.062
22	189	1039	1.670	0	442.186	222.816		0.023	0.012	0.000	0.062	0.063
22	190	1039	1.280	0	443.213	223.446		0.008	0.007	0.000	0.062	0.062
22	191	1035	1.460	0	444.238	224.075		0.014	0.001	0.000	0.061	0.061
22	192	1035	1.750	0	445.265	224.706		0.032	0.003	0.000	0.060	0.060
22	193	1140	2.020	0	446.339	225.367		0.041	0.001	0.000	0.067	0.067
22	194	1141	1.110	0	447.367	226.000		0.005	0.001	0.000	0.067	0.067
22	195	1141	1.300	0	448.395	226.633		0.008	0.005	0.000	0.066	0.066
22	196	1142	1.530	0	449.423	227.267		0.014	0.009	0.000	0.066	0.066
22	197	1142	1.160	0	450.450	227.901		0.006	0.002	0.000	0.065	0.065
22	198	1142	1.120	0	451.478	228.536		0.005	0.005	0.000	0.065	0.065
22	199	938	1.530	0	452.417	229.117		0.062	0.000	0.000	0.044	0.044
22	199	1048	1.620	0	452.467	229.148		0.049	0.002	0.000	0.058	0.058
22	199	1143	1.530	0	452.506	229.172		0.016	0.007	0.000	0.064	0.064
22	199	1203	1.540	0	452.520	229.181		0.030	0.001	0.000	0.070	0.070
21	199	1205	1.450	0	452.522	229.182		0.028	0.009	0.000	0.061	0.062
22	199	1313	1.530	0	452.570	229.212		0.032	0.015	0.000	0.062	0.064
22	199	1415	1.460	0	452.615	229.239		0.045	0.001	0.000	0.052	0.052
22	200	1143	0.945	0	453.534	229.808		0.003	0.002	0.000	0.064	0.064
22	201	1144	1.060	0	454.562	230.446		0.005	0.002	0.000	0.063	0.063
22	201	1426	1.080	0	454.677	230.517		0.008	0.002	0.000	0.049	0.050
22	202	1144	1.340	0	455.589	231.083		0.010	0.003	0.000	0.063	0.063
22	203	1144	2.000	0	456.617	231.721		0.055	0.011	0.000	0.062	0.063
22	204	1145	0.993	0	457.645	232.360		0.004	0.003	0.000	0.062	0.062
22	205	1145	1.180	0	458.673	232.999		0.007	0.003	0.000	0.061	0.061
21	206	1036	1.030	0	459.651	233.609		0.008	0.005	0.000	0.049	0.050
21	207	1231	0.877	0	460.760	234.300		0.004	0.002	0.000	0.058	0.058
22	208	1147	1.030	0	461.756	234.922		0.005	0.002	0.000	0.060	0.060
22	209	1147	1.350	0	462.784	235.563		0.011	0.004	0.000	0.059	0.060
22	210	1147	1.520	0	463.811	236.206		0.018	0.001	0.000	0.059	0.059
22	211	1148	1.250	0	464.840	236.849		0.009	0.006	0.000	0.059	0.059
22	212	1038	1.580	0	465.817	237.461		0.041	0.000	0.000	0.050	0.050
22	213	1147	0.929	0	466.894	238.136		0.004	0.002	0.000	0.058	0.058
22	214	1149	0.969	0	467.923	238.782		0.004	0.002	0.000	0.057	0.057
22	215	1149	1.290	0	468.950	239.427		0.011	0.001	0.000	0.057	0.057
22	216	1150	1.690	0	469.978	240.074		0.033	0.021	0.000	0.057	0.060
22	217	1150	1.320	0	471.006	240.720		0.012	0.000	0.000	0.056	0.056

CAM	SOL	TIME	TAU	K	DAY	LS	LIMITATION TAG	EDG	EDV	EV	ES	ETOT
22	218	1236	1.460	0	472.066	241.388		0.018	0.006	0.000	0.057	0.057
22	219	1151	1.190	0	473.062	242.016		0.008	0.003	0.000	0.056	0.056
22	220	938	0.993	0	473.994	242.604		0.022	0.008	0.000	0.032	0.033
21	221	1130	0.892	0	475.102	243.303		0.005	0.003	0.000	0.049	0.049
22	221	1320	0.975	2	475.180	243.353	UPPER BOUND	0.003	0.002	0.000	0.054	0.054
22	233	1130	0.879	0	487.432	251.139		0.003	0.108	0.000	0.049	0.119
22	233	1319	0.999	2	487.509	251.189	UPPER BOUND	-1.000	0.000	0.000	0.000	-1.000
21	245	1130	1.790	1	499.761	259.062	LOWER BOUND	0.173	0.002	0.000	0.043	0.043
22	245	1319	1.420	0	499.839	259.112		0.025	0.019	0.000	0.049	0.053
22	257	1129	0.989	0	512.091	267.312		0.009	0.004	0.000	0.043	0.043
22	257	1319	1.020	0	512.169	267.362		0.007	0.003	0.000	0.048	0.048
21	269	1130	1.650	1	524.421	275.100	LOWER BOUND	0.160	0.002	0.000	0.040	0.040
22	269	1320	1.780	1	524.500	275.149	LOWER BOUND	0.186	0.002	0.000	0.049	0.049
22	281	1130	1.710	1	536.751	282.762	LOWER BOUND	0.160	0.002	0.000	0.042	0.042
22	281	1320	2.060	1	536.830	282.811	LOWER BOUND	0.192	0.002	0.000	0.050	0.050
21	293	1130	1.700	1	549.081	290.298	LOWER BOUND	0.164	0.002	0.000	0.041	0.041
22	293	1320	1.930	1	549.160	290.346	LOWER BOUND	0.202	0.002	0.000	0.053	0.053
22	305	1129	2.040	1	561.410	297.709	LOWER BOUND	0.173	0.002	0.000	0.045	0.045
22	305	1319	2.300	1	561.489	297.755	LOWER BOUND	0.214	0.002	0.000	0.056	0.056
21	317	1129	2.120	1	573.740	304.994	LOWER BOUND	0.186	0.002	0.000	0.046	0.046
22	329	1129	1.660	0	586.070	312.153		0.022	0.011	0.000	0.053	0.054
22	329	1319	1.720	0	586.148	312.198		0.022	0.010	0.001	0.066	0.067
22	341	1319	0.778	2	598.478	319.231	UPPER BOUND	0.002	0.013	0.001	0.072	0.073
22	353	1129	0.748	2	610.730	326.095	UPPER BOUND	0.001	0.022	0.000	0.064	0.068
22	353	1319	0.848	2	610.808	326.139	UPPER BOUND	0.002	0.014	0.002	0.078	0.079
21	365	1129	1.090	2	623.060	332.878	UPPER BOUND	0.003	0.066	0.000	0.065	0.093
22	377	1101	1.460	0	635.370	339.524		0.010	0.001	0.000	0.069	0.069
22	377	1611	0.959	0	635.591	339.642		0.007	0.003	0.012	0.068	0.069
22	378	1612	1.540	0	636.619	340.191		0.028	0.006	0.013	0.068	0.069
22	379	1102	1.350	0	637.425	340.622		0.008	0.004	0.000	0.070	0.070
22	379	1607	1.210	0	637.643	340.738		0.013	0.003	0.015	0.070	0.071
22	380	1048	1.130	0	638.443	341.164		0.005	0.003	0.000	0.066	0.067
22	380	1608	1.110	0	638.671	341.285		0.010	0.003	0.016	0.070	0.072
22	381	1048	0.949	0	639.470	341.710		0.003	0.002	0.000	0.067	0.067
22	381	1608	1.080	0	639.699	341.831		0.010	0.004	0.016	0.070	0.072
22	382	948	1.500	0	640.455	342.233		0.035	0.003	0.000	0.048	0.048
22	382	1048	1.580	0	640.498	342.256		0.028	0.006	0.000	0.068	0.068
22	384	1049	1.420	0	642.553	343.345		0.018	0.007	0.000	0.069	0.069
22	386	1050	1.040	0	644.609	344.430		0.007	0.003	0.000	0.070	0.070
22	387	1040	1.290	0	645.629	344.968		0.007	0.003	0.000	0.068	0.068
22	388	1041	1.210	0	646.658	345.508		0.006	0.004	0.000	0.069	0.069
22	389	1041	1.050	0	647.685	346.048		0.004	0.001	0.000	0.069	0.070
22	389	1156	1.010	0	647.739	346.076		0.006	0.002	0.011	0.087	0.088
22	390	1042	1.480	0	648.713	346.587		0.010	0.014	0.000	0.070	0.072
22	392	1042	1.390	0	650.768	347.661		-1.000	0.000	0.000	0.000	-1.000
22	394	1043	0.929	2	652.824	348.733	UPPER BOUND	0.003	0.002	0.000	0.073	0.073
22	396	1044	1.110	0	654.880	349.801		0.008	0.002	0.000	0.074	0.074
22	397	1044	1.660	0	655.907	350.333		0.025	0.007	0.000	0.075	0.075
22	400	1046	1.020	0	658.991	351.927		0.006	0.003	0.001	0.077	0.077
21	404	1757	0.833	0	663.409	354.195		0.006	0.001	0.001	0.039	0.039
22	405	1058	1.130	0	664.137	354.567		0.007	0.001	0.001	0.083	0.083
22	405	1148	0.992	0	664.173	354.586		0.006	0.002	0.001	0.080	0.080
22	405	1623	0.642	0	664.369	354.686		0.005	0.002	0.032	0.076	0.083
21	405	1703	0.655	0	664.398	354.700		0.005	0.002	0.011	0.059	0.060
21	405	1718	0.633	0	664.408	354.706		0.002	0.001	0.004	0.054	0.054
21	405	1803	0.651	0	664.440	354.722		0.003	0.001	0.000	0.038	0.038
22	406	853	0.813	0	665.075	355.046		0.003	0.001	0.000	0.040	0.040
22	406	943	0.788	0	665.111	355.065		0.002	0.002	0.000	0.059	0.059
22	406	1008	0.800	0	665.129	355.074		0.004	0.002	0.000	0.068	0.068
22	406	1058	0.766	0	665.165	355.092		0.004	0.001	0.001	0.084	0.084

CAM	SOL	TIME		TAU	K	DAY	LS	LIMITATION TAG	EDG	EDV	EV	ES	ETOT
22	406	1208		0.605	0	665.215	355.117		0.004	0.002	0.038	0.098	0.106
22	406	1623		0.755	0	665.397	355.210		0.006	0.002	0.033	0.076	0.083
22	407	1059	1.220		0	666.193	355.616		0.009	0.003	0.001	0.084	0.084
22	409	1024	1.300		0	668.223	356.648		0.012	0.003	0.000	0.075	0.075
22	410	1025	0.798		0	669.251	357.170		0.004	0.001	0.000	0.076	0.076
22	411	1025	1.440		0	670.279	357.690		0.015	0.006	0.000	0.077	0.077
22	413	946	1.420		0	672.306	358.714		0.021	0.005	0.000	0.064	0.065
21	413	1656		0.657	0	672.613	358.869		0.005	0.002	0.018	0.064	0.066
22	414	1057	1.070		0	673.384	359.257		0.006	0.002	0.001	0.087	0.087
22	415	1012	0.746		0	674.379	359.758		0.004	0.002	0.000	0.074	0.075
22	416	1012	1.120		0	675.407	0.274		0.008	0.003	0.000	0.075	0.075
22	417	1012	1.190		0	676.434	0.789		0.009	0.002	0.000	0.076	0.076
22	418	1013	0.602		0	677.462	1.304		0.003	0.001	0.000	0.077	0.077
22	419	1014	1.010		0	678.491	1.817		0.006	0.004	0.002	0.077	0.077
22	420	829	0.860		0	679.443	2.293		0.004	0.002	0.000	0.038	0.038
22	420	859	0.892		0	679.465	2.303		0.004	0.001	0.000	0.050	0.050
22	420	949	0.893		0	679.500	2.321		0.005	0.001	0.000	0.069	0.069
22	420	1029	0.876		0	679.529	2.335		0.004	0.002	0.001	0.083	0.083
22	420	1130	0.778		0	679.572	2.357		0.005	0.003	0.030	0.098	0.103
21	420	1704		0.507	0	679.811	2.476		0.004	0.001	0.018	0.063	0.066
21	420	1734		0.607	2	679.832	2.486	UPPER BOUND	0.002	0.001	0.003	0.053	0.053
21	420	1809		0.513	0	679.857	2.499		0.002	0.001	0.001	0.039	0.039
21	421	1659		0.785	0	680.835	2.985		0.007	0.003	0.020	0.065	0.068
22	422	1026	0.703		0	681.582	3.357		0.003	0.001	0.001	0.083	0.083
22	423	1026	0.863		0	682.609	3.866		0.004	0.001	0.001	0.083	0.083
21	423	1650		0.482	0	682.883	4.002		0.004	0.002	0.030	0.069	0.075
22	426	1101	0.710		0	685.717	5.403		0.004	0.003	0.019	0.095	0.097
21	426	1656		0.449	0	685.970	5.528		0.004	0.001	0.028	0.068	0.073
21	426	1806		0.490	2	686.020	5.553	UPPER BOUND	0.002	0.001	0.001	0.042	0.042
21	428	1657		0.599	0	688.026	6.540		0.005	0.002	0.029	0.068	0.074
21	429	1658		0.519	0	689.054	7.044		0.005	0.001	0.030	0.068	0.075
22	431	1034	1.170		0	690.835	7.917		-1.000	0.000	0.000	0.000	-1.000
22	432	1033	0.885		0	691.862	8.418		0.004	0.002	0.002	0.090	0.090
22	433	1034	1.030		0	692.890	8.920		0.006	0.002	0.007	0.091	0.091
22	435	1035	0.634		2	694.945	9.920	UPPER BOUND	0.003	0.002	0.011	0.092	0.093
22	437	1036	0.733		0	697.001	10.916		0.003	0.002	0.014	0.094	0.095
22	439	1037	0.783		0	699.057	11.909		0.004	0.002	0.017	0.095	0.096
22	442	1013	0.823		0	702.122	13.383		0.004	0.002	0.001	0.089	0.089
21	442	1703		0.453	0	702.415	13.524		0.005	0.002	0.037	0.070	0.079
21	442	1758		0.436	0	702.454	13.542		0.003	0.002	0.001	0.049	0.049
21	445	1744		0.535	0	705.526	15.011		0.003	0.002	0.010	0.055	0.056
22	446	734	0.760		0	706.119	15.294		0.005	0.002	0.000	0.029	0.029
21	446	736	0.776		0	706.120	15.294		0.006	0.002	0.000	0.028	0.028
22	446	817	0.782		0	706.149	15.308		0.003	0.001	0.000	0.047	0.047
21	446	819	0.785		0	706.151	15.309		0.004	0.001	0.000	0.045	0.045
22	446	1000	0.749		0	706.223	15.343		0.003	0.001	0.001	0.087	0.087
21	446	1744		0.550	0	706.554	15.501		0.004	0.002	0.010	0.056	0.056
22	447	1000	0.679		0	707.250	15.832		0.003	0.001	0.001	0.088	0.088
21	447	1740		0.459	0	707.579	15.988		0.003	0.001	0.012	0.057	0.059
22	448	1016	0.652		2	708.289	16.326	UPPER BOUND	0.003	0.002	0.011	0.093	0.094
21	448	1741		0.464	0	708.607	16.476		0.003	0.001	0.013	0.057	0.059
22	449	1016	0.637		2	709.317	16.813	UPPER BOUND	0.003	0.003	0.012	0.094	0.094
21	449	1741		0.446	0	709.634	16.963		0.003	0.001	0.013	0.057	0.059
21	450	1826		0.628	0	710.694	17.464		0.006	0.001	0.001	0.040	0.040
22	451	1002	0.812		0	711.362	17.780		-1.000	0.000	0.000	0.000	-1.000
21	451	1827		0.535	0	711.722	17.950		0.004	0.001	0.001	0.040	0.040
22	452	952	0.666		2	712.382	18.261	UPPER BOUND	0.003	0.002	0.001	0.087	0.087
22	453	953	0.635		2	713.410	18.745	UPPER BOUND	0.003	0.001	0.001	0.088	0.088
21	453	1748		0.525	2	713.749	18.904	UPPER BOUND	0.003	0.002	0.011	0.056	0.057
22	454	953	0.622		2	714.438	19.228	UPPER BOUND	0.003	0.001	0.001	0.089	0.089

CAM	SOL	TIME	TAU	K	DAY	LS	LIMITATION TAG	EDG	EDV	EV	ES	ETOT
21	454	1743	0.745	0	714.773	19.385		0.003	0.002	0.013	0.058	0.059
22	455	953	0.627	2	715.465	19.710	UPPER BOUND	0.003	0.002	0.001	0.089	0.089
21	455	1743	0.449	0	715.801	19.867		0.003	0.002	0.013	0.058	0.059
22	458	940	0.701	0	718.539	21.146		0.003	0.001	0.001	0.086	0.086
21	458	1755	0.514	0	718.892	21.311		0.003	0.003	0.009	0.054	0.055
22	461	941	0.656	0	721.622	22.579		0.003	0.002	0.001	0.088	0.088
21	461	1751	0.602	0	721.971	22.741		0.004	0.002	0.011	0.056	0.057
22	463	942	0.626	2	723.677	23.530	UPPER BOUND	0.003	0.003	0.001	0.089	0.089
21	463	1752	0.518	0	724.027	23.692		0.003	0.001	0.012	0.056	0.057
21	465	1758	0.581	0	726.086	24.640		0.004	0.000	0.009	0.054	0.055
22	466	933	0.660	0	726.753	24.947		0.003	0.001	0.001	0.088	0.088
21	466	1758	0.581	0	727.114	25.112		0.004	0.001	0.009	0.054	0.055
22	468	919	0.880	0	728.798	25.885		0.005	0.002	0.001	0.083	0.083
21	468	1754	0.668	0	729.166	26.053		0.005	0.002	0.012	0.056	0.058
22	471	915	0.633	0	731.878	27.290		0.003	0.002	0.001	0.083	0.083
21	471	1750	0.508	0	732.246	27.457		0.004	0.002	0.015	0.058	0.060
22	473	916	0.605	2	733.934	28.224	UPPER BOUND	0.003	0.002	0.001	0.085	0.085
21	473	1801	0.552	0	734.308	28.393		-1.000	0.000	0.000	0.000	-1.000
22	474	916	0.607	2	734.961	28.689	UPPER BOUND	0.003	0.002	0.001	0.085	0.085
22	476	917	0.617	2	737.017	29.618	UPPER BOUND	0.003	0.003	0.001	0.086	0.087
21	476	1802	0.442	0	737.392	29.786		0.003	0.001	0.010	0.054	0.055
22	479	728	0.633	0	740.022	30.968		0.004	0.003	0.000	0.044	0.044
22	479	758	0.637	0	740.043	30.978		0.003	0.002	0.000	0.057	0.057
22	479	823	0.653	0	740.061	30.986		0.003	0.002	0.000	0.067	0.067
22	479	853	0.650	0	740.082	30.996		0.003	0.001	0.000	0.079	0.079
22	479	918	0.638	2	740.100	31.004	UPPER BOUND	0.003	0.002	0.001	0.088	0.088
21	479	1743	0.421	0	740.460	31.165		0.003	0.001	0.020	0.062	0.065
21	479	1758	0.422	0	740.471	31.170		0.003	0.001	0.012	0.056	0.058
21	479	1823	0.416	0	740.489	31.178		0.002	0.001	0.001	0.046	0.046
22	480	909	0.601	2	741.121	31.461	UPPER BOUND	0.003	0.003	0.001	0.085	0.085
21	480	1809	0.450	0	741.507	31.633		0.003	0.002	0.007	0.052	0.053
22	481	909	0.605	2	742.149	31.920	UPPER BOUND	0.003	0.003	0.001	0.086	0.086
21	481	1804	0.403	0	742.530	32.091		0.002	0.001	0.010	0.054	0.055
22	482	910	0.609	0	743.177	32.378		0.003	0.003	0.001	0.086	0.086
22	482	1010	0.467	0	743.220	32.396		0.004	0.004	0.049	0.106	0.117
21	482	1740	0.389	0	743.541	32.537		0.003	0.002	0.025	0.064	0.069
21	482	1805	0.373	0	743.559	32.545		0.002	0.001	0.010	0.054	0.055
22	486	652	0.598	0	747.188	34.139		0.003	0.001	0.000	0.032	0.032
21	486	1907	0.635	0	747.713	34.369		0.005	0.001	0.000	0.030	0.030
22	487	652	0.560	0	748.216	34.590		0.003	0.001	0.000	0.032	0.032
21	487	1802	0.468	0	748.694	34.800		0.003	0.001	0.012	0.056	0.058
22	488	652	0.469	0	749.243	35.041		0.002	0.001	0.000	0.033	0.033
21	488	1813	0.509	0	749.729	35.255		0.003	0.001	0.007	0.052	0.053
22	489	858	0.607	0	750.361	35.532		0.003	0.001	0.001	0.085	0.085
22	491	859	0.577	2	752.416	36.435	UPPER BOUND	0.003	0.000	0.001	0.086	0.086
21	491	1809	0.477	0	752.809	36.608		0.003	0.002	0.010	0.054	0.055
22	493	639	0.445	0	754.372	37.295		0.002	0.001	0.000	0.030	0.030
22	493	749	0.459	0	754.421	37.317		0.002	0.001	0.000	0.059	0.059
22	493	819	0.506	2	754.443	37.326	UPPER BOUND	0.002	0.000	0.000	0.072	0.072
22	493	859	0.586	2	754.471	37.339	UPPER BOUND	0.003	0.000	0.001	0.087	0.087
21	493	1809	0.408	0	754.864	37.511		0.003	0.001	0.001	0.054	0.054
21	493	1844	0.418	0	754.889	37.522		0.003	0.001	0.001	0.040	0.040
22	495	900	0.594	2	756.527	38.243	UPPER BOUND	0.003	0.000	0.001	0.088	0.088
21	495	1815	0.464	0	756.923	38.417		0.003	0.001	0.007	0.052	0.053
22	497	846	0.563	2	758.572	39.142	UPPER BOUND	0.002	0.000	0.001	0.084	0.084
21	497	1816	0.461	0	758.979	39.321		0.003	0.001	0.007	0.052	0.053
21	499	1812	0.361	0	761.031	40.224		0.002	0.002	0.009	0.054	0.055
22	500	657	0.420	0	761.577	40.464		0.002	0.001	0.000	0.041	0.041
21	500	1812	0.443	0	762.058	40.676		0.003	0.001	0.009	0.054	0.055
22	502	658	0.397	0	763.633	41.369		0.002	0.001	0.000	0.042	0.042

CAM	SOL	TIME	TAU	K	DAY	LS	LIMITATION TAG	EDG	EDV	EV	ES	ETOT
21	502	1808	0.390	0	764.111	41.579		0.002	0.003	0.012	0.056	0.057
22	503	653	0.370	0	764.656	41.820		0.002	0.001	0.000	0.040	0.040
22	506	820	0.529	2	767.801	43.205	UPPER BOUND	0.002	0.000	0.000	0.077	0.077
21	506	1805	0.334	0	768.218	43.388		0.002	0.001	0.014	0.058	0.059
22	509	656	0.382	0	770.824	44.536		0.002	0.001	0.000	0.044	0.044
21	511	1817	0.415	0	773.364	45.656		0.003	0.001	0.009	0.053	0.054
22	512	657	0.413	0	773.907	45.895		0.002	0.002	0.000	0.046	0.046
22	514	613	0.375	0	775.930	46.788		0.001	0.004	0.000	0.028	0.028
21	514	1813	0.326	0	776.444	47.014		0.002	0.002	0.011	0.055	0.056
21	515	1814	0.312	0	777.472	47.468		0.002	0.001	0.011	0.055	0.056
22	516	614	0.398	0	777.986	47.695		0.001	0.001	0.000	0.029	0.029
21	517	1819	0.439	0	779.531	48.376		0.003	0.002	0.008	0.053	0.054
22	518	615	0.469	0	780.042	48.602		0.002	0.001	0.000	0.030	0.030
22	520	616	0.430	0	782.097	49.509		0.001	0.001	0.000	0.031	0.031
21	520	1821	0.407	0	782.615	49.737		0.002	0.002	0.008	0.053	0.054
22	522	617	0.404	0	784.153	50.417		0.001	0.001	0.000	0.033	0.033
21	522	1816	0.360	0	784.666	50.643		0.002	0.001	0.011	0.055	0.056
22	523	617	0.471	0	785.181	50.871		0.002	0.001	0.000	0.033	0.033
22	525	603	0.546	0	787.226	51.774		0.003	0.001	0.000	0.028	0.028
21	525	1818	0.645	0	787.750	52.006		0.005	0.027	0.010	0.055	0.062
22	528	604	0.599	0	790.309	53.136		0.004	0.012	0.000	0.030	0.032
21	528	1814	0.783	0	790.830	53.367		0.007	0.146	0.013	0.056	0.157
22	537	602	0.438	0	799.555	57.226		0.003	0.001	0.000	0.032	0.032
21	537	1818	0.449	0	800.080	57.459		0.006	0.002	0.012	0.056	0.057
22	538	603	0.437	0	800.583	57.681		0.003	0.001	0.000	0.033	0.033
21	538	1818	0.455	0	801.107	57.914		0.006	0.002	0.012	0.055	0.057
22	541	549	0.435	0	803.655	59.042		0.003	0.001	0.000	0.028	0.028
21	541	1819	0.377	0	804.191	59.279		0.005	0.002	0.011	0.055	0.056
22	544	551	0.413	0	806.739	60.408		0.003	0.002	0.000	0.030	0.030
21	544	1816	0.415	0	807.271	60.644		0.005	0.001	0.013	0.057	0.058
21	548	1827	0.413	0	811.389	62.469		0.006	0.002	0.016	0.058	0.060
22	549	548	0.411	0	811.875	62.685		0.003	0.001	0.000	0.030	0.030
22	552	549	0.433	0	814.958	64.052		0.003	0.001	0.000	0.031	0.031
21	552	1824	0.434	0	815.497	64.291		0.005	0.002	0.010	0.054	0.055
22	553	549	0.400	0	815.985	64.508		0.002	0.001	0.000	0.032	0.032
21	553	1824	0.423	0	816.524	64.747		0.005	0.002	0.009	0.054	0.055
22	555	540	0.436	0	818.034	65.417		0.003	0.001	0.000	0.029	0.029
21	555	1820	0.464	0	818.576	65.658		0.006	0.002	0.012	0.056	0.057
21	557	1820	0.414	0	820.631	66.570		0.005	0.003	0.012	0.055	0.057
22	558	536	0.378	0	821.113	66.785		0.002	0.001	0.000	0.028	0.028
21	559	1817	0.422	0	822.684	67.482		0.006	0.002	0.014	0.057	0.059
21	567	1830	0.402	0	830.913	71.140		-1.000	0.000	0.000	0.000	-1.000
22	568	535	0.405	0	831.388	71.351		-1.000	0.000	0.000	0.000	-1.000
21	571	1826	0.376	0	835.020	72.967		-1.000	0.000	0.000	0.000	-1.000
22	572	537	0.378	0	835.499	73.180		-1.000	0.000	0.000	0.000	-1.000
22	579	605	0.379	0	842.711	76.391		-1.000	0.000	0.000	0.000	-1.000
22	579	635	0.404	0	842.733	76.401		-1.000	0.000	0.000	0.000	-1.000
22	579	705	0.421	0	842.754	76.411		-1.000	0.000	0.000	0.000	-1.000
22	579	735	0.437	0	842.776	76.420		-1.000	0.000	0.000	0.000	-1.000
21	579	1905	0.364	0	843.268	76.639		-1.000	0.000	0.000	0.000	-1.000
22	583	522	0.428	0	846.791	78.209		0.003	0.001	0.000	0.027	0.027
22	584	522	0.405	0	847.818	78.668		0.003	0.001	0.000	0.028	0.028
21	584	1822	0.390	0	848.375	78.916		0.005	0.003	0.012	0.056	0.057
22	587	523	0.428	0	850.901	80.043		0.003	0.001	0.000	0.029	0.029
22	590	524	0.377	0	853.985	81.418		-1.000	0.000	0.000	0.000	-1.000
21	590	1819	0.340	0	854.538	81.665		0.004	0.001	0.013	0.056	0.058
22	591	525	0.377	0	855.013	81.877		0.002	0.001	0.000	0.030	0.030
21	591	1820	0.402	0	855.566	82.124		0.005	0.002	0.013	0.056	0.058
21	592	1830	0.404	0	856.600	82.586		0.005	0.001	0.007	0.052	0.053
22	593	520	0.333	0	857.064	82.793		0.003	0.001	0.000	0.028	0.028

CAM	SOL	TIME	TAU	K	DAY	LS	LIMITATION TAG	EDG	EDV	EV	ES	ETOT
21	593	1831	0.397	0	857.629	83.045		0.005	0.002	0.007	0.052	0.053
22	594	521	0.410	0	858.092	83.252		0.003	0.001	0.000	0.029	0.029
22	595	522	0.442	0	859.121	83.711		0.003	0.001	0.000	0.029	0.029
21	595	1832	0.447	0	859.684	83.963		0.005	0.002	0.007	0.052	0.052
22	597	522	0.541	0	861.176	84.629		0.005	0.002	0.000	0.029	0.030
21	597	1832	0.470	0	861.739	84.881		0.006	0.002	0.006	0.051	0.052
22	600	523	0.603	0	864.259	86.007		-1.000	0.000	0.000	0.000	-1.000
22	601	524	0.502	0	865.287	86.467		-1.000	0.000	0.000	0.000	-1.000
21	601	1829	0.488	0	865.847	86.717		-1.000	0.000	0.000	0.000	-1.000
22	605	520	0.400	0	869.394	88.303		-1.000	0.000	0.000	0.000	-1.000
21	605	1830	0.332	0	869.958	88.555		-1.000	0.000	0.000	0.000	-1.000
21	608	1902	0.353	0	873.063	89.945		-1.000	0.000	0.000	0.000	-1.000
22	609	522	0.404	0	873.506	90.143		-1.000	0.000	0.000	0.000	-1.000
22	613	519	0.412	0	877.613	91.982		-1.000	0.000	0.000	0.000	-1.000
21	613	1829	0.428	0	878.177	92.235		-1.000	0.000	0.000	0.000	-1.000
22	616	520	0.398	0	880.697	93.363		-1.000	0.000	0.000	0.000	-1.000
21	616	1829	0.381	0	881.260	93.616		-1.000	0.000	0.000	0.000	-1.000
22	619	516	0.420	0	883.776	94.744		-1.000	0.000	0.000	0.000	-1.000
21	619	1826	0.384	0	884.340	94.996		-1.000	0.000	0.000	0.000	-1.000
21	623	1828	0.390	0	888.451	96.840		-1.000	0.000	0.000	0.000	-1.000
22	624	518	0.487	0	888.915	97.048		-1.000	0.000	0.000	0.000	-1.000
22	625	519	0.562	0	889.943	97.509		-1.000	0.000	0.000	0.000	-1.000
21	625	1824	0.376	0	890.503	97.761		-1.000	0.000	0.000	0.000	-1.000
22	627	514	0.489	0	891.995	98.430		-1.000	0.000	0.000	0.000	-1.000
22	629	450	0.515	0	894.033	99.345		-1.000	0.000	0.000	0.000	-1.000
22	629	515	0.456	0	894.050	99.353		-1.000	0.000	0.000	0.000	-1.000
22	629	630	0.572	0	894.104	99.377		-1.000	0.000	0.000	0.000	-1.000
22	629	730	0.591	0	894.147	99.396		-1.000	0.000	0.000	0.000	-1.000
21	629	1825	0.441	0	894.614	99.606		-1.000	0.000	0.000	0.000	-1.000
22	631	701	0.388	0	896.181	100.310		-1.000	0.000	0.000	0.000	-1.000
22	631	1726	0.440	0	896.627	100.510		-1.000	0.000	0.000	0.000	-1.000
22	634	710	0.602	0	899.270	101.697		-1.000	0.000	0.000	0.000	-1.000
21	634	1732	0.472	0	899.714	101.897		-1.000	0.000	0.000	0.000	-1.000
22	640	709	0.543	0	905.434	104.468		-1.000	0.000	0.000	0.000	-1.000
21	640	1728	0.485	0	905.876	104.667		-1.000	0.000	0.000	0.000	-1.000
22	646	705	0.409	0	911.596	107.241		-1.000	0.000	0.000	0.000	-1.000
21	646	1722	0.490	0	912.036	107.439		-1.000	0.000	0.000	0.000	-1.000
22	653	659	0.601	0	918.784	110.478		-1.000	0.000	0.000	0.000	-1.000
21	653	1724	0.457	0	919.230	110.679		-1.000	0.000	0.000	0.000	-1.000
22	665	659	0.372	0	931.114	116.039		-1.000	0.000	0.000	0.000	-1.000
21	665	1725	0.362	0	931.561	116.241		-1.000	0.000	0.000	0.000	-1.000
21	667	1727	0.380	0	933.617	117.170		-1.000	0.000	0.000	0.000	-1.000
22	668	654	0.394	0	934.193	117.430		-1.000	0.000	0.000	0.000	-1.000
22	671	710	0.440	0	937.287	118.827		0.004	0.030	0.000	0.071	0.077
21	671	1726	0.338	0	937.727	119.026		0.004	0.007	0.036	0.067	0.077
22	677	706	0.468	0	943.449	121.618		0.004	0.007	0.000	0.069	0.069
21	677	1728	0.387	0	943.893	121.824		0.004	0.008	0.029	0.065	0.072
22	683	703	0.361	0	949.612	124.493		0.003	0.008	0.000	0.067	0.067
21	683	1717	0.359	0	950.050	124.699		0.008	0.023	0.038	0.068	0.081
22	690	657	0.398	0	956.800	127.889		0.003	0.006	0.000	0.063	0.063
21	690	1720	0.292	0	957.245	128.100		0.005	0.024	0.028	0.065	0.074
22	696	704	0.465	0	962.970	130.839		0.004	0.008	0.000	0.065	0.066
21	696	1722	0.317	0	963.411	131.051		0.005	0.007	0.021	0.062	0.066
22	702	700	0.510	0	969.132	133.819		0.002	0.024	0.000	0.062	0.066
21	702	1725	0.328	0	969.578	134.036		0.002	0.038	0.016	0.059	0.072
22	704	659	0.539	0	971.186	134.820		0.002	0.002	0.000	0.061	0.061
21	704	1726	0.292	0	971.634	135.038		0.002	0.006	0.015	0.058	0.060
22	708	709	0.470	0	975.303	136.837		0.002	0.012	0.000	0.065	0.066
21	708	1726	0.347	0	975.744	137.053		0.002	0.002	0.013	0.057	0.058
22	714	706	0.370	2	981.466	139.883	UPPER BOUND	0.002	0.027	0.000	0.062	0.068

CAM	SOL	TIME	TAU	K	DAY	LS	LIMITATION TAG	EDG	EDV	EV	ES	ETOT
21	714	1732	0.264	2	981.913	140.105	UPPER BOUND	0.002	0.010	0.000	0.052	0.053
22	720	703	0.419	2	987.629	142.963	UPPER BOUND	0.002	0.031	0.000	0.059	0.067
21	720	1722	0.409	0	988.071	143.185		0.002	0.008	0.009	0.054	0.055
22	727	657	0.401	2	994.817	146.597	UPPER BOUND	0.002	0.004	0.000	0.054	0.054
21	727	1724	0.421	0	995.265	146.824		0.002	0.042	0.003	0.050	0.066
22	733	704	0.340	2	1000.987	149.752	UPPER BOUND	0.001	0.019	0.000	0.056	0.059
22	739	659	0.490	0	1007.149	152.936		0.002	0.002	0.000	0.052	0.052
21	739	1720	0.315	0	1007.592	153.166		0.002	0.023	0.001	0.047	0.052
21	745	1726	0.422	0	1013.761	156.390		0.003	0.020	0.000	0.042	0.046
22	751	709	0.534	0	1019.486	159.411		0.003	0.030	0.000	0.052	0.060
21	751	1729	0.368	0	1019.928	159.645		0.002	0.020	0.001	0.038	0.043
22	757	705	0.558	0	1025.648	162.695		0.003	0.010	0.000	0.048	0.049
21	757	1722	0.402	0	1026.088	162.931		0.003	0.003	0.001	0.038	0.038
22	764	659	0.448	0	1032.836	166.567		0.002	0.017	0.000	0.043	0.046
21	764	1724	0.365	0	1033.282	166.809		0.002	0.003	0.000	0.034	0.034
21	770	708	0.453	0	1039.007	169.928		0.003	0.020	0.000	0.042	0.046
21	776	1727	0.443	0	1045.614	173.563		0.002	0.003	0.000	0.027	0.028
22	778	659	0.629	0	1047.221	174.452		0.003	0.049	0.000	0.037	0.061
21	779	1722	0.508	0	1048.693	175.269		0.003	0.003	0.000	0.028	0.028
22	784	1434	0.792	0	1053.710	178.069		0.007	0.014	0.000	0.089	0.090
22	792	1427	0.928	0	1061.925	182.699		0.009	0.036	0.000	0.087	0.094
22	800	1431	0.606	0	1070.148	187.393		0.005	0.010	0.000	0.082	0.082
21	808	959	0.760	0	1078.174	192.032		0.009	0.013	0.001	0.079	0.080
22	808	1004	0.800	0	1078.177	192.034		0.007	0.007	0.000	0.085	0.085
22	808	1444	0.669	0	1078.377	192.150		0.006	0.010	0.000	0.074	0.074
22	816	1437	0.710	0	1086.592	196.958		0.007	0.010	0.000	0.071	0.072
22	824	1421	1.040	0	1094.801	201.820		0.014	0.012	0.000	0.071	0.072
22	832	1339	0.969	0	1102.991	206.731		0.011	0.008	0.000	0.076	0.076
22	840	1347	1.560	0	1111.216	211.721		0.012	0.006	0.000	0.070	0.070
22	848	1356	1.320	0	1119.443	216.771		0.008	0.010	0.000	0.065	0.065
22	856	1359	0.993	0	1127.665	221.878		0.004	0.007	0.000	0.061	0.061
22	864	1402	1.670	0	1135.887	227.043		0.030	0.013	0.000	0.056	0.058
22	872	908	0.731	0	1143.897	232.133		0.003	0.004	0.000	0.033	0.034
22	872	913	0.734	0	1143.900	232.135		0.010	0.005	0.000	0.035	0.035
22	872	953	0.693	0	1143.929	232.153		0.005	0.018	0.000	0.045	0.049
22	872	1043	0.772	0	1143.965	232.176		0.010	0.007	0.000	0.055	0.056
22	872	1048	0.741	0	1143.968	232.178		0.002	0.017	0.000	0.056	0.059
22	872	1148	0.835	0	1144.011	232.206		0.010	0.008	0.000	0.062	0.063
22	872	1253	0.875	0	1144.057	232.235		0.011	0.013	0.000	0.062	0.063
22	872	1303	0.879	0	1144.065	232.240		0.003	0.006	0.000	0.061	0.062
22	872	1333	0.936	0	1144.086	232.253		0.014	0.007	0.000	0.058	0.058
22	872	1343	0.909	0	1144.093	232.258		0.003	0.005	0.000	0.057	0.057
22	872	1448	1.220	0	1144.139	232.288		0.019	0.007	0.000	0.044	0.044
22	872	1553	0.989	1	1144.186	232.317	LOWER BOUND	0.070	0.022	0.000	0.025	0.033
21	872	1648	0.349	1	1144.225	232.342	LOWER BOUND	0.023	0.007	0.000	0.008	0.011

REFERENCES

Abramowitz, M., and I. Sagun, Handbook of Mathematical Functions, (New York, Dover, 1968).

American Institute of Physics Handbook, (New York, McGraw Hill) 1963, page 4-301.

Deardorff, J. W., Efficient prediction of ground surface temperature and moisture, with inclusion of a layer of vegetation, J. Geophys. Res. 83, 1889-1903, 1978.

Farmer, C. B., D. W. Davies, A. L. Holland, D. D. LaPorte, and P. E. Doms, Mars: water vapor observations from the Viking orbiters, J. Geophys. Res. 82, 4225-4248, 1977.

Gooding, J. L., Martian dust particles as condensation nuclei: A preliminary assessment of mineralogical factors, Icarus 66, 56-74, 1986.

Haberle, R. M., C. B. Leovy, and J. B. Pollack, Some effects of global dust storms on the atmospheric circulation of Mars, Icarus 50, 322-367, 1982.

Hanel, R., B. Conrath, W. Hovis, V. Kunde, P. Lowman, W. Maguire, J. Pearl, J. Pirraglia, C. Prabhakara, and B. Schlachman, Investigation of the martian environment by infrared spectroscopy on Mariner 9, Icarus 17, 423-442, 1972.

Hart, H. M., and B. M. Jakosky, Composition and stability of the condensate observed at the Viking Lander 2 site on Mars, Icarus 66, 134-142, 1986.

Jakosky, B. M., The seasonal cycle of water on Mars, Space Science Reviews 41, 131-200, 1985.

Jakosky, B. M., and C. B. Farmer, The seasonal and global behavior of water vapor in the Mars atmosphere: Complete global results of the Viking Atmospheric Water Detector experiment, J. Geophys. Res. 87, 2999-3019, 1982.

Jaquin, F., P. Gierasch, and R. Kahn, The vertical structure of limb hazes in the martian atmosphere, Icarus 68, 442-461, 1986.

Jones, K. L., R. E. Arvidson, E. A. Guinness, S. L. Bragg, S. D. Wall, C. E. Carlston, and D. G. Pidek, One Mars year: Viking lander imaging observations, Science 204, 799-806, 1979.

Kieffer, H. H., Soil and surface temperatures at the Viking lander sites, Science 194, 1344-1346, 1976.

Leovy, C. B., J. E. Tillman, W. R. Guest, and J. Barnes, Interannual variability of martian weather, Recent Advances in Planetary Meteorology, G. E. Hunt, editor, Cambridge University Press, 69-84, 1985.

Mayo, A. P., W. T. Blackshear, R.H. Tolson, and W. H. Michael, Jr., Lander locations, Mars physical ephemeris, and solar system parameters: Determination from Viking lander tracking data, J. Geophys. Res. 82, 4297-4303, 1977.

Pollack, J. B., D. Colburn, R. Kahn, J. Hunter, W. Van Camp, C. E. Carlston, and M. R. Wolf, Properties of aerosols in the martian atmosphere, as inferred from Viking lander imaging data, J. Geophys. Res. 82, 4479-4496, 1977.

Pollack, J. B., D. S. Colburn, F. M. Flasar, R. Kahn, C. E. Carlston, and D. Pidek, Properties and effects of dust particles suspended in the martian atmosphere, J. Geophys. Res. 84, 2929-2945, 1979.

Pollack, J. B., C. B. Leovy, P. W. Greiman, and Y. Mintz, A martian general circulation experiment with large topography, J. Atmos. Sci. 38, 3-29, 1981.

Toon, O. B., J. B. Pollack, and C. Sagan, Physical properties of the particles composing the martian dust storm of 1971-1972, Icarus 30, 663-696, 1977.
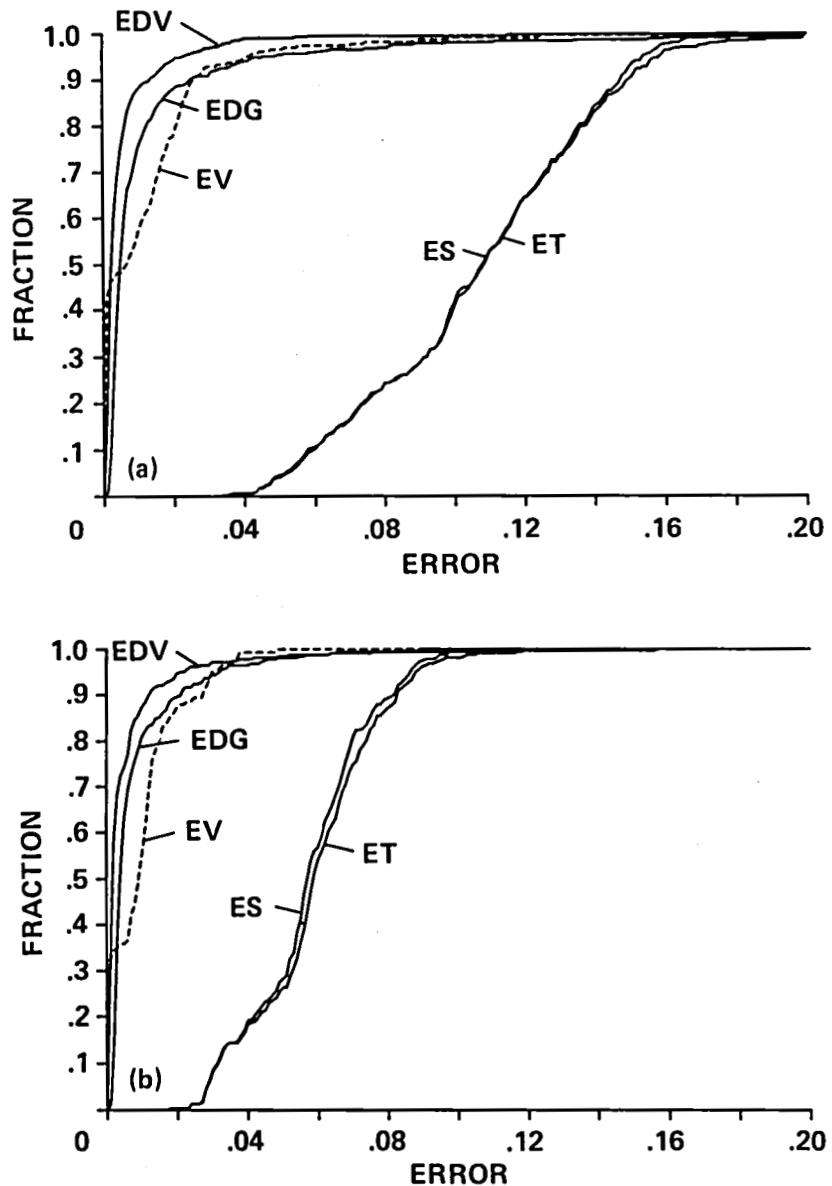
Figure 1.- Histogram of errors associated with optical depth measurements. (a) VL1. (b) VL2.
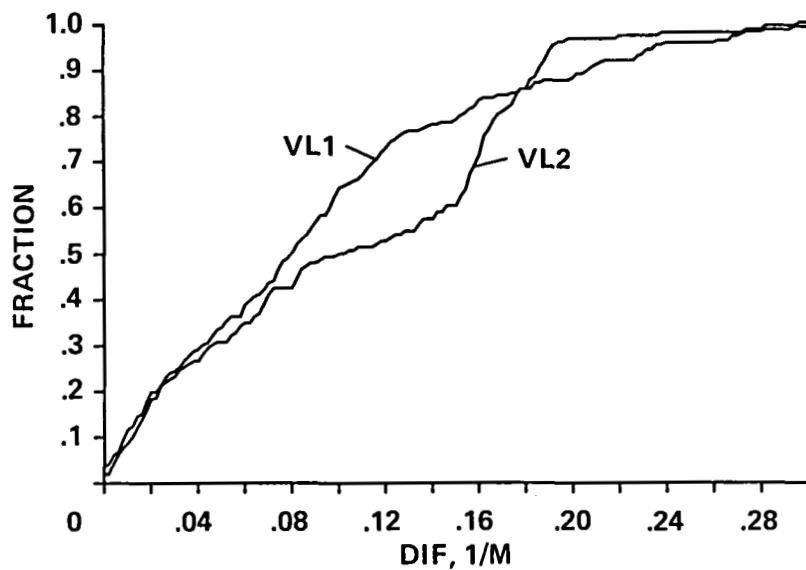
Figure 2.- Histogram of the difference in reciprocal airmasses associated with the AM-PM differences determined by optical depth measurements. The difference is a factor in the error in AM-PM differences.
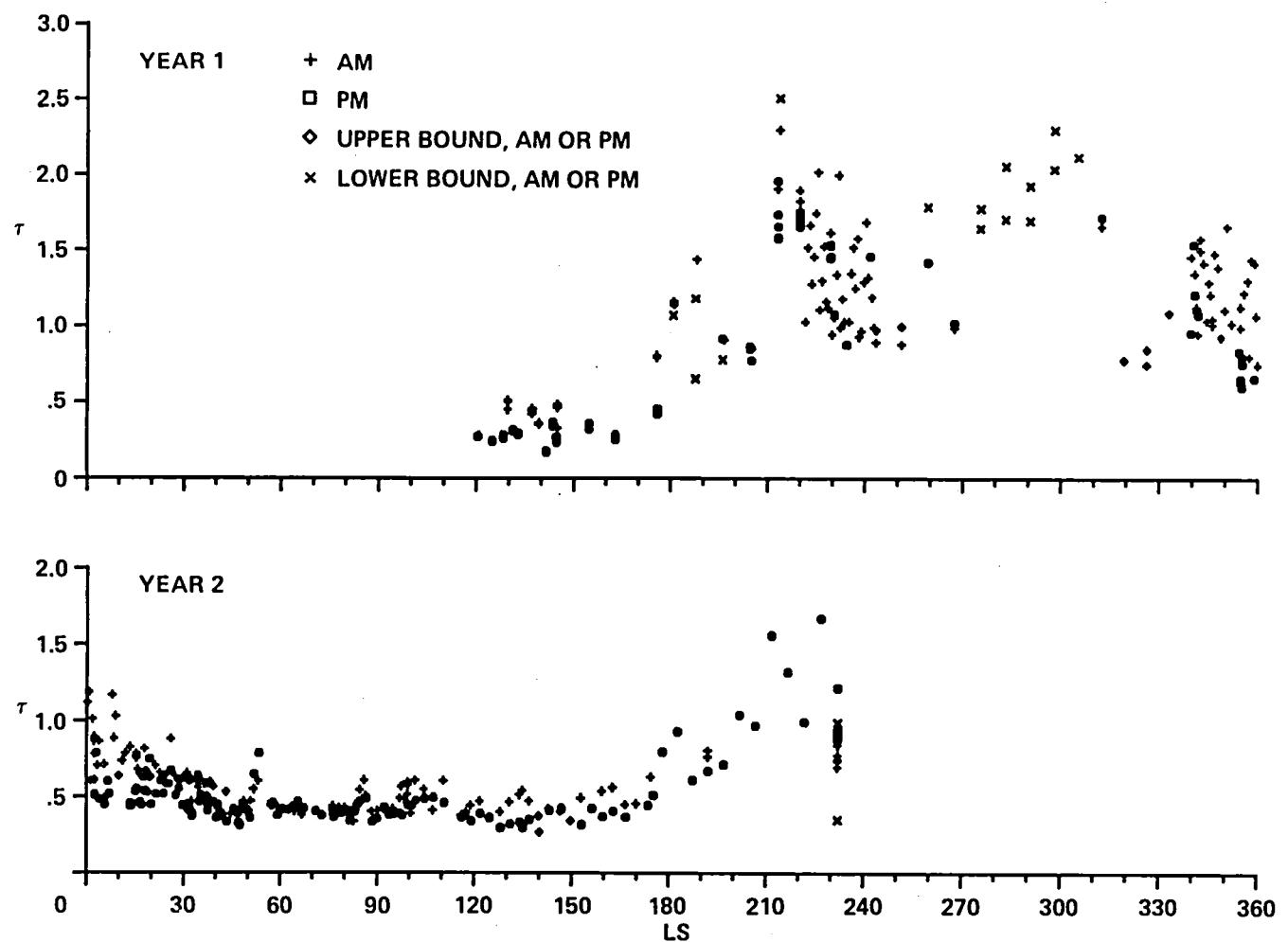
Figure 3.- Concluded. (b) Measured by VL2.
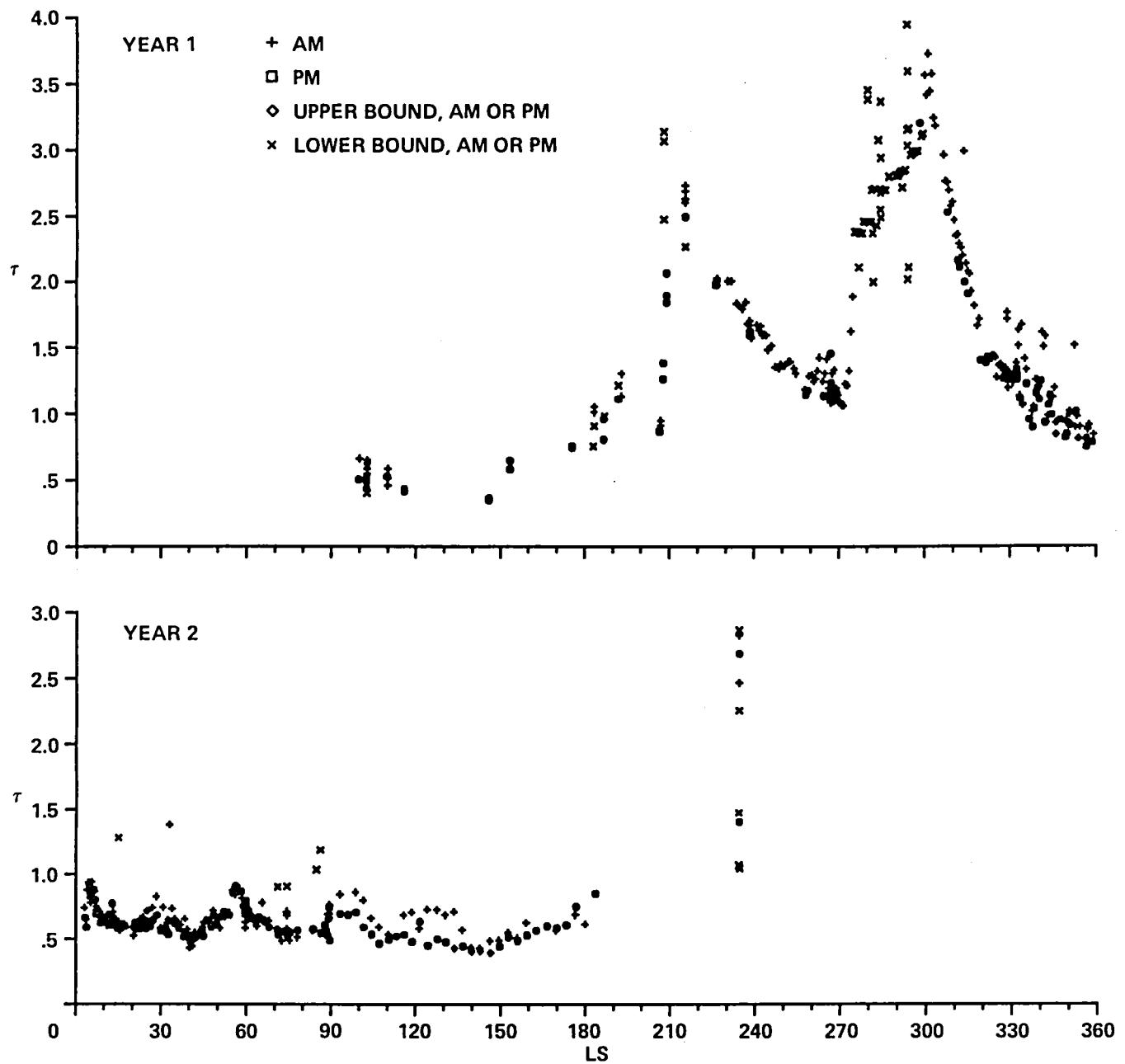
Figure 3.- Complete set of optical depths. (a) Measured by VL1.
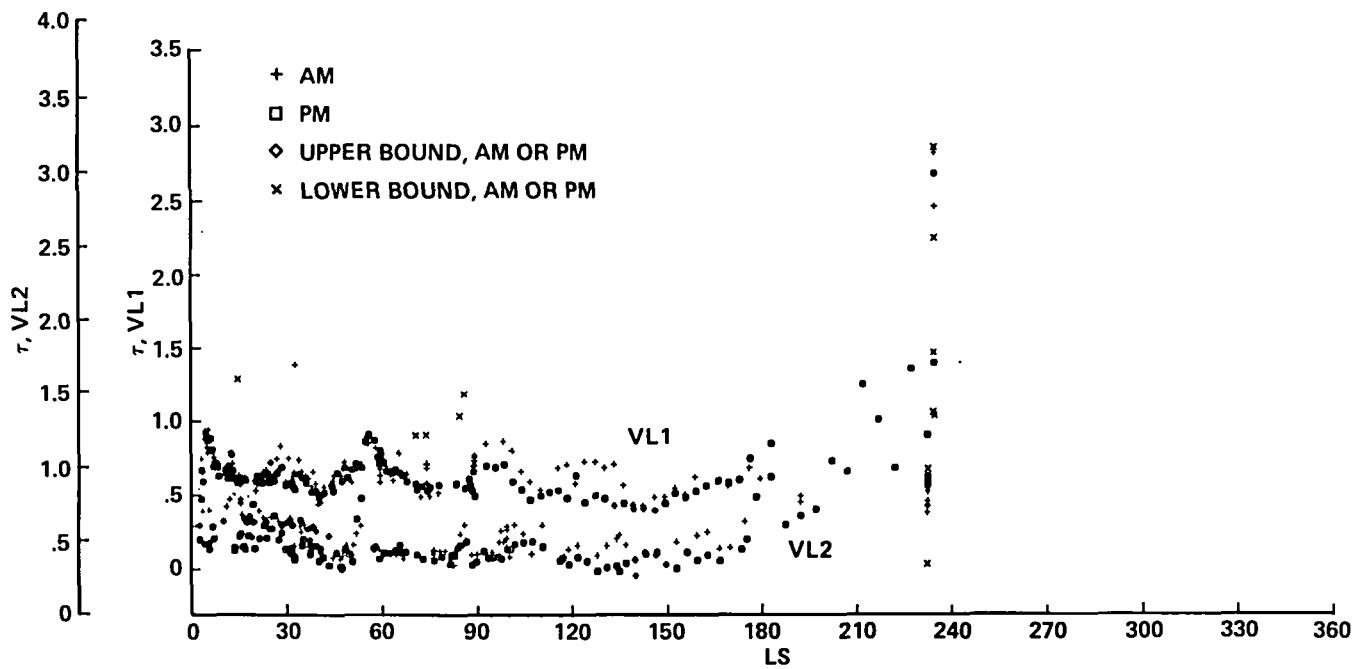
Figure 4.- Comparison of optical depths at the two lander sites in the second martian year. Values for VL1 are offset by approximately 0.3 optical depth units.
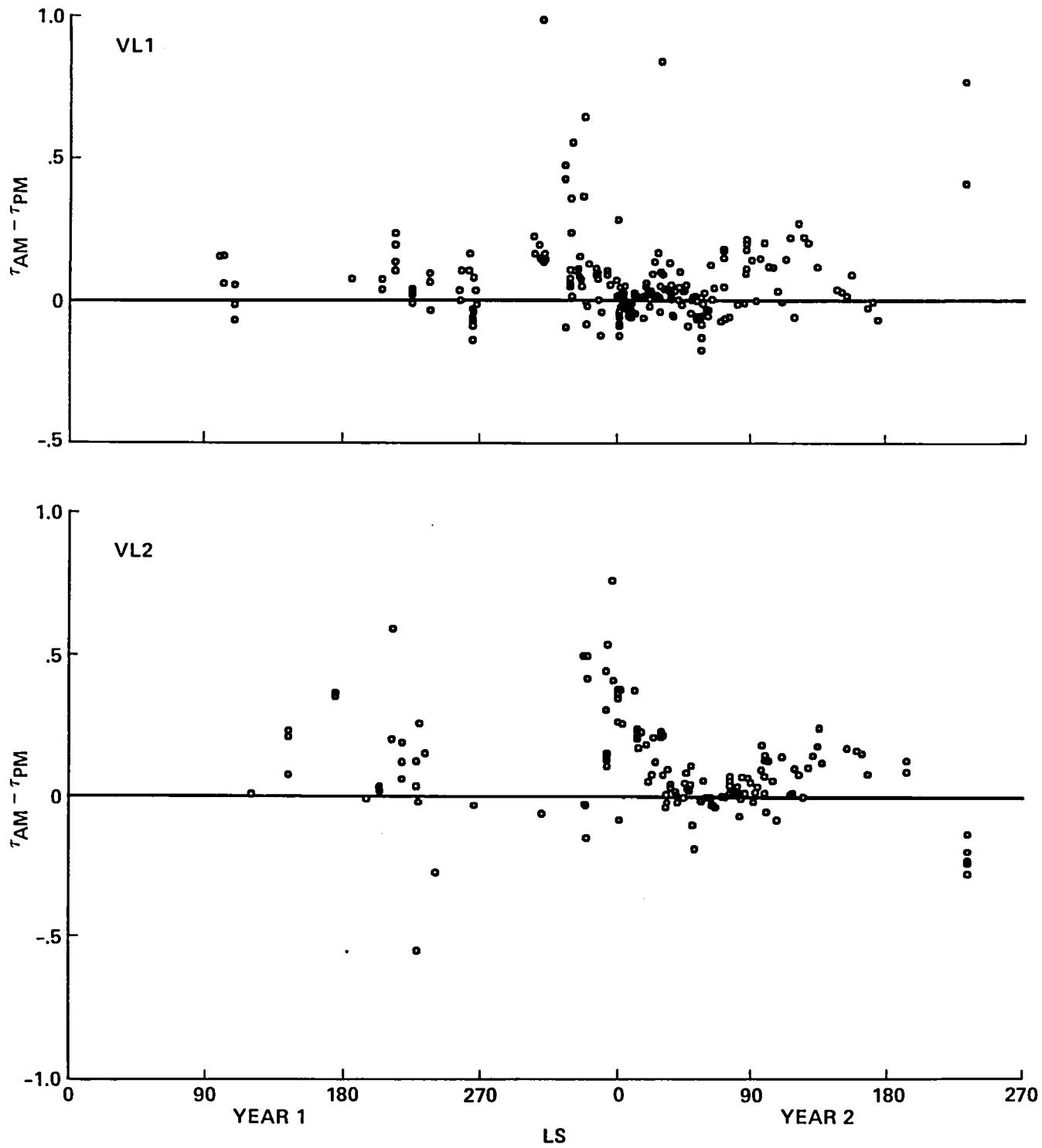
Figure 5.- AM-PM differences measured at the two lander sites. Each plotted point is the difference between a morning optical depth and the average of all afternoon optical depths on that sol and the preceding one.

44
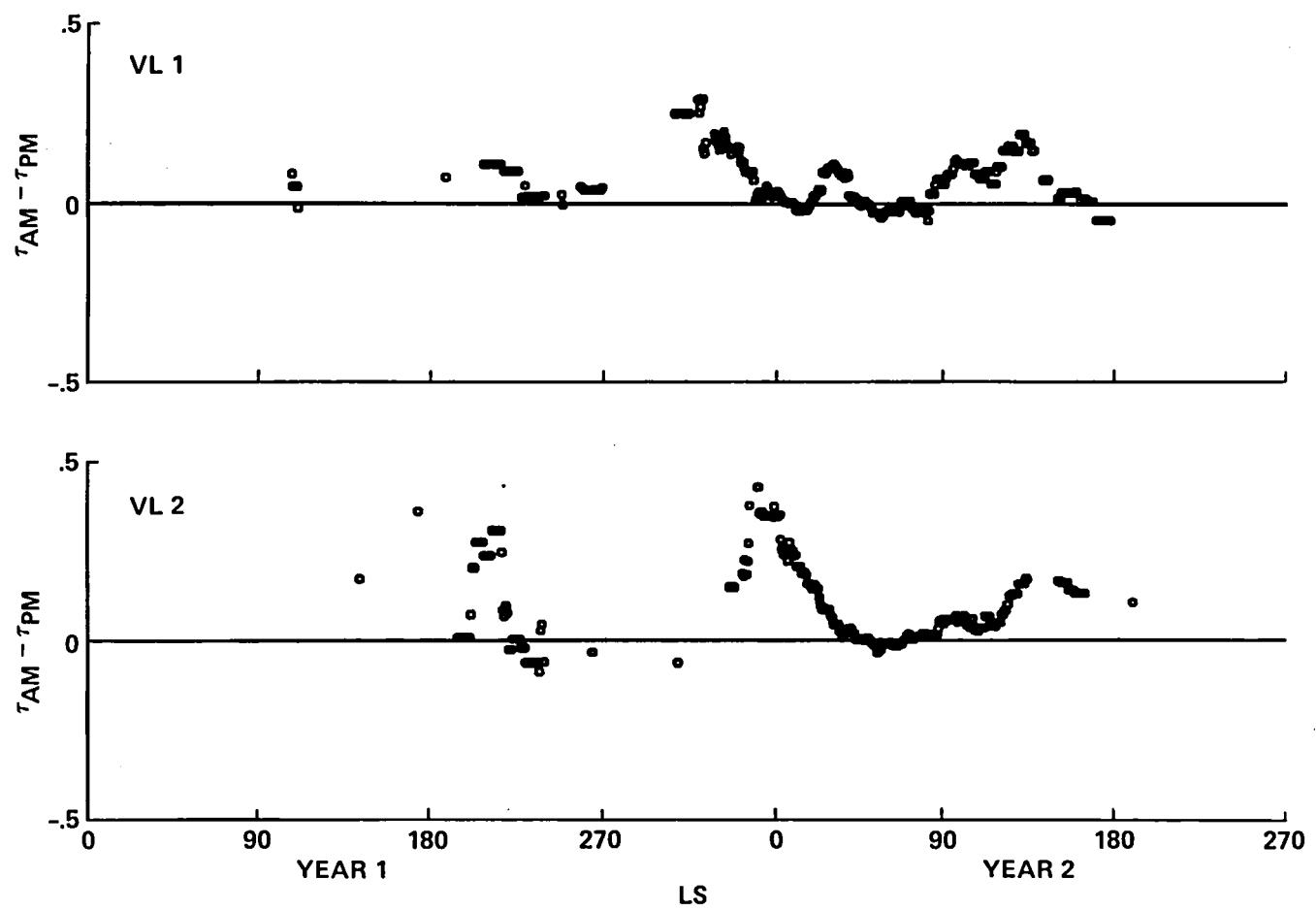
Figure 6.- AM-PM differences smoothed by a running average.
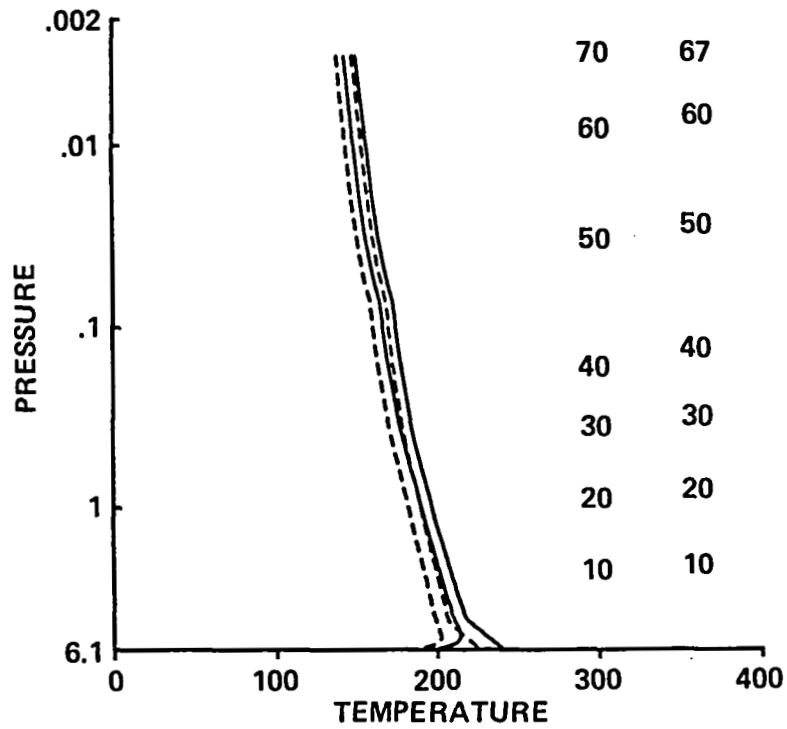
Figure 7.- VL1 temperature profiles computed by the model. Abscissa is temperature in K, and ordinate is atmospheric pressure in millibars. On the right are altitude levels expressed in km: column on left denotes average altitudes for solid curves, column on right, dotted curves. Each pair of profiles has PM profile on right and AM on left. Solid lines, Ls = 90; dotted lines, Ls = 270. Optical depth = 0.3.
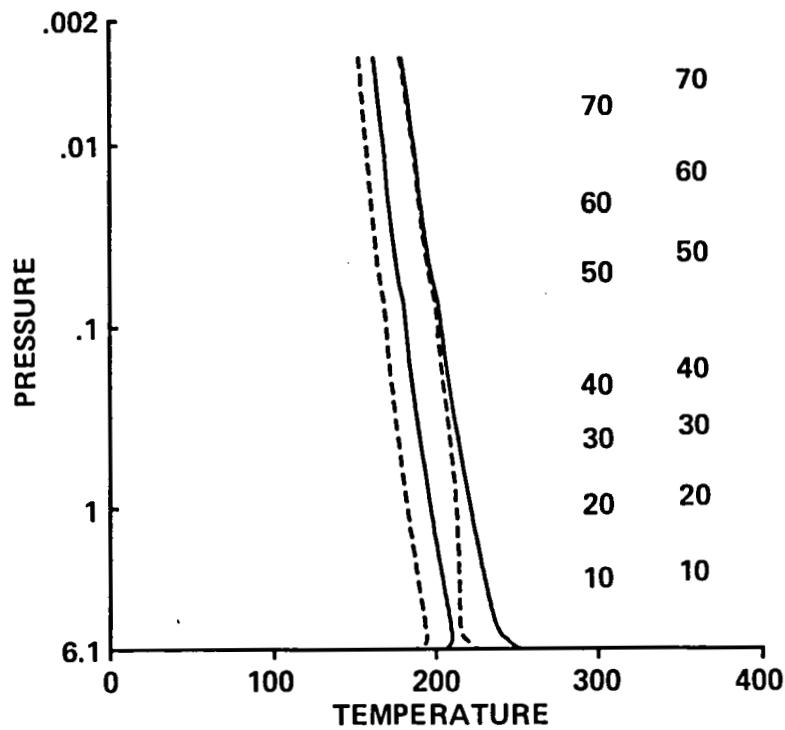
Figure 8.- VL1 temperature profiles as in figure 7, but with optical depth = 2.0.
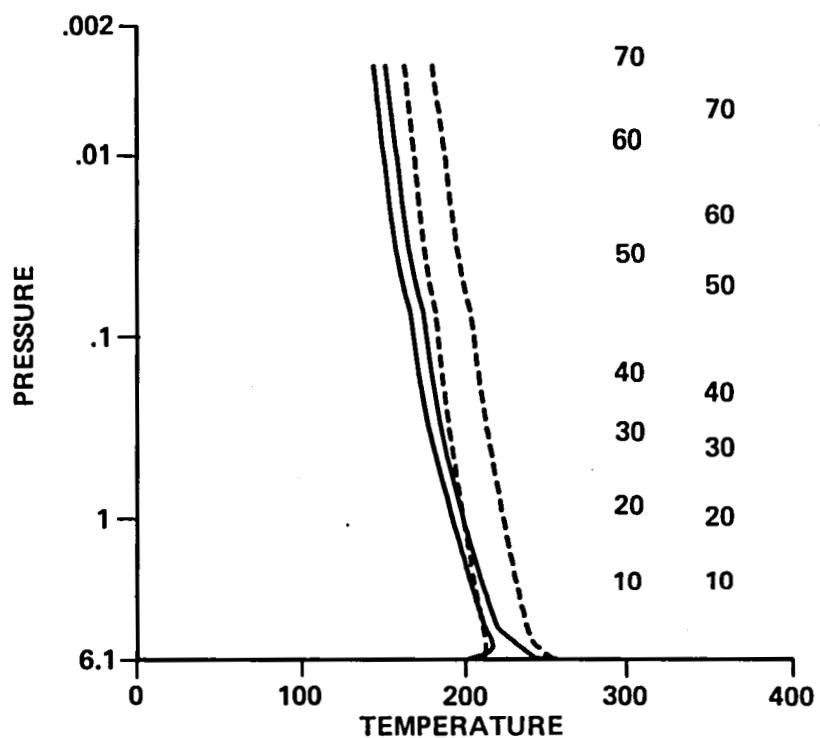
Figure 9.- VL1 temperature profiles as in figure 7, but with solid lines, optical depth = 0.3; dotted lines, optical depth = 2.0. Ls = 90.
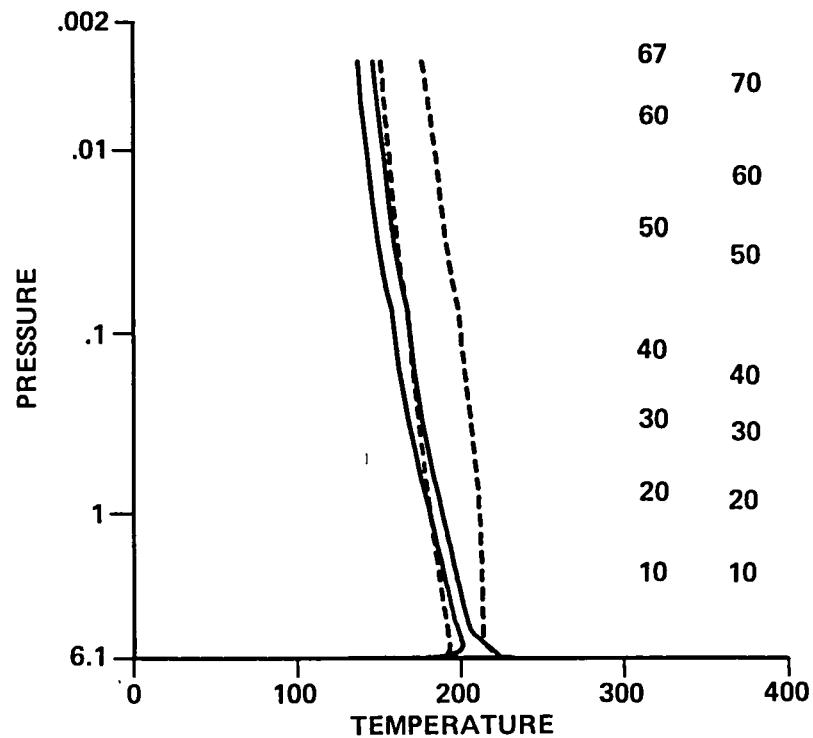
Figure 10.- VL1 temperature profiles as in figure 9, but with Ls = 270.
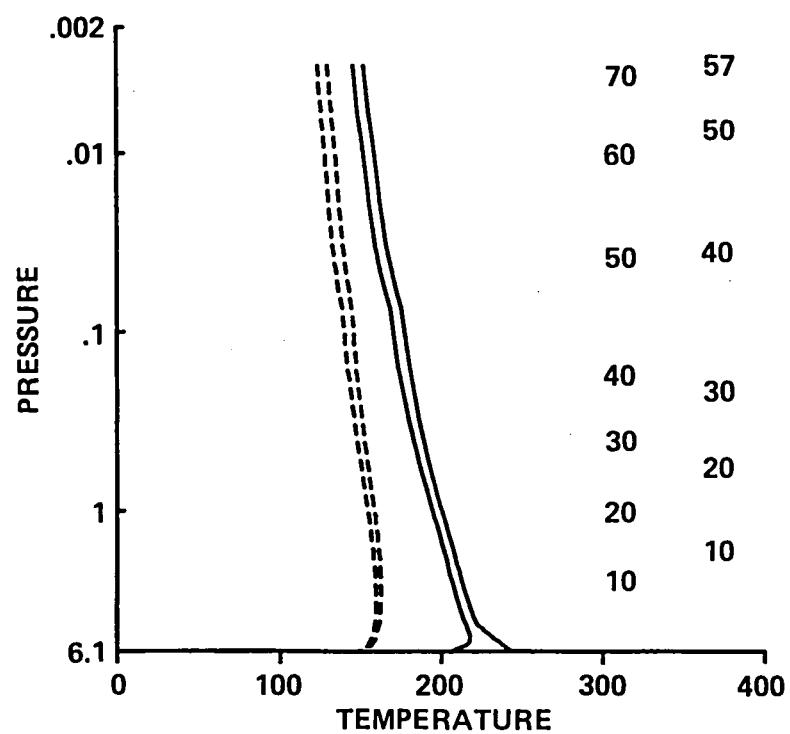
Figure 11.- VL2 temperature profiles as in figure 7. Solid lines, Ls = 90; dotted lines, Ls = 270. Optical depth = 0.3.
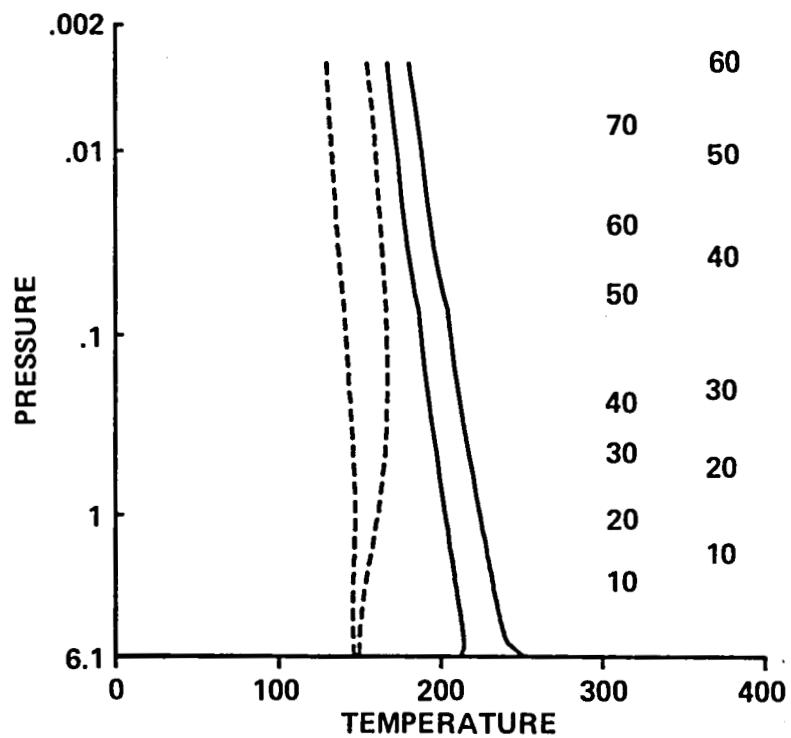
Figure 12.- VL2 temperature profiles as in figure 11, but with optical depth = 2.0.
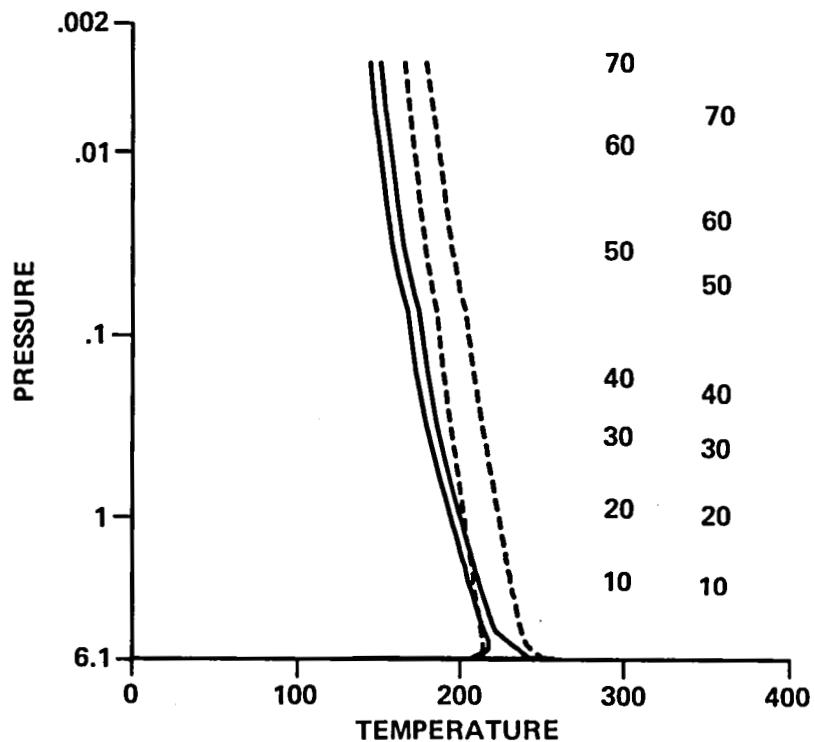
Figure 13.- VL2 temperature profiles as in figure 11, but with solid lines, optical depth = 0.3; dotted lines, optical depth = 2.0. Ls = 90.
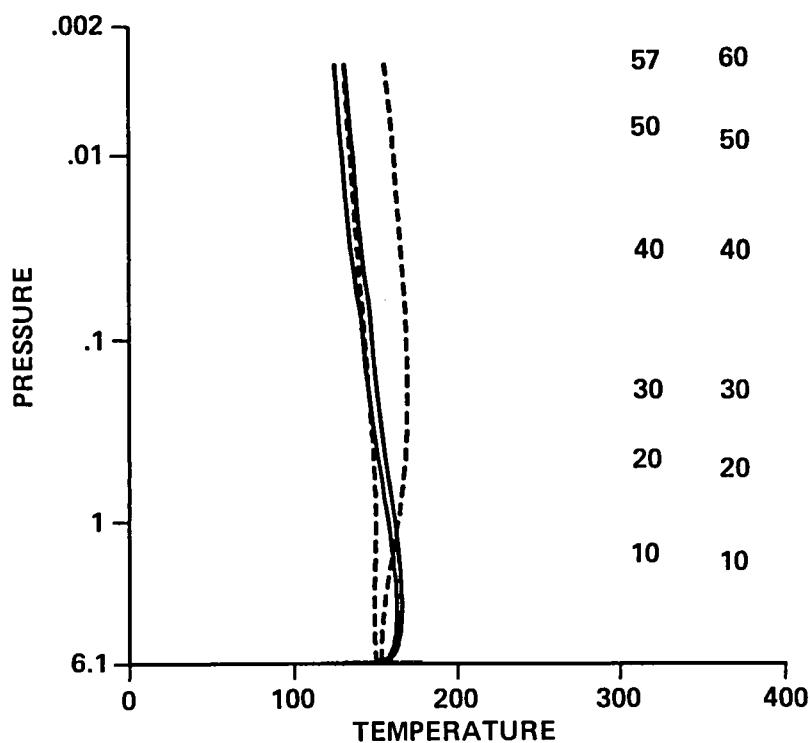
Figure 14.- VL2 temperature profiles as in figure 13, but with Ls = 270.
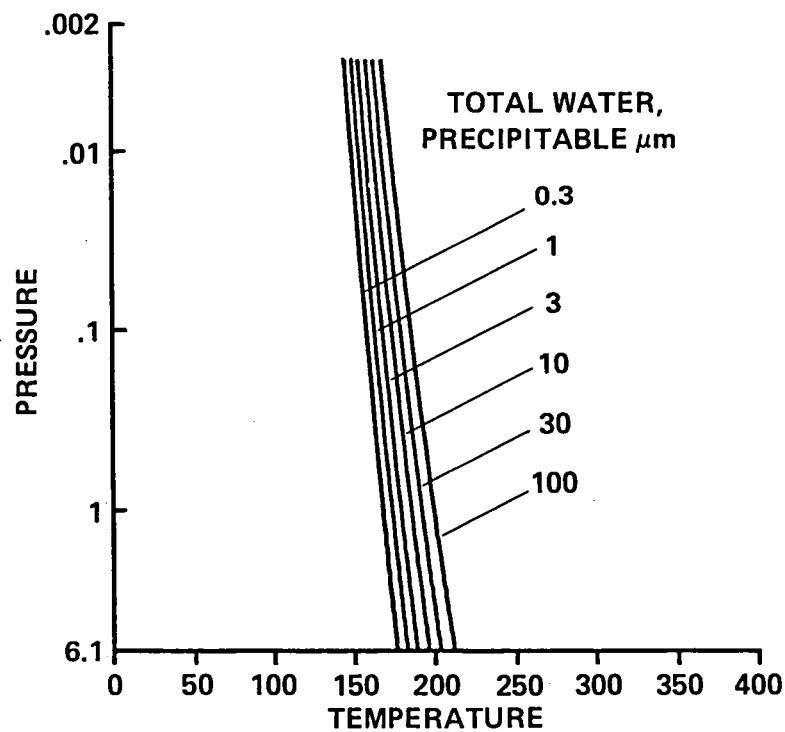
Figure 15.- Dewpoint temperature in K as a function of atmospheric pressure for various amounts of water vapor content. The profiles are independent of latitude, season or time of day. One precipitable micrometer is the amount of water in an atmospheric column that would condense to a liquid layer one micrometer thick. These profiles assume a mixing ratio constant with altitude.

50
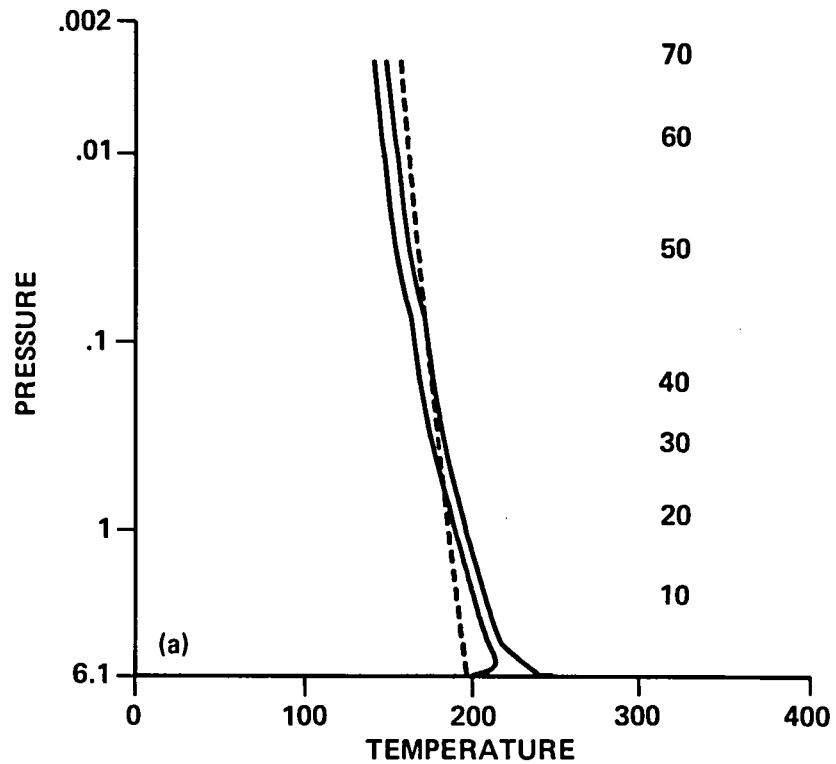
Figure 16.- VL1 temperature and condensation profiles for Ls = 90 and optical depth = 0.3. (a) The temperature profile is as shown in figure 7 with a dewpoint profile for 11 pr μm.
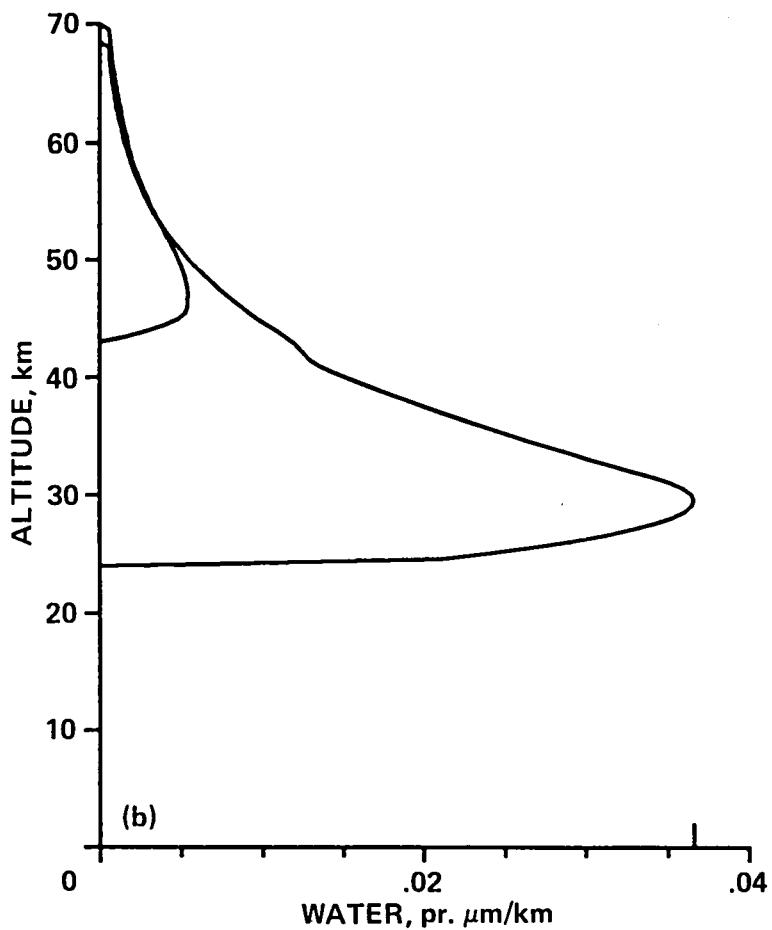
Figure 16.- Concluded. (b) Water density profiles show predicted condensed water in pr μm /km. Curve on right is AM and curve on left is PM. Tick mark on horizontal axis shows maximum AM density.
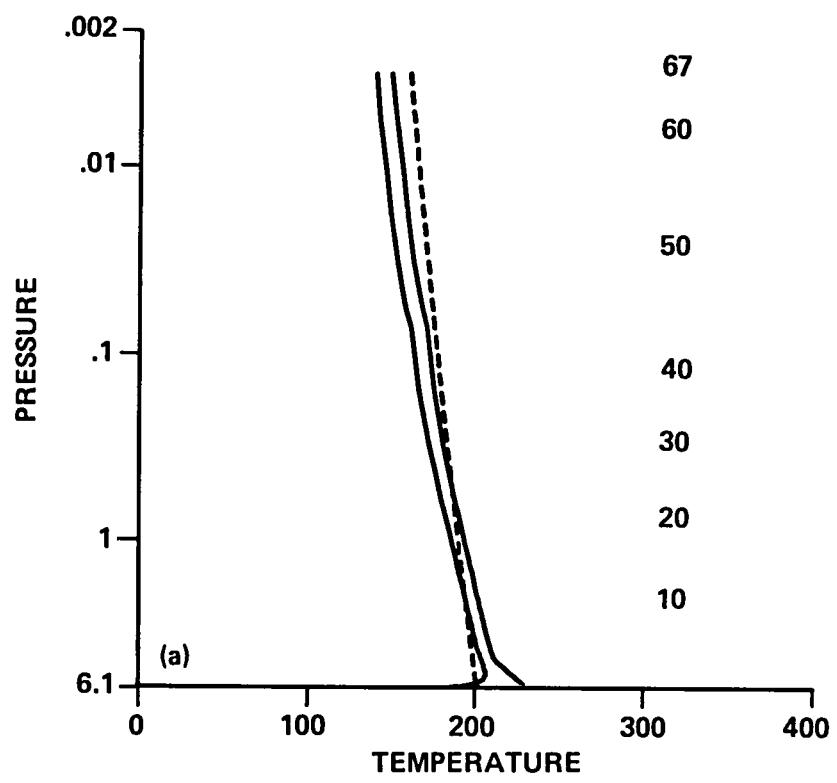
Figure 17.- VL1 profiles as in figure 16 but with Ls = 270. (a) Temperature profile.
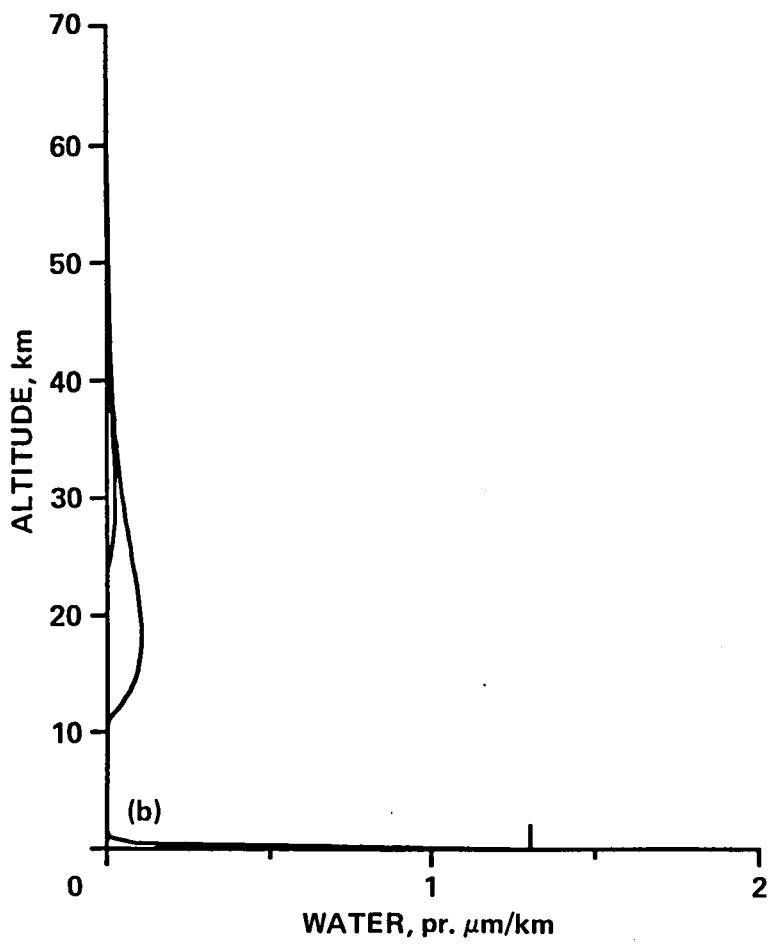
Figure 17.- Concluded. (b) Water density profile.
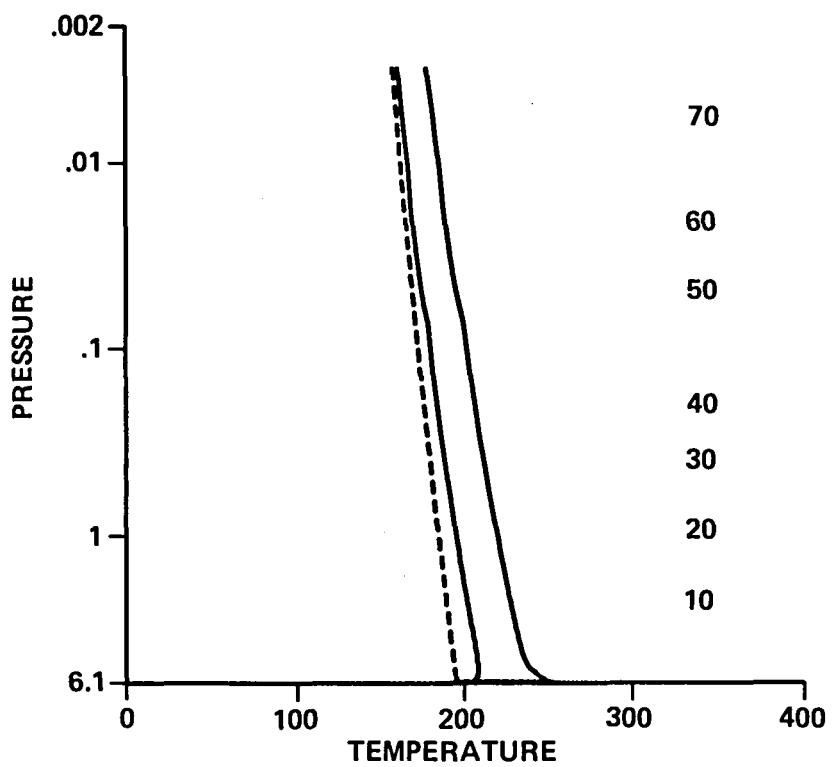
Figure 18.- VL1 temperature profiles as in figure 16 but with optical depth = 2.0. No water condensation is predicted.
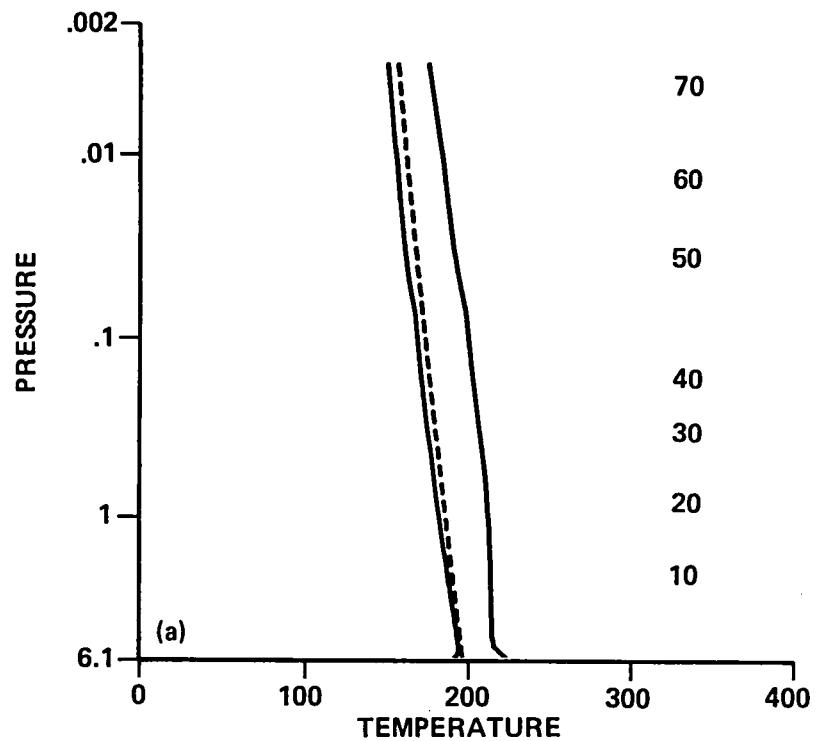
Figure 19.- VL1 profiles as in figure 16 but with Ls = 270 and optical depth = 2.0. No PM condensation is predicted. (a) Temperature profile.
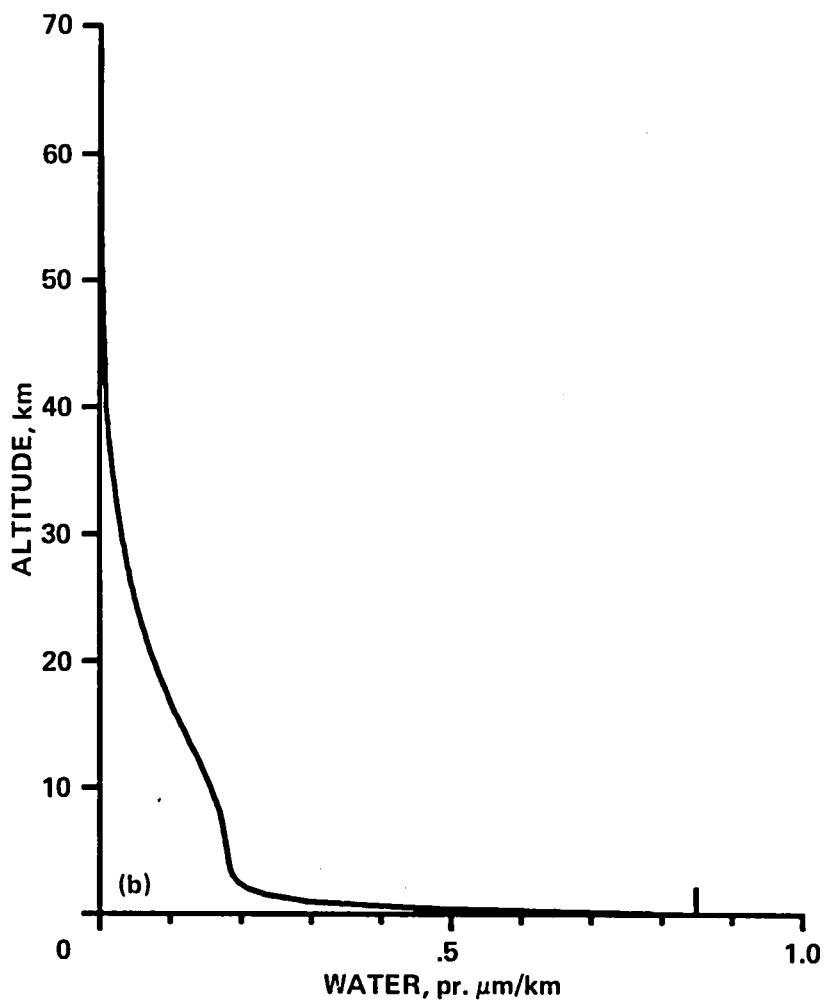
Figure 19.- Concluded. (b) Water density profile.
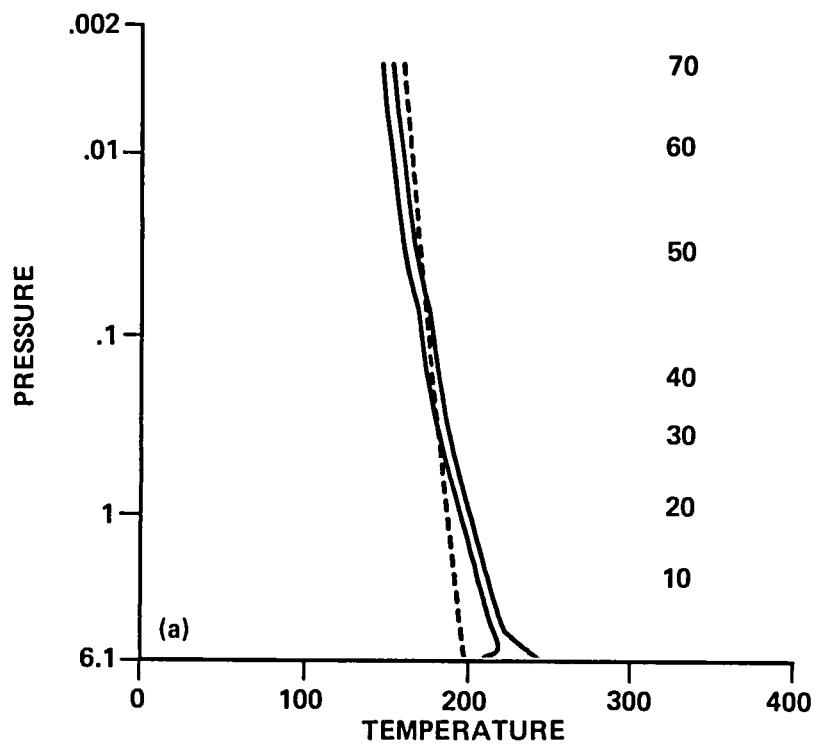
Figure 20.- VL2 profiles as in figure 16. Ls = 90 and optical depth = 0.3. (a) Temperature profile.
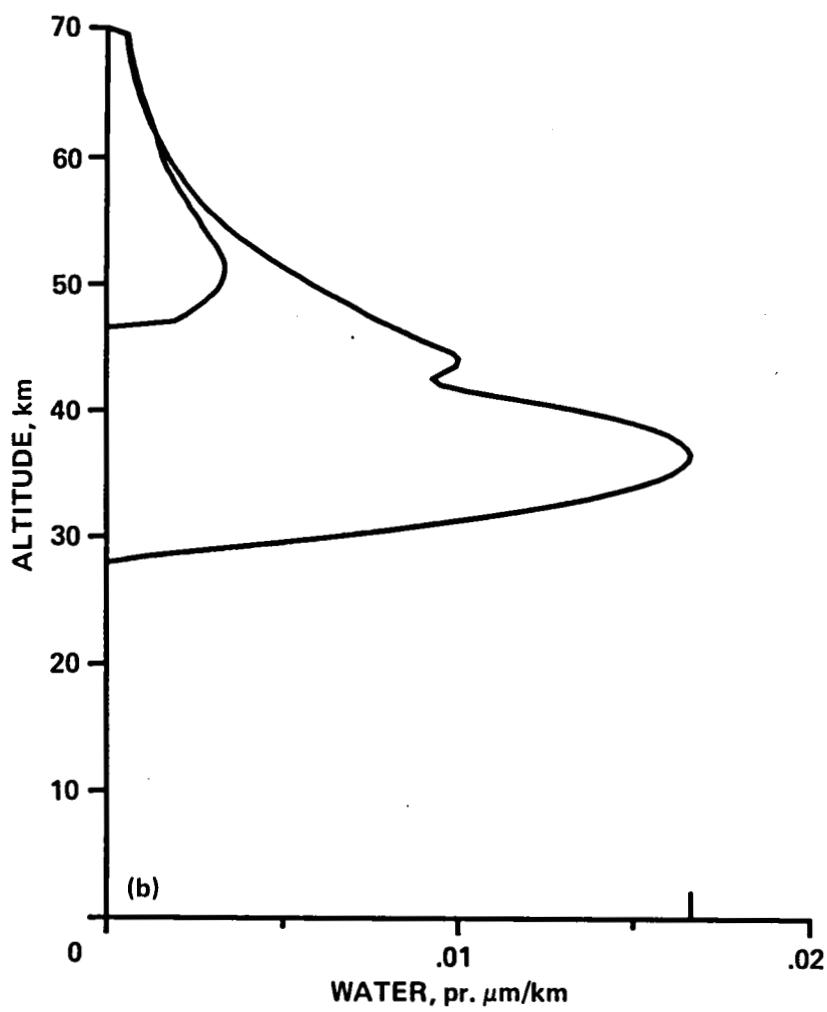
Figure 20.- Concluded. (b) Water density profile.
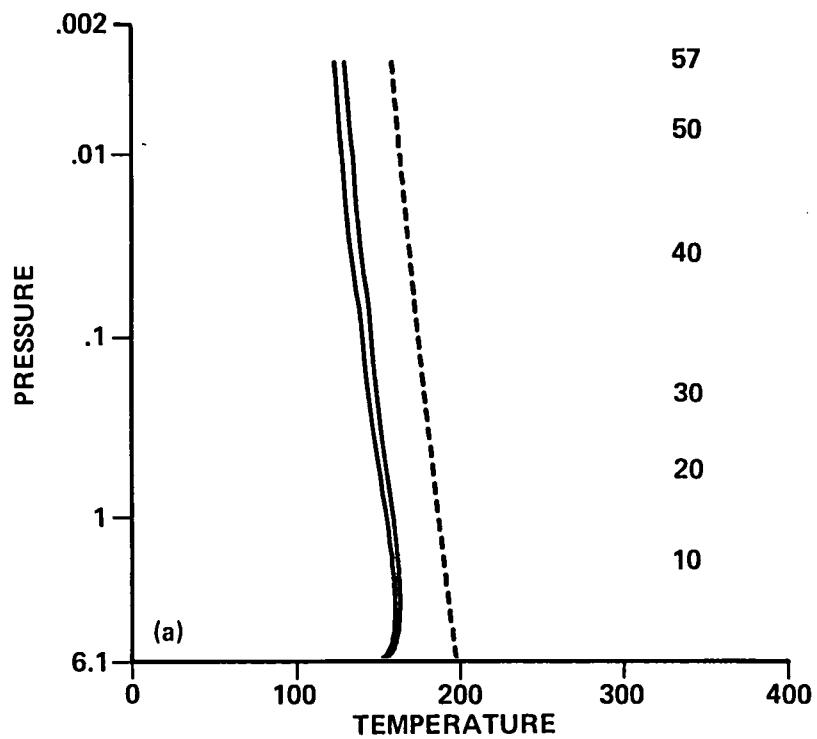
Figure 21.- VL2 profiles as in figure 20 but with Ls = 270. Condensation is essentially complete in both AM and PM because of the cold temperatures. (a) Temperature profile.
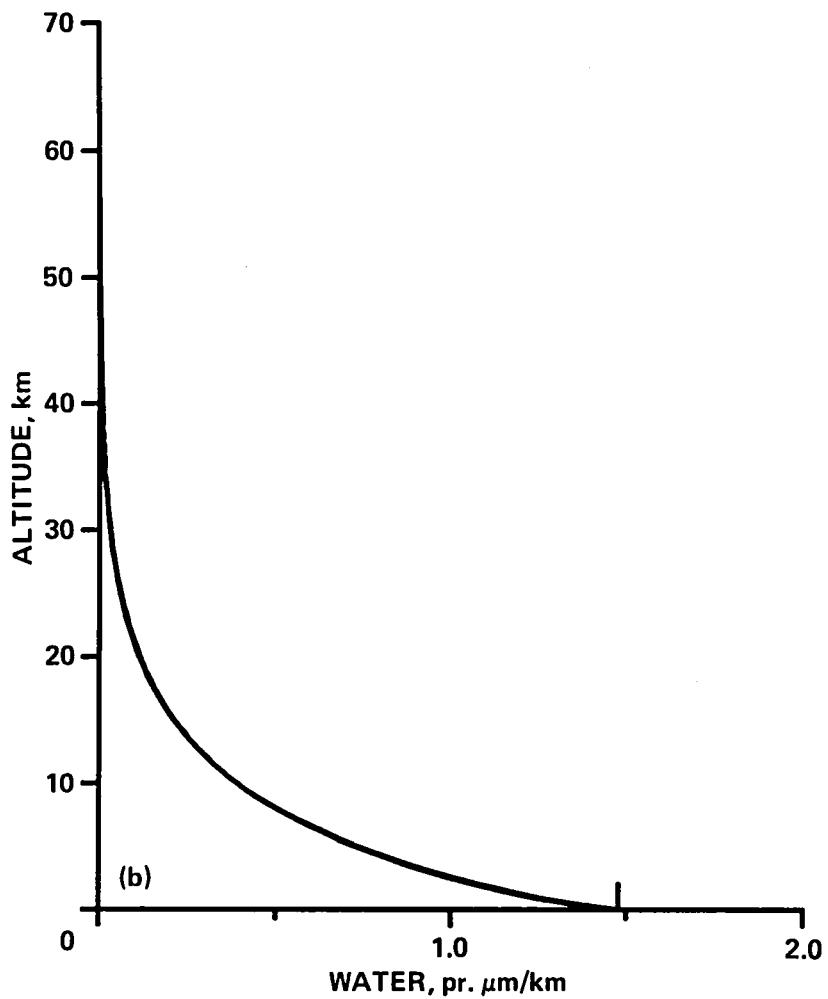
Figure 21.- Concluded. (b) Water density profile.
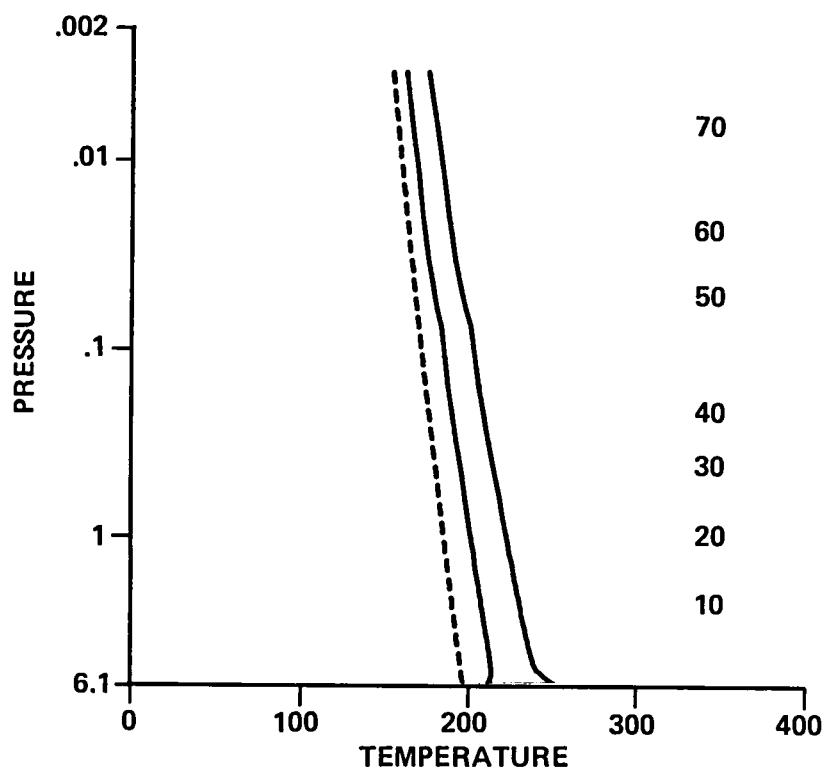
Figure 22.- VL2 temperature profiles as in figure 20 but with optical depth = 2.0. No water condensation is predicted.
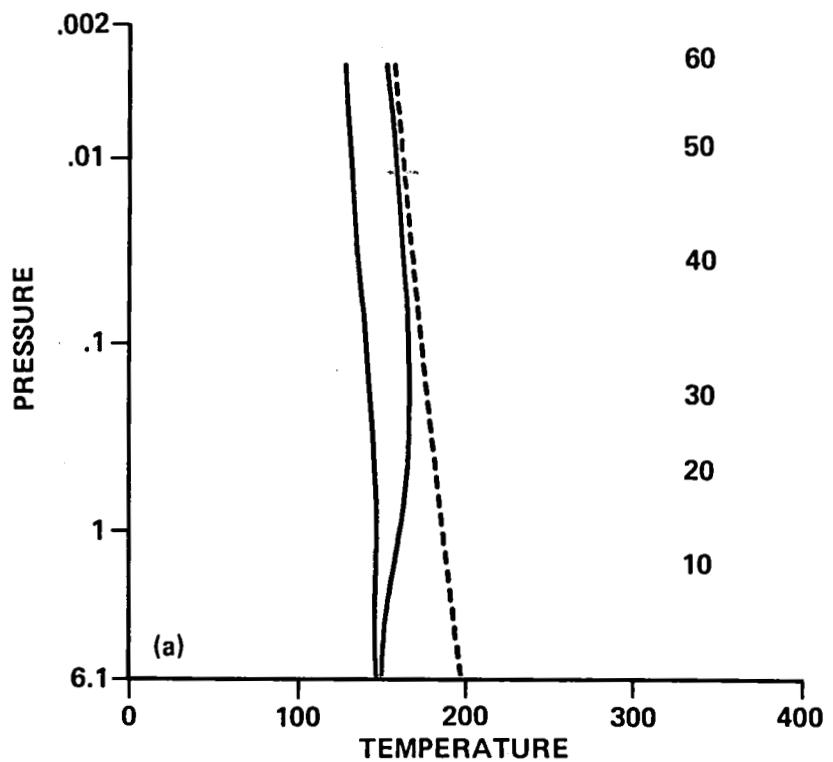
Figure 23.- VL2 temperature profiles as in figure 20 but with Ls = 270 and optical depth = 2.0. AM and PM condensations are nearly complete. (a) Temperature profile.
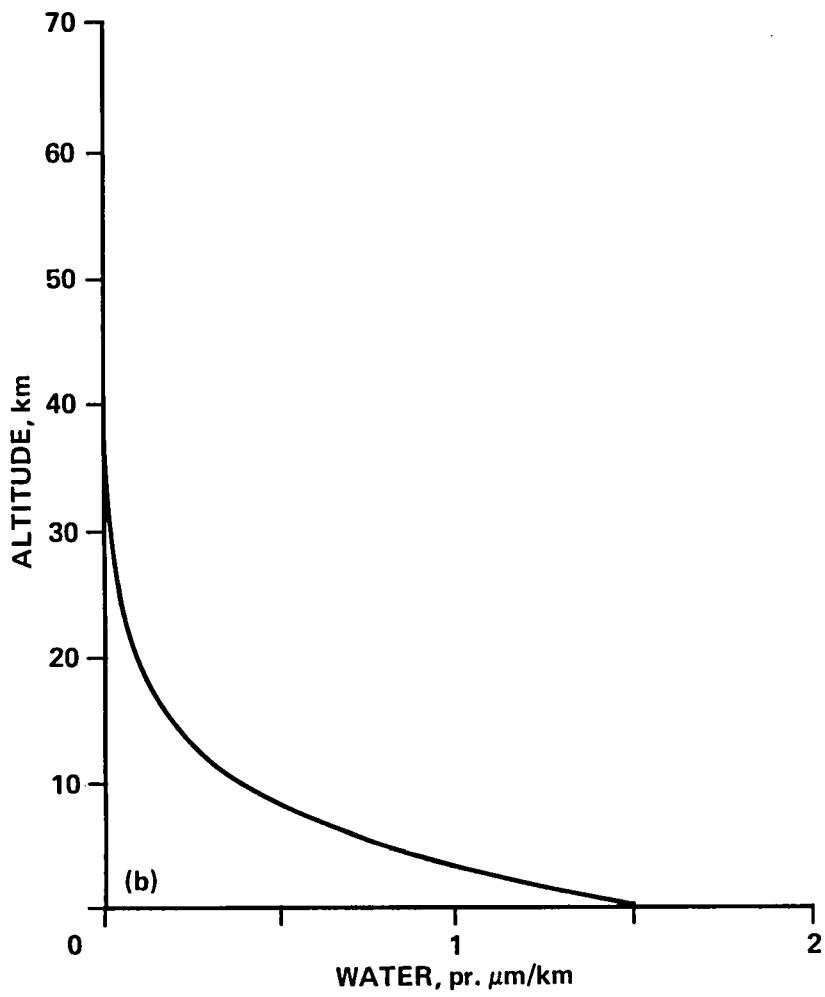
Figure 23.- Concluded. (b) Water density profile.
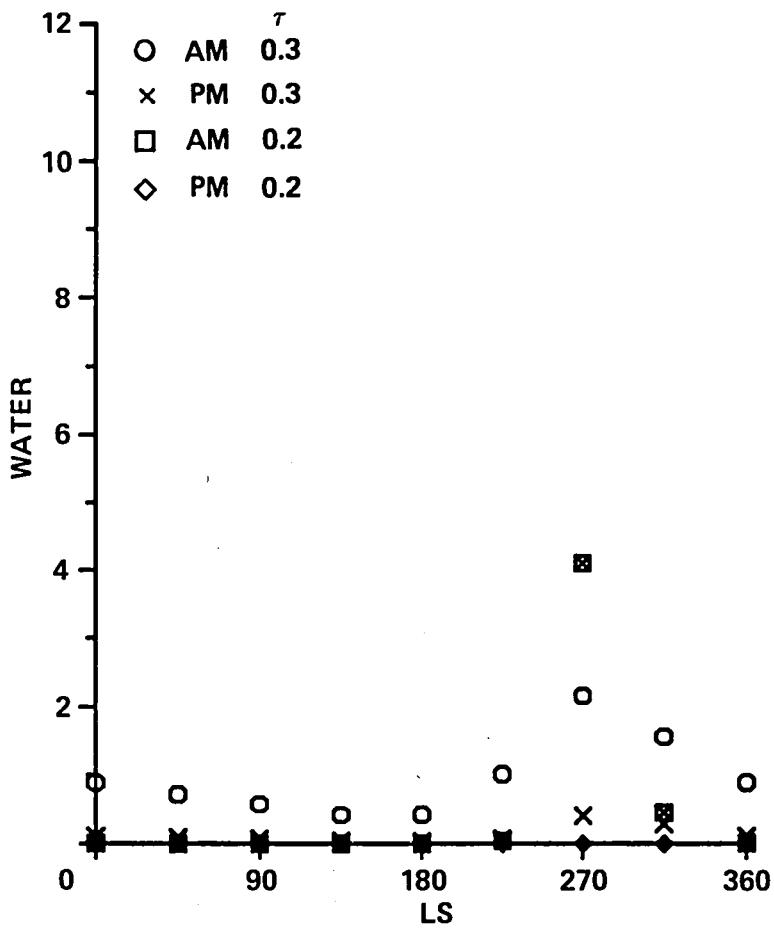
Figure 24.- Parametric study of condensation at the latitude of Lander 1 as a function of the season. Water vapor content is 11.0 pr μm.
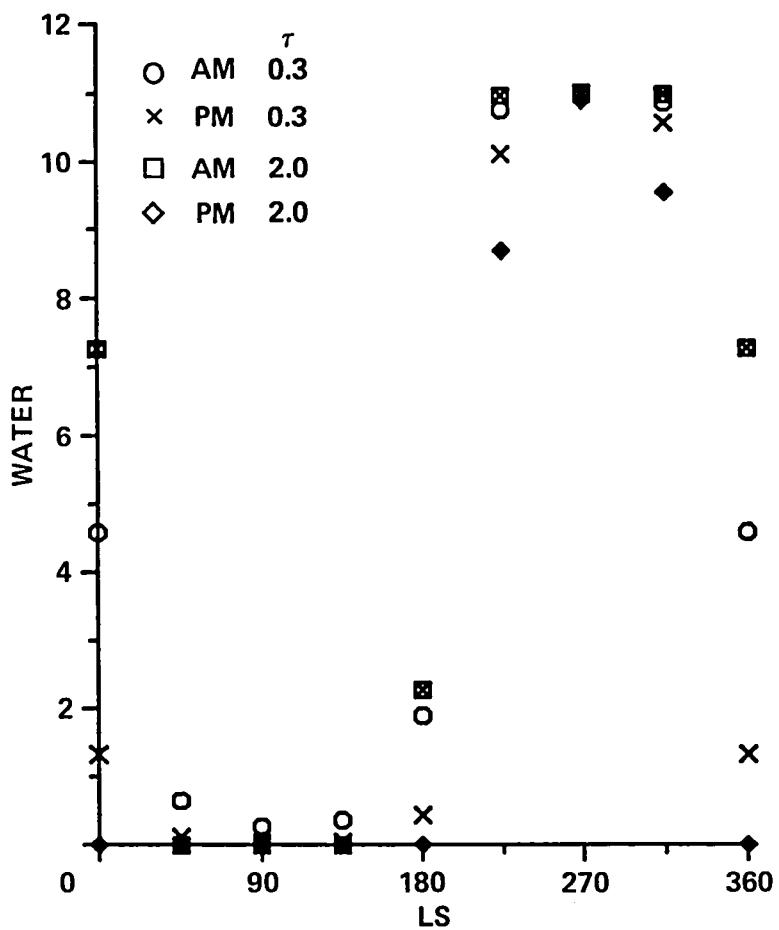
Figure 25.- Parametric study as in figure 24 but for the latitude of VL2.
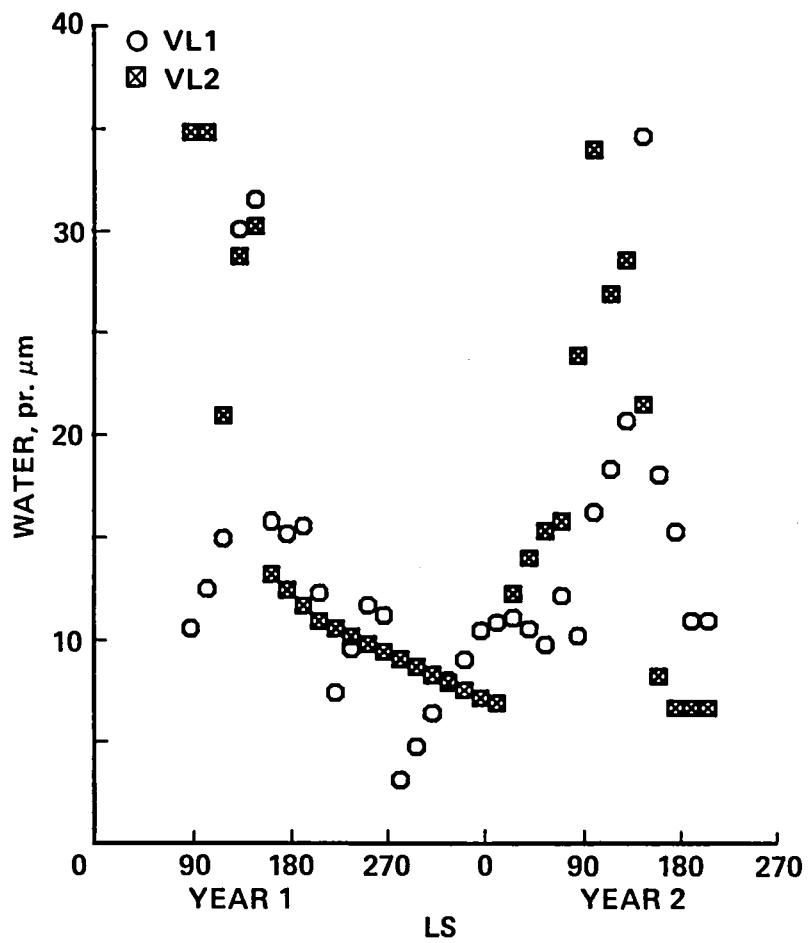
Figure 26.- Water vapor content at the two lander sites as measured by the MAWD experiment. Where measurements were insufficient, linear interpolation was used.
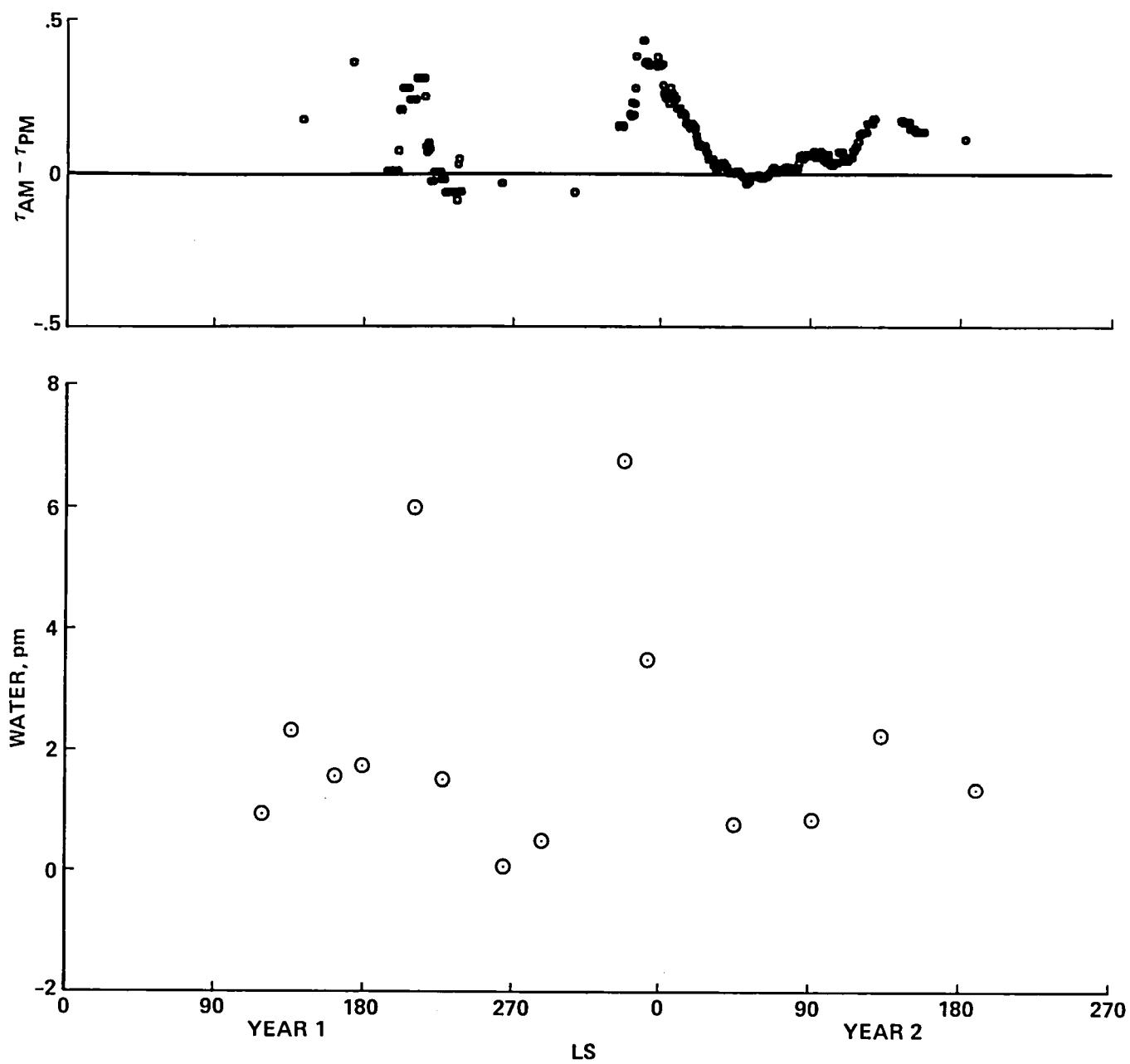
Figure 27.- Comparison of measured AM-PM differences and model predictions, VL2. The model uses water vapor values from the MAWD experiment and optical depths from PM lander observations.
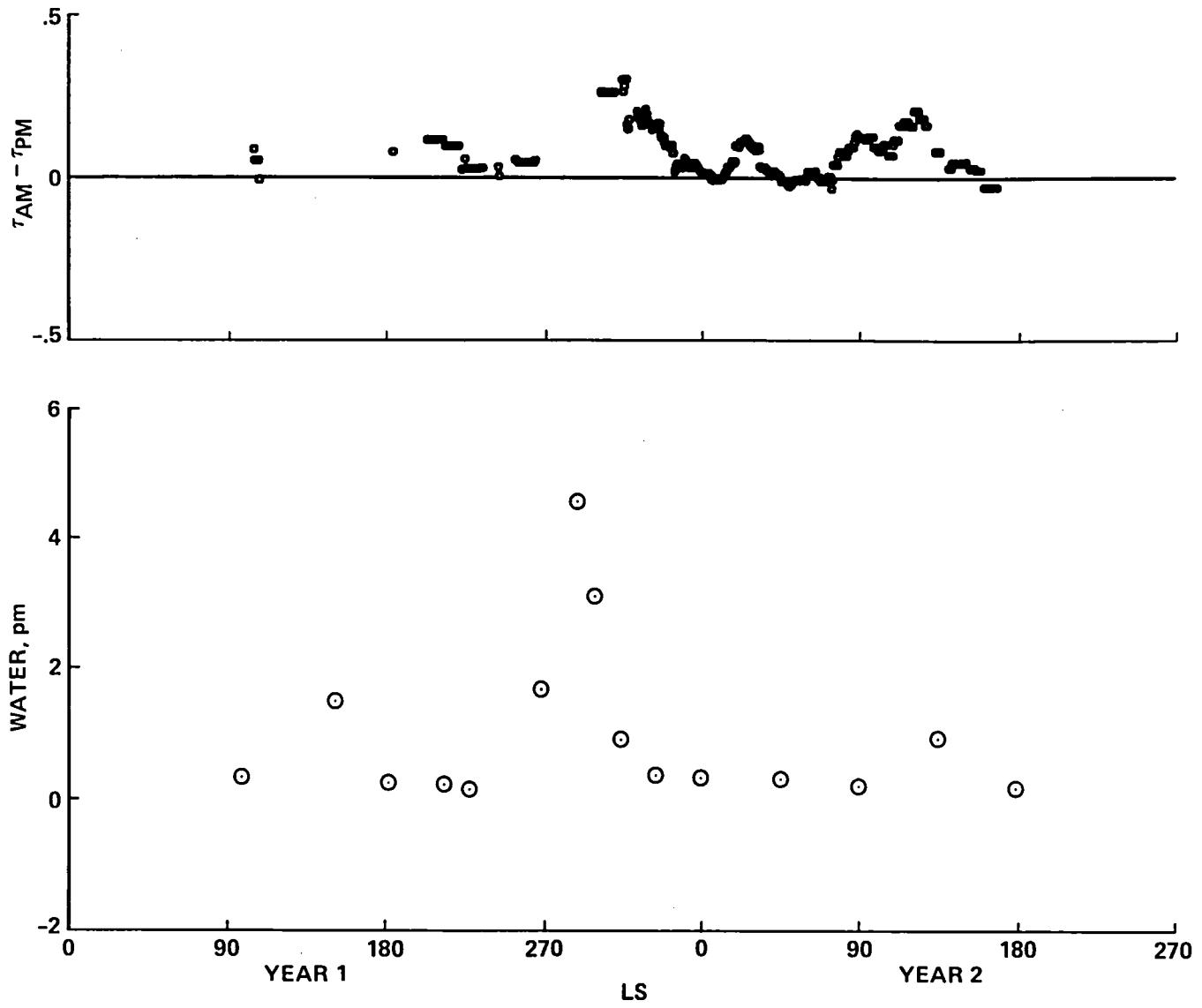
Figure 28.- Comparison of measured AM-PM differences and model predictions, VL1.
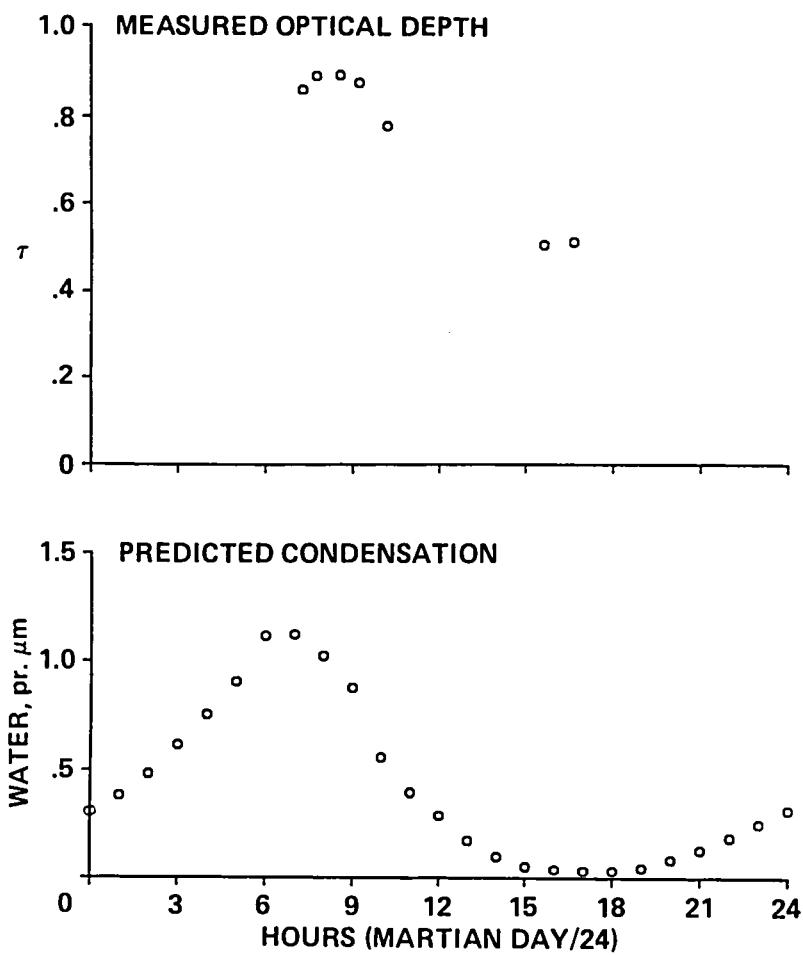
Figure 29.- Comparison of measured optical depths and predicted water condensation for Sol 420, VL2.
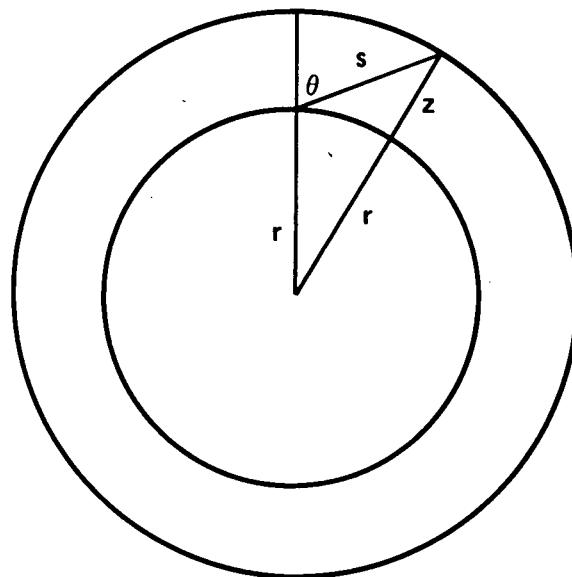

Figure 30.- Relation of slant height to altitude above a spherical surface.

1. Report No. NASA TM-100057	2. Government Accession No.	3. Recipient's Catalog No.
4. Title and Subtitle Diurnal Variations in Optical Depth at Mars: Observations and Interpretations		**5. Report Date** May 1988
		6. Performing Organization Code
7. Author(s) D. S. Colburn, J. B. Pollack, and R. M. Haberle		**8. Performing Organization Report No.** A-88067
		10. Work Unit No. 154-20-80-16
9. Performing Organization Name and Address Ames Research Center Moffett Field, CA 94035		**11. Contract or Grant No.**
		13. Type of Report and Period Covered Technical Memorandum
12. Sponsoring Agency Name and Address National Aeronautics and Space Administration Washington, DC 20546-0001		**14. Sponsoring Agency Code**

15. Supplementary Notes

Point of Contact: D. S. Colburn, Ames Research Center, MS 245-3, Moffett Field, CA 94035, (415) 694-5495 or FTS 464-5495

16. Abstract

Viking lander camera images of the Sun were used to compute atmospheric optical depth at two sites over a period of 1-1/3 martian years. The complete set of 1044 optical depth determinations is presented in graphical and tabular form. Error estimates are presented in detail. Optical depths in the morning (AM) are generally larger than in the afternoon (PM). The AM-PM differences are ascribed to condensation of water vapor into atmospheric ice aerosols at night and their evaporation in midday. A smoothed time series of these differences shows several seasonal peaks. These are simulated using a one-dimensional radiative-convective model which predicts martian atmospheric temperature profiles. A calculation combining these profiles with water vapor measurements from the Mars Atmospheric Water Detector (MAWD, on the Viking orbiters) is used to predict when the diurnal variations of water condensation should occur. The model reproduces a majority of the observed peaks and shows the factors influencing the process. Diurnal variation of condensation is shown to peak when the latitude and season combine to warm the atmosphere to the optimum temperature, cool enough to condense vapor at night and warm enough to cause evaporation at midday. The diurnal variation is

17. Key Words (Suggested by Author(s)) Mars Mars atmosphere Optical depth	18. Distribution Statement Unclassified – Unlimited Subject Category – 91

19. Security Classif. (of this report) Unclassified	20. Security Classif. (of this page) Unclassified	21. No. of pages 71	22. Price A04